The development of frother optimisation techniques in full scale flotation plants

by

Luke Venkatesan

BSc Eng (Chemical), University of Kwazulu Natal

A thesis submitted to the University of Cape Town as fulfilment of the requirement for the degree of Master of Science in Chemical Engineering

Supervised by: Dr Belinda Mcfadzean and Mr Martin Harris

CENTRE FOR MINERALS RESEARCH

Department of Chemical Engineering

University of Cape Town

September 2013

Synopsis

In 2012, Anglo American Platinum assembled a technical task team of metallurgists for their concentrator operations. Although there has been extensive research in literature regarding the flotation response and behaviour of reagents, there still exists a gap between fundamental laboratory scale research and plant scale application. This thesis will focus on the development of techniques for optimising and characterising frother on a full scale plant using the Anglo American Platinum Bubble Sizer (AAPBS) which is a commonly used tool by the plant metallurgist. The techniques developed have been based on the application of fundamental research of frothers in literature.

This thesis consists of three main focus areas:

1) Developing a technique for measuring the relationship between sauter mean bubble diameter and frother concentration on a full scale plant.
2) Developing a technique for estimating frother concentrations in process streams in full scale plant
3) Establishing whether the relationship between sauter mean bubble diameter and superficial gas velocity in a flotation bank of identical cells in series in a plant operating at frother concentration above the CCC is identical, and whether this can be used to detect the decrease of frother concentration to below the CCC at any point in the bank. Furthermore, the metallurgical performance of a bank with a decrease in frother concentration below the CCC midway through the bank was determined before and after the addition of frother, which was added as such that all the cells in the bank operate with a frother concentration above the CCC.

There were two techniques investigated for measuring the relationship between sauter mean bubble diameter and frother concentration. Both techniques involved using the AAPBS and the use of forced air mechanically agitated tank cells. Technique 1 involved using the first rougher cell on a flotation plant, dosing frother at different rates into the cell to target different frother concentrations and then measuring the resultant bubble size whilst operating at a fixed air rate. The coalescence mechanism here was occurring in a three phase solids/aqueous/air system occurring in a continuous stirred tank. Similarly Technique 2 involved using the first rougher cell; however, the first cell was depleted of frother by bypassing the frother dosage line into the next cell. This was done to isolate the first rougher cell and to minimise disturbance to the rest of the rougher bank. Known concentrations of frother were made up in potable water and these were added into the AAPBS. Bubbles from the pulp phase enter the bubble riser tube which is long and narrow (3m x 25mm diameter) which is representative of two phase aqueous/air “plug flow” system. These bubbles coalesce to different degrees based on the known frother concentration. The resulting bubble size distribution was then be measured by taking photographs at the viewing pane of the AAPBS. The air rate in the cell was kept constant to within 0.7-0.9 cm/s and the photographs were analysed using software provided by stone three to determine the sauter mean bubble diameter and the bubble size distribution.

Technique 1 was applied to Plant A UG2 concentrator which was using a polyglycol type frother called Betafroth 206C which has an undisclosed composition and a molecular weight of approximately 200 g/mol. The first rougher cell used was an Outokumpu 70 m^3 forced air mechanically agitated tank cell. The results showed no clear relationship between sauter mean bubble diameter and frother concentration. Furthermore, the sauter mean bubble diameter was already very small and it appeared that the changes in between runs were more strongly linked to the superficial gas velocity than frother concentration. The fact that the sauter mean bubble diameter obtained was already small implied that the frother concentration in the cell was already high. This could have been due to an additional source of frother due to spillage or in the process water that potentially elevated the actual frother concentrations in the cell. Technique 1 also resulted in significant disturbances to the entire rougher bank because it involved changing the frother dosages to the bank. This would affect the flotation performance of the bank for a prolonged period and affect plant performance. Hence it was decided that technique 1 would not be suitable.

Technique 2 was applied in Plant A UG2 Concentrator on the same rougher cell as above using the same frother, Betafroth 206C. The results obtained were in excellent agreement with the relationships observed in literature for a similar frother type. Furthermore, the data could be modelled to fit an exponential decay relationship with an excellent fit. The CCC obtained for betafroth 206C was approximately 8 ppm. The reproducibility of this technique was then tested at Plant B UG2 concentrator by applying it on the first rougher cell on each of two parallel rougher banks. These rougher cells were of the same size, type and of same internals but it could be expected that the gas dispersion and bubble size distribution would not be identical because of differences in wear of the cell internals. The roughers cells were Outokumpu 70 m^3 forced air mechanically agitated tank cells, and the frother being tested was a polyglycol type called Sasfroth 200 which is a mixture of polyglycol ethers and alcohols and has a molecular weight of approximately 200 g/mol. The results showed that the relationships for both cells were very similar and that technique 2 was reproducible. Furtermore, the CCC for both tests were approximately the same at 10 ppm for Sasfroth 200.

A comparison of the relationship between sauter mean bubble diameter and frother concentration was made between betafroth 206C and sasfroth 200 which showed that betafroth 206C had a stronger effect on reducing bubble coalescence. Furthermore, the CCC obtained for Betafroth 206C was approximately 8 ppm which was lower than that of Sasfroth 200 which was found to be approximately 10 ppm. This difference was outside an experimental error of 10%. This implied that Betafroth 206C was a stronger frother than Sasfroth 200.

Technique 2 was applied to Plant C UG2 concentrator which also used Sasfroth 200. The first rougher cell used was a 50 m^3 Outokumpu forced air cell which was a smaller cell than previously tested; this was done to test the robustness of the technique on a different size cell. The measurement was also repeated on the same cell on a different day to investigate the repeatability of the measurement with different plant operating conditions. The results showed that the same exponential decay relationship as found in literature was obtained with an excellent fit to the model. The results obtained were similar to the results obtained at Plant B UG2 concentrator and was reproducible on a different cell size. All the results obtained for Sasfroth 200 from Plant B and Plant C UG2 concentrator where then compared to each other which were representative of different plants, cell sizes and operating conditions. The data points for sauter mean bubble diameter and frother concentration relationship overlapped and appeared to lie on a common line for all tests. Furthermore, the CCC obtained for all tests were on average 10.6 ppm with a relative standard error of 4.4%. This was within the estimate of experimental error which was approximately 10%. Technique 2 is also simple to perform by a plant metallurgist and it introduces minimal disturbance to plant operation by isolating the first rougher cell from the rest of the bank as opposed to technique 1. Hence technique 2 was found to be reproducible, repeatable and a robust measurement for full scale plant application. Furthermore, there is also potential for using Technique 2 to compare different frothers on plant scale by using the CCC as an indication of relative strength.

The technique for estimating frother concentration in the process streams was an extension of technique 2. The methodology was to use the effect of the aqueous solution from process streams on bubble coalescence as a proxy for frother concentration. Similarly to technique 2, the process stream aqueous solution was added to the AAPBS, and the resultant bubble size was measured. Using the known relationship between sauter mean bubble diameter and frother concentration for the frother, this bubble size was translated into an equivalent frother concentration (EFC). This technique was applied to Plant B and Plant C UG2 concentrator which use Sasfroth 200 as the plant frother. The rougher banks were surveyed in each plant and a mass balance for frother was performed and compared to results obtained in literature using different frother concentration measurement methods. The results showed that a frother balance could be applied successfully with good data consistency between measured and balanced data. It was observed that a small portion of frother leaves in the concentrates in the bank and the bulk of the frother remained in the bulk water stream which was in agreement with literature. Similarly, the equivalent frother recovery and water recovery in

concentrates of the bank had a straight line relationship for both plants. This was also in agreement with literature which indicates that polyglycol frothers are very water soluble and tend to follow the water stream. A trend between concentrate percentage solids and EFC was observed. The trend showed that higher percent solids had higher EFCs. There are two transport methods of frother into the concentrate, the first by attachment of frother at the air/water interface of bubbles and the second is with water recovery to the concentrate by entrainment. It can be expected that the former would be at a higher concentration than the latter. The concentrate percentage solids is an indication water recovery by entrainment, hence it can be possible that the higher percentage solids implied lower water recovery by entrainment, and resulted in a higher concentration.

It has been shown in literature that dissolved ions in solution affect bubble coalescence and these are present in process plants which recycle process water. Because the EFC measurement is dependant on bubble size and is aimed at estimating a frother concentration; the dissolved ions present may affect the EFC measurement and the estimation of the frother concentration. Hence measurements of the dissolved ions and ionic strength of the process streams on the rougher bank on Plant C UG2 concentrator was performed. The ionic strength of the process stream aqueous solutions were compared to measurements made in literature of the effect of ionic strength on bubble coalescence. The ionic strength of the process streams were in the region of 0.03 mol/l and would not have had a significant effect on bubble coalescence. The main effect on bubble coalescence would have been due to frother and hence the EFC could be used as a proxy for frother concentration.

The relationship between sauter mean bubble diameter and superficial gas velocity was investigated in Plant D UG2 concentrator. Plant D UG2 Concentator treats Platreef ore and uses Betafroth 206 as the plant frother. The secondary cleaner and scavenger cleaner banks were used for the investigation. The secondary cleaner bank operated with identical forced air mechanically agitated tank cells operating with the same impeller speed. Frother was dosed in the feed to the secondary cleaner bank was this was considered to be higher than the CCC. The results showed that relationships between sauter mean bubble diameter and superficial gas velocity for the first four cells in the secondary cleaner bank were on the same common straightline.

The secondary cleaner tails stream is the feed stream to the cleaner scavenger bank which received no frother. The cleaner scavenger bank consisted of six identical cells in series and showed poor visual froth stability. Measurements of the relationship between sauter mean bubble diameter and superficial gas velocity were linear and on the same line for the first two cells of this bank, however from cell three to six, the straight lines were shifting upwards implying larger bubbles for the same superficial gas velocity. Frother was dosed on the third cell at a concentration equivalent to 15 ppm based on the water flowrate in the feed to the bank. There was a significant visual improvement in froth stability and measurements of the sauter mean bubble diameter and superficial gas velocities showed that all the relationships for all the cells were linear and now on the same straightline. The metallurgical performance of the cleaner scavenger bank was performed before and after the addition of frother. The results showed a significant increase in nickel and 4E PGM grade of approximately 30% after the addition of frother. Furthermore there was a significant increase in copper recovery of 27%, and the nickel and 4E PGM recovery increased by 100%.

Plagiarism Agreement

I declare that this thesis, submitted for the degree of Master of Science in Engineering at the University of Cape Town, is my own work and has not been submitted prior to this for any degree at this university or any other institution. I understand the meaning of plagiarism and declare that all the work in the document, except for that which is properly acknowledged, is my own work.

Luke Venkatesan

Acknowledgements

“Now all glory to God, who is able to keep you from falling away and will bring you with great joy into his glorious presence without a single fault. All glory to him who alone is God, our Saviour through Jesus Christ our Lord. All glory, majesty, power, and authority are his before all time, and in the present, and beyond all time! Amen!” Jude 24-25

First and foremost I would like to dedicate this thesis to the Lord Jesus Christ who is the source of all wisdom, knowledge and understanding. He has given me the strength, wisdom and understanding to whom I am eternally grateful. I would like to thank my parents, Sandra and Willie Venkatesan, and my love Nickieta Singh, for all the encouragement, support and sacrifices. I would also like to thank my siblings Daniel, Matthew and Annette for encouragement. I would like to specially thank the late Mark Greyling, Andrew Harris, and the Technical Task Team (TTT) for all the encouragement, support and hard work! I want to thank Dr Neville Plint and Anglo American Platinum for the encouragement and financial support for this thesis. I would also like to thank Dr Belinda Mcfadzean for all the help and guidance, and support with the write up of this thesis. I appreciate all your help and effort! I also want to thank Mr Martin Harris for all the advice.

Table of Contents

List of Figures

List of Tables

1. Introduction

In 2012, Anglo American Platinum assembled a technical task team for their concentrator operations. The main objective of the team was to develop a methodology and strategy for full scale flotation optimisation with the aim of mass pull reduction in their concentrator operations. The main levers for flotation optimisation were air addition, froth depth, circuit configuration and flotation reagents. Although extensive research has been done in literature on the flotation behaviour and response to reagents, there still exists a gap between fundamental research and plant scale application. Hence this master's project will be focussed on applying the knowledge available in literature to develop simple robust applications that can be used for optimisation in full scale plants. The focus will be on developing plant scale techniques and strategies for dosing frother.

Frother is an important flotation reagent in that it affects both the pulp phase and the froth phase in a flotation cell. In the pulp phase it controls the bubble size and in the froth phase provides froth stability (Capuccitti and Finch, 2008). Furthermore, it has been shown by Gorain et al (1998) that bubble size is directly related to flotation kinetics which makes frother a very important reagent. In current plant operations, frother is typically dosed based on past experience and visually observing the froth with very little technical methodology.

The characterisation of different frothers based on their effect on bubble size and inferred effect on froth stability have been extensively studied on a laboratory scale (Cho and Laskowski, 2002; Finch et al, 2008; Nesset et al, 2006; Nesset et al, 2007; Grau et al, 2005). However most of the reagent suppliers keep the compositions of their frothers a trade secret. Hence on a plant scale independent characterisation of the frother will be required and this costs time and money. There exists a need to develop a simple and robust plant scale technique that allows frother to be characterised and for frother concentration to be estimated in process streams in order to determine frother dosages. Techniques have been developed by (Hadler et al, 2005; Tsatouhas et al, 2005, Gelinas and Finch, 2007, Weber et al, 2003) to estimate and measure frother concentrations in process streams. However, the limitations of these techniques are that they require specialised personnel in a sophisticated and well equipped laboratory without providing a robust measurement.

Two techniques using the currently available Anglo Platinum Bubble Sizer will be investigated to measure the effect of frother concentration on bubble size. A technique to estimate the frother concentration in process streams will be investigated which uses the effect of the process stream aqueous solution on bubble coalescence as a proxy for frother concentration. In addition, the effect of frother concentration on the relationship between sauter mean bubble diameter and superficial gas velocity for a bank of identical cells in series will be investigated. This relationship between sauter mean bubble diameter and superficial gas velocity will be used to detect decrease of frother to below the critical coalescence concentration (CCC) in a bank of identical cells in series. These techniques use already existing equipment and require no capital investment and are simple to operate.

2. Literature Review

2.1 The Bushveld Igneous Complex

The Bushveld Igneous Complex (BIC) as shown in Figure 1 is the largest layered intrusion in the world (Cawthorn, 1999). It has an area of more than 65000 km^2 and a depth of close to 7 km (Cawthorn, 1999). The complex was formed by a large volume of magma that cooled very slowly into layers allowing for concentration of valuable minerals (Cawthorn, 1999). There are three different ore bodies: the Merensky reef, the Upper Group 2 (UG2) chromitite reef and the Platreef. The Merensky reef and UG2 reef can be traced on the surface for 300kms in two separate arcs and the Platreef extends for over 30 km (Cawthorn, 1999). These reefs are mined for their valuable platinum group metals which are platinum, palladium, rhodium, ruthenium, osmium and iridium.

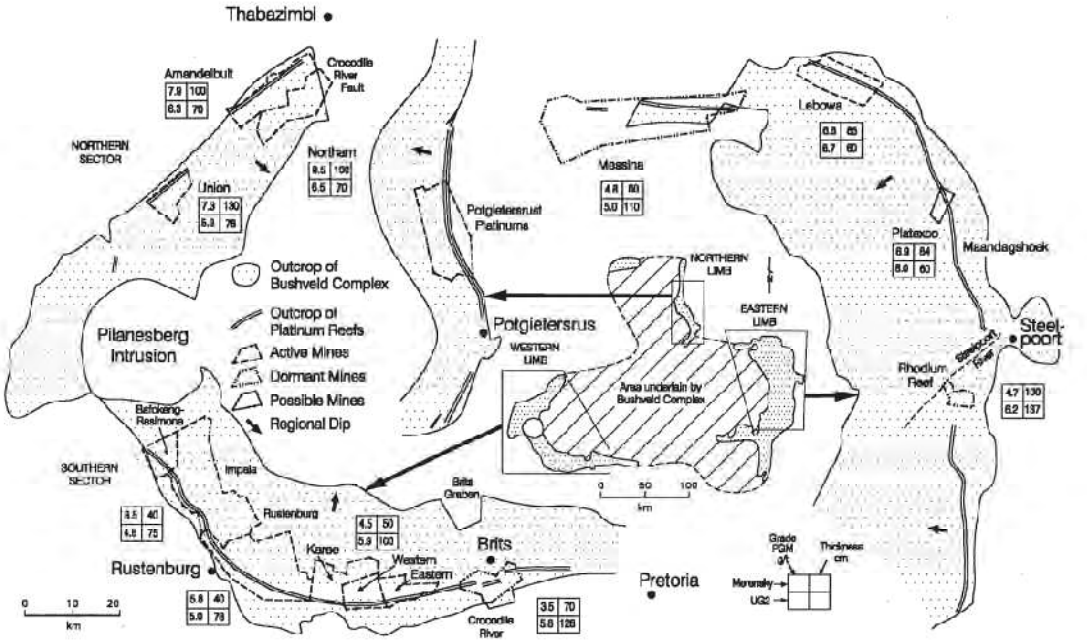

Figure 1: Schematic of Bushveld Igneous Complex (adapted from Cawthorn, 1999)

2.2 Anglo American Platinum Operations

Anglo American Platinum is the world's largest primary producer of platinum group metals and is responsible for 40% of the world's newly mined platinum. The company has operations spreading throughout the Bushveld Igneous Complex as shown in Figure 2. These include fully owned mines and joint ventures.

Figure 2: Anglo American Platinum operations in Bushveld Complex (adapted from Anglo American Platinum Annual Report 2012)

After the ore is mined, it is treated in concentrator plants. There are a total of 14 concentrators in the group, of which one is situated in Zimbabwe. Concentrators use froth flotation as the separation and concentration process to upgrade the ore before it is sent to smelters. There are three smelting complexes which include the Waterval, Mortimer and Polokwane smelters. The smelters produce a furnace matte which is treated at the Waterval Converter. The converter matte is then sent to the base metals refinery and then the precious metals refinery. The final products include platinum, palladium, rhodium, ruthenium, osmium, iridium and gold. By-products include copper, nickel, cobalt sulphate, sodium sulphate and sulphuric acid.

2.3 Froth Flotation

Froth flotation is a separation process used widely in the current PGM concentrator plants at Anglo American Platinum. This process follows a series of comminution steps which crush and grind the ore in order to liberate the valuable minerals using crushers, ball mills and attrition mills (Isamills). Once the ore is ground it is pumped as slurry into flotation cells. Air is bubbled through the slurry and the valuable hydrophobic (water repelling) minerals attach onto air bubbles and float to the surface or froth where it is recovered as the concentrate. A flotation cell consists of a rotor and stator to agitate and suspend the slurry, and to also disperse air into the cell. There are 2 distinct phases which are the pulp phase which is a turbulent mixture of slurry and air, and an air-rich froth phase which contains water, air and concentrated valuable minerals. Chemical reagents are added to enhance the separation process: collector, to enhance the hydrophobicity of the valuable minerals; frother, to ensure small pulp-phase bubbles and a stable froth; and depressant to depress the unwanted naturally floating gangue. This thesis will be focussing on the frother.

2.4 Frother

2.4.1 Role of frother in Flotation

Frothers have many functions in the flotation process. They affect both the pulp zone and the froth zone. In the pulp zone, they reduce the bubble size by preventing bubble coalescence. In the froth zone, they affect the stability of the froth to hold valuable minerals, allow for drainage of water and entrained particles, affect mobility of froth to transport valuable minerals into the cell launders and

affect the break-up of the froth in the launders to allow for pumping of the concentrate (Capuccitti and Finch, 2008).

2.4.2 Types of frothers

Frothers are also termed surfactants and the widely used frothers in flotation include the following: “1) Natural oils such as terpineol (e.g. pine oil) and cresols, 2) C_5 – C_8 aliphatic alcohols, 3) polypropylene glycols and their alkyl ethers, 4) mixed ethers, aldehydes and ketone products, 5) alkoxyalkanes such as TEB (tri-ethyl butane)” (Capuccitti and Finch, 2008). Each frother is typically selected based on its desired effect on the pulp and the froth. The commonly used frothers in PGM flotation include polypropylene glycols and their alkyl ethers. The compositions of some frothers are known but are commonly kept as trade secrets by reagent manufacturers.

2.4.3 Effect of frother on bubble size and foam stability

Frothers are surface active compounds and this surface activity can be explained by their molecular structure shown in Figure 3 (Finch et al, 2008). Frothers are typically heteropolar molecules that contain both hydrophilic and hydrophobic groups. The hydrophilic group consists of the OH groups as in alcohols but can include the alkoxy groups ($O\text{-}C_n\text{-}H_{n+1}$) as in polyglycols. The hydrophobic component is the hydrocarbon chain. This bi-polar molecular structure allows the frother molecules to adsorb onto the air-water interface on a bubble with the hydrophilic component on the water side and the hydrophobic component on the air side. This interrupts the hydrogen bonding between the water molecules and reduces the surface tension (Finch et al, 2008).

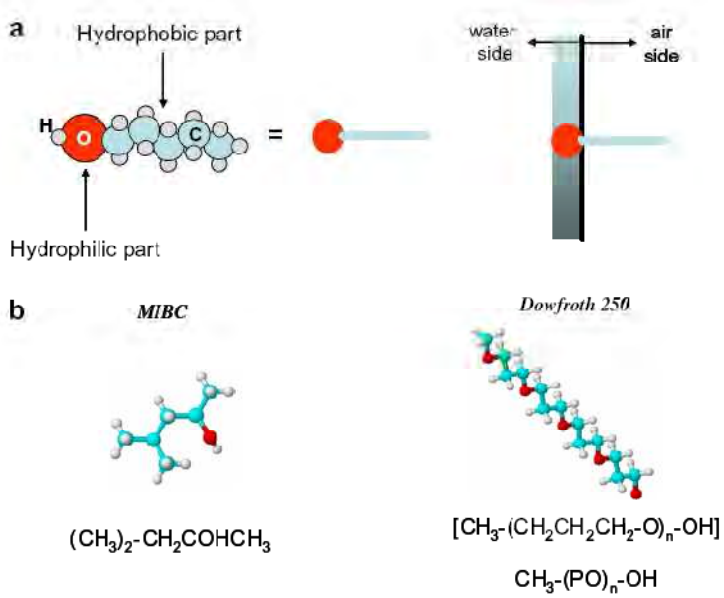

Figure 3: Frother molecular structure for an a) alcohol type (MIBC) and b) polyglycol type (Dowfroth 250) (Finch et al, 2008)

The effect of frother on surface tension and bubble size was investigated by Sweet et al (1997) in a two phase air/water system. The tests showed that the effects of frother on bubble size occurred at frother concentrations much lower than those at which the surface tension was affected. Hence this effect of frother on bubble size is apparent at small concentrations of frother in water. This effect has been further studied by (Cho and Laskowski, 2002). The objective of their experiment was to test the effects of flotation frothers on bubble size and foam stability in two phase air/water system. Foam stability was measured using the dynamic foamability index, the methodology originally published by (Malysa et al, 1979, 1981). The term foam is used instead of froth to describe a system with air and water only. The methodology uses the retention time (rt) which is defined as the slope of the linear

part of the dependence of the total gas volume (solution and air) on the gas flow rate. The dynamic foamability index is defined as the slope of the rt vs. frother concentration relationship as the concentration approaches zero.

Tests were carried out with 5 different frothers, which included MIBC (methyl isobutyl carbinol) and different hexanol isomers and derivatives which included: 1) 1-hexanol 2) Di-ethoxy mono-propoxy hexanol 3) Di-eothoxy hexanol 4) Mono propoxy-di ethoxy hexanol. The tests were performed in 3-1 Plexiglass tank using distilled water at 21 ^{o}C as well as in an open top Leeds cell. Both multiple hole and single hole spargers were used to generate the bubbles and the UCT bubble sizer was used to measure bubble size (Tucker et al, 1994). In addition, dynamic foamability measurements were performed on each frother. There was no effect of frother on bubble size with single hole spargers because there was limited collision between the bubbles. However, in the 3 hole sparger and the open top Leeds cell, the results showed that increasing frother concentration decreased bubble size. This effect was attributed to frother preventing bubble coalescence. Figure 4 shows the relationship between Sauter mean bubble diameter and frother concentration in the three-hole sparger (Cho and Laskowski, 2002). In the relationship, Cho and Laskowski, (2002) showed that there existed a frother concentration above which there is little or no change in bubble size. This concentration was called the critical coalescence concentration (CCC).

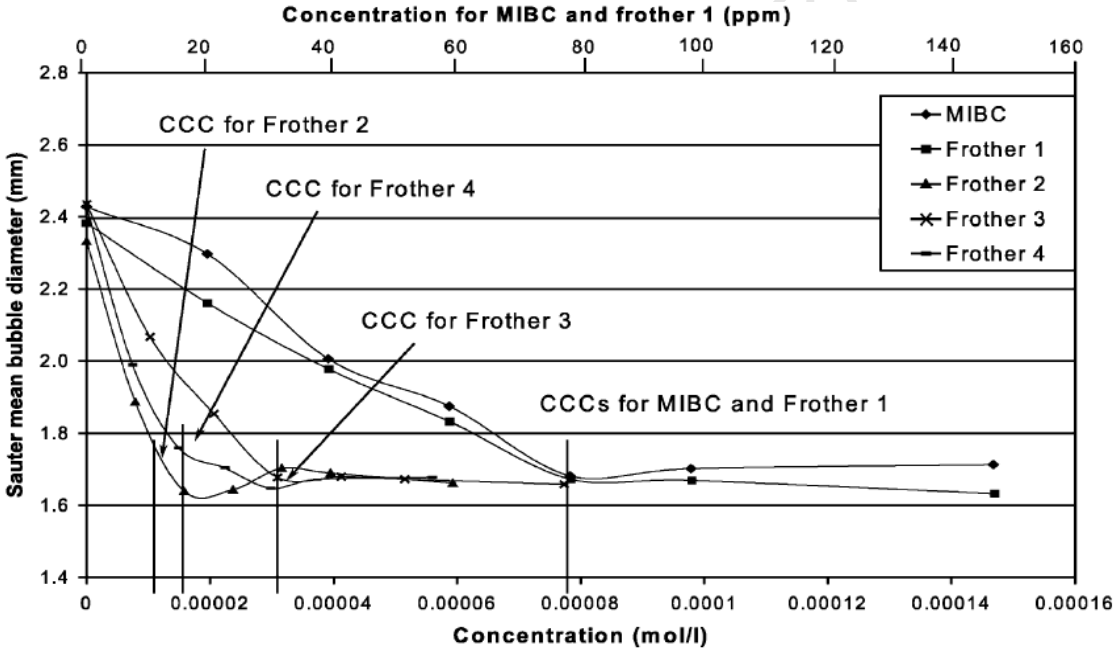

Figure 4: Sauter mean bubble size vs. frother concentration carried out in a 0.1 mm three-hole bronze sparger (Cho and Laskowski, 2002)

This relationship can be described in Figure 5, which shows the difference regions of frother concentration. Frother concentrations below the CCC (zone 1) show bubble size being controlled via coalescence, whereas concentrations above the CCC (zone 2) show bubble size as a result of the bubble generation mechanism.

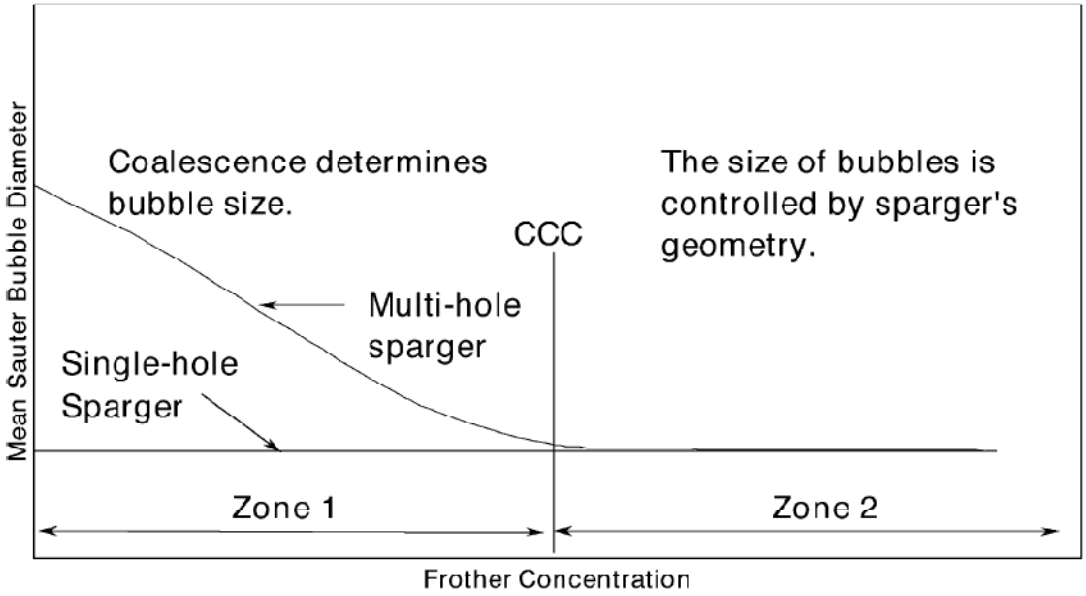

Figure 5: Schematic of Sauter Mean Bubble Size and Frother Concentration (Cho and Laskowski, 2002)

Figure 6 shows the method used by Grau et al (2005) to determine the CCC graphically. Grau et al (2005) defined the CCC as the intersection of the horizontal asymptote to the curves with the sloped line approximating the curve at lower concentrations as shown in Figure 6. Similarly Nesset et al (2007) used a concept called the CCC95, which is the concentration at which there is a 95% size reduction in the sauter mean bubble diameter.

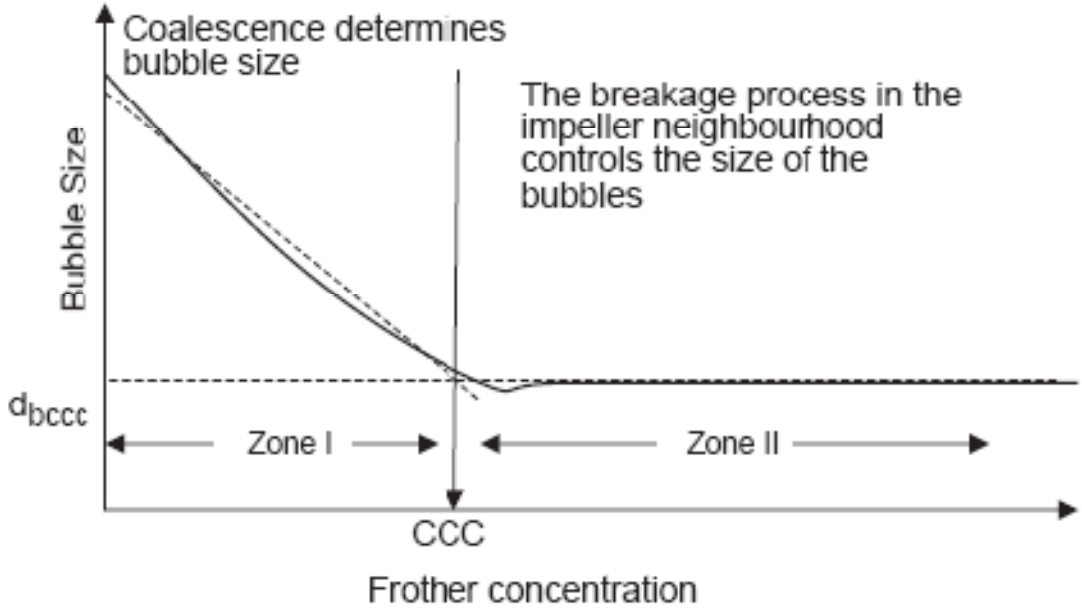

Figure 6: Graph showing graphical determination of the CCC (Grau et al, 2005)

Table 1 shows a comparison of the CCC values obtained in the three hole sparger apparatus as well as in a flotation cell. The CCC values obtained are almost identical, implying the CCC values are independent of the flotation cell used. Hence the CCC for a given frother can be used as a material constant (Grau et al, 2005). It is clear that the different frothers had different effects on bubble size

and gave different CCCs. Dynamic foamability measurements were also performed for each frother and were plotted against the CCC shown in Figure 7.

Table 1: CCC values obtained in three-hole sparger and in open top Leeds cell (Cho and Laskowski, 2002)

Frothers	Three-hole sparger CCC values (mol/l)	Open-top flotation cell CCC values (mol/l)
MIBC	0.000079	0.000083
Frother 1	0.000079	0.000083
Frother 2	0.000013	0.000015
Frother 3	0.000031	0.000037
Frother 4	0.000016	0.000015

Figure 7 shows the relationship between DFI and the CCC (Cho and Laskowksi, 2002). The frothers that generated lower CCC values also resulted in higher DFI values. This implies that stronger frothers require a lower dosage in order to produce the same bubble size and also result in more stable froths. Hence this implies that the CCC can be used to characterise the strength of frothers.

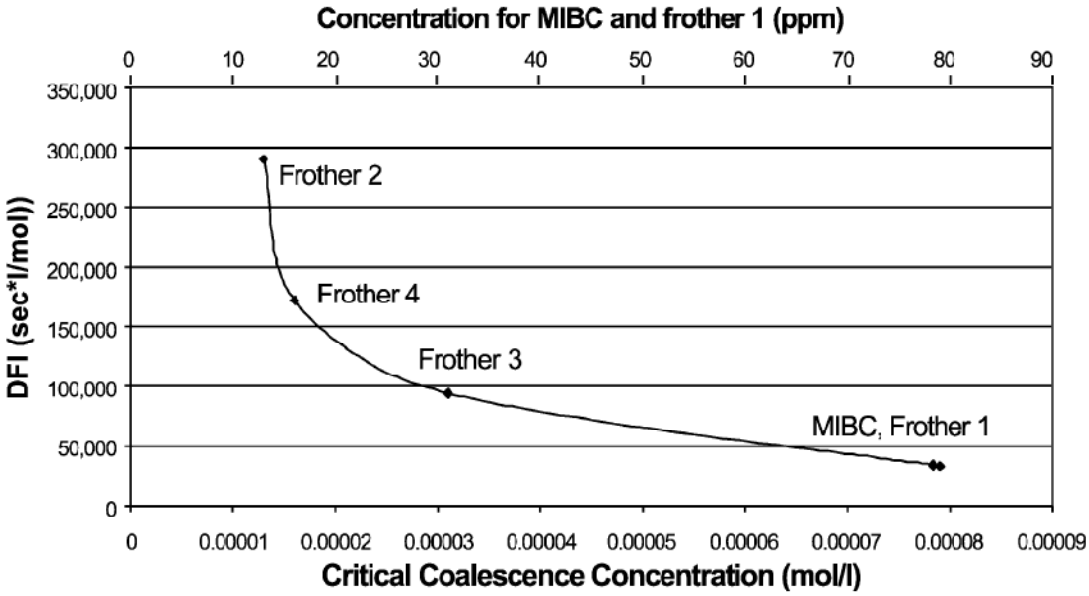

Figure 7: DFI vs. CCC relationship for the tested frothers (Cho and Laskowski, 2002)

2.4.4 Effect of frother concentration on bubble size in a mechanically agitated flotation cell

Nesset et al (2006, 2007) investigated the effect of operating variables and gas dispersion characteristics that affect bubble size in a mechanical forced air flotation cell. An important parameter investigated was frother type and concentration. The mechanical cell used was a 0.8 m^3 Metso pilot cell as shown in Figure 8. The cell was fitted with gas velocity and gas hold up probes. Bubble size measurements were performed with the Bubble Viewer, which used image analysis. Measurements were carried in a two phase air/water system. Montreal tap water was used in the cell and frother was dosed and mixed without air for 10 minutes before bubble size measurements were taken.

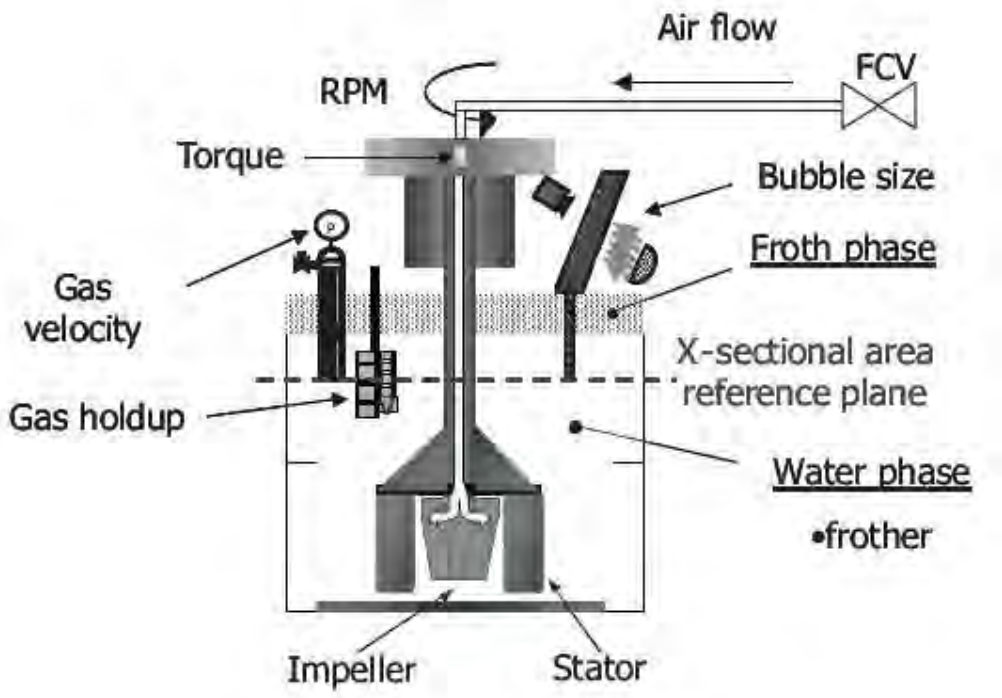

Figure 8: Schematic of the 0.8 m^3 Metso Cell used by Nesset et al (2006, 2007).

Figure 9 shows the effect of frother concentration on the bubble size distribution for an air/water system in a mechanical flotation cell (Nesset et al, 2006). Initially at zero frother concentration, the bubble size distribution is bimodal, and as the frother concentration increases the bubble size distribution gets finer and narrower and approaches a unimodal distribution. By comparing the bubble size distribution to a single sauter mean bubble diameter shown below, it can be seen that increasing frother concentration decreases the sauter mean bubble diameter up to a minimum. This minimum is called the critical coalescence concentration (Laskowski, 2003).

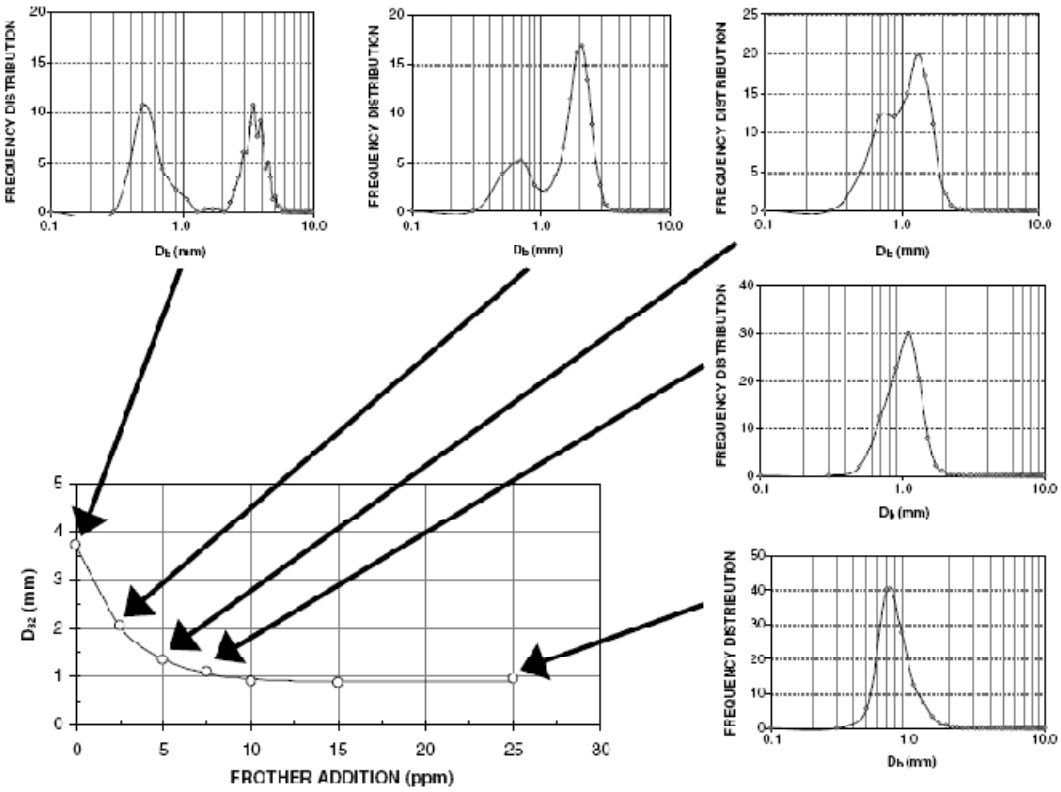

Figure 9: Effect of frother concentration on the bubble size frequency distribution in a mechanically agitated flotation cell (Nesset et al, 2006)

Nesset et al, 2007 further investigated the relationship with five different frother types. Figure 10 shows that the relationship between Sauter mean bubble diameter and frother concentration is a similar exponential decay relationship. However, although the final bubble sizes were found to be consistent with all frothers, the amount of frother required to reach this bubble size was different for all frothers. Pentanol had the least effect on reducing bubble size and F-150 had the greatest effect on reducing bubble size. These effects were also characterised by the CCC95 shown in Figure 10. The CCC95 was calculated from the exponential decay equation and is the frother concentration at which the bubble size is reduced by 95%. It was shown by Finch et al, 2008 that the relationship between sauter mean bubble diameter and frother concentration for all the frothers in Figure 10 could be normalised to fall on a common line as shown in Figure 11. This was done by plotting the sauter mean bubble diameter against the frother concentration divided by the CCC95.

Finch et al, 2008 investigated the coalescence mechanism in a slot sparger using high speed images as shown in Figure 12. The sequence of bubble contact and coalescence is clearly evident in tap water alone (a). The bubbles contact each other, distort and thereafter coalesce and a fine bubble is released as a result. In the case where frother is added to the Montreal tap water (b), the bubbles contact each other but do not coalesce as a result of the frother present. This mechanism was investigated with a sparger; however it can also explain the bubble size distributions seen in Figure 9 measured in a mechanical flotation cell. This can be explained as an initial bimodal bubble size distribution because of coalescence which produces coarser and finer bubbles. As the frother concentration increases coalescence decreases hence the bubble size distribution gets narrower and finer and approaches a unimodal distribution.

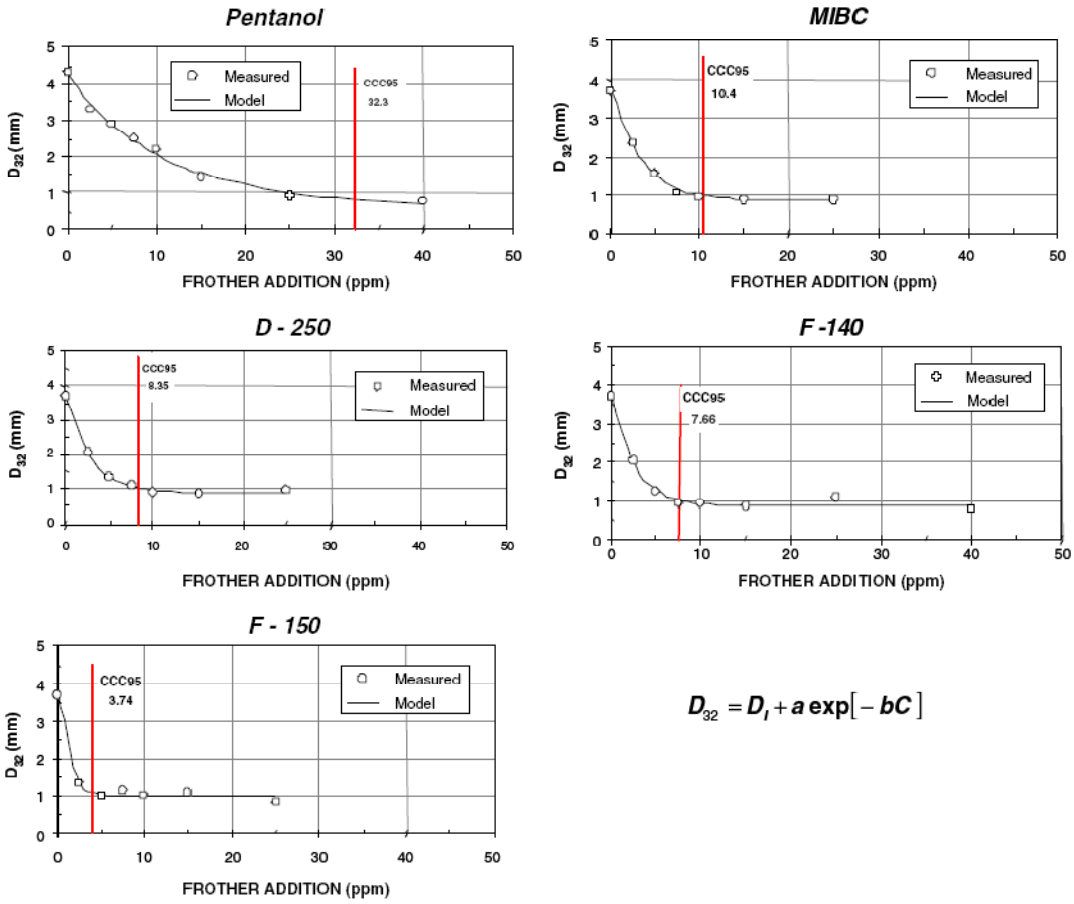

Figure 10: Sauter mean bubble diameter vs. frother concentration for five different frothers obtained from a 0.8 m^3 mechanically agitated flotation cell (Nesset et al, 2007)

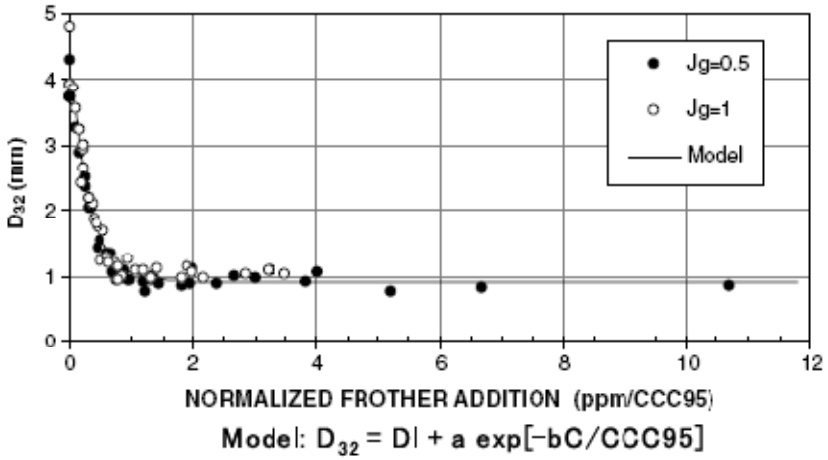

Figure 11: Relationship between Sauter mean bubble diameter and normalised frother addition (Finch et al, 2008)

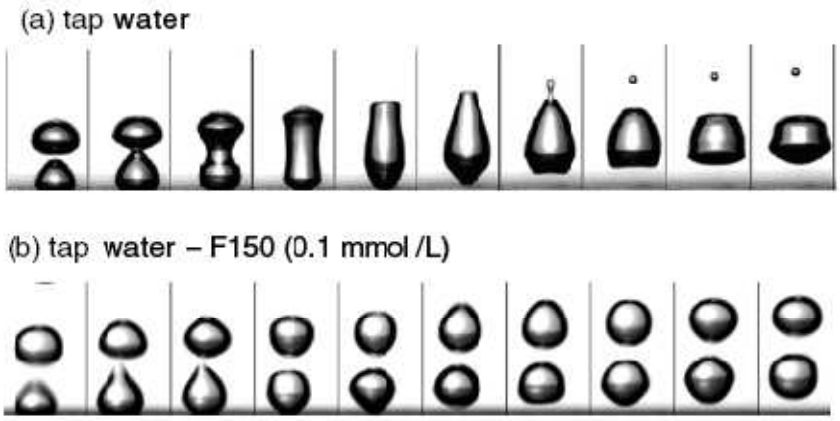

Figure 12: Sequence of high speed images (2000 frames/s) investigating bubble coalescence using a slot sparger with (a) tap water and (b) with frother added (Finch et al, 2008)

2.4.5 Mathematical Relationship between frother concentration and bubble size

Comley et al. (2002) showed that this relationship between bubble size and frother concentration can be described mathematically by an exponential decay relationship. This relationship can be defined by the following equation:

$$d_{32} = d_{lim} + Aexp(-BC_{frother}) \quad (1)$$

Where: d_{32} : Sauter mean bubble diameter (mm)

$$d_{32} = \frac{\sum_1^n d_i^3}{\sum_1^n d_i^2} \quad (2)$$

d_{lim} :limiting bubble size at frother concentration>> CCC

$C_{frother}$: Frother concentration in solution

A,B : fitted parameters describing shape of exponential decay relationship

Hence by knowing this relationship, the Sauter mean bubble diameter can be predicted if the frother concentration is known and vice versa. The Sauter mean bubble diameter is used in flotation because it gives a bubble size that corresponds to the average bubble surface area and volume which are important to flotation.

2.4.6 Effect of Salts on Bubble Size

In addition to the effect of frothers on bubble size, it has been shown that dissolved salts also affect bubble size. This is important because process plants typically recycle the process water which contains dissolved salts. Quin et al. (2007) tested the effect of different salts which are common in process water of plants on both bubble size and gas hold up in both 2 and 3-phase. In addition, the effects of NaCl on bubble size, gas hold up and froth overflow rate was compared to MIBC. Bubble size is strongly related to gas hold up; smaller bubbles rise up at lower rates and hence spend more time in the pulp and hence increase gas hold up (Quinn et al, 2007). Hence an increase in gas hold up can be related to a decrease in bubble size.

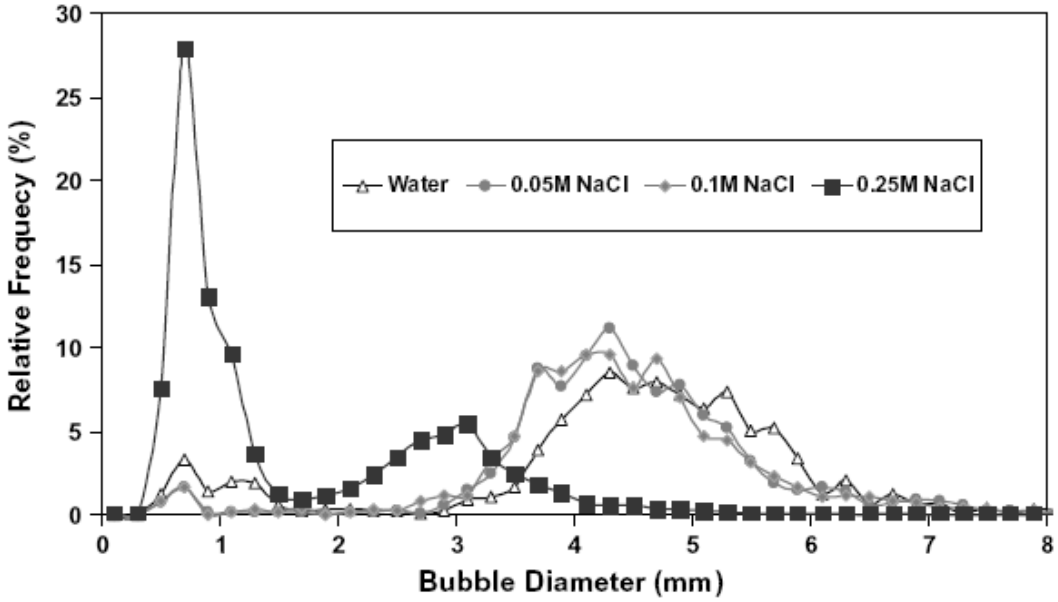

Figure 13: Bubble size distributions with water and different concentrations of NaCl in 2 phase system (Quinn et al, 2007)

Figure 13 shows the bubble size distributions (BSD) obtained for water and different concentrations of NaCl. It can be seen that with water the BSD is wide, but as the NaCl concentration increases the BSD narrows. In addition, for lower NaCl concentrations, the BSD is similar to water but there is a significant difference at 0.25M NaCl, and the effect on reducing bubble size becomes very clear. In addition, the effect of different salts on gas holds up and hence bubble size can be seen in Figure 14. Figure 14 shows for both low and high air rates, that as the molar concentration of each of the salts increases the gas hold up increases and hence bubble size increases. It can also be seen that the different salts have different effects on gas hold up. NaCl seems to have the smallest effect and that as the charge or valence of these salts increase, the greater the effects on gas hold up. However, the ionic strength which takes into account the effect of the charge of the ions in the salt shows that the salts have more or less the same effect on bubble size at the same ionic strength, as shown in Figure 15. This implies that the ionic strength can be used to best describe the combined effect of these salts on bubble size. The effect of ionic strength on flotation performance was investigated by Manono et al, 2012. Batch flotation tests were conducted with synthetic water at different multiples of the ionic strength which is typical of plant process water. It was shown that increasing ionic strength increased both mass and water recovery which is an effect observed with increasing frother dosage

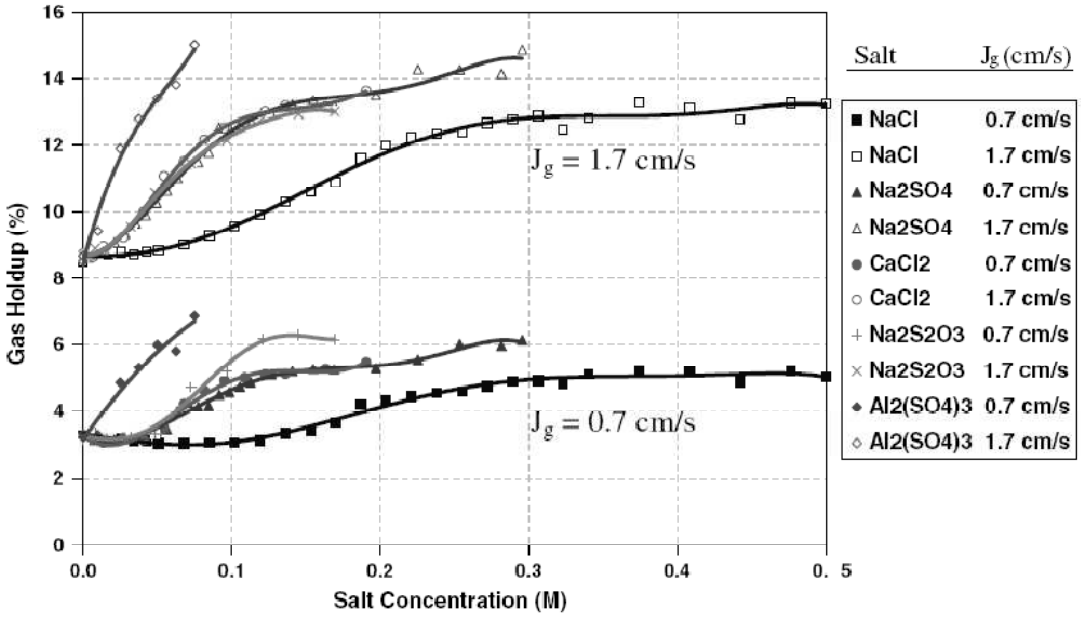

Figure 14: Effect of different salts on gas hold up at different superficial gas velocities (Quinn et al, 2007)

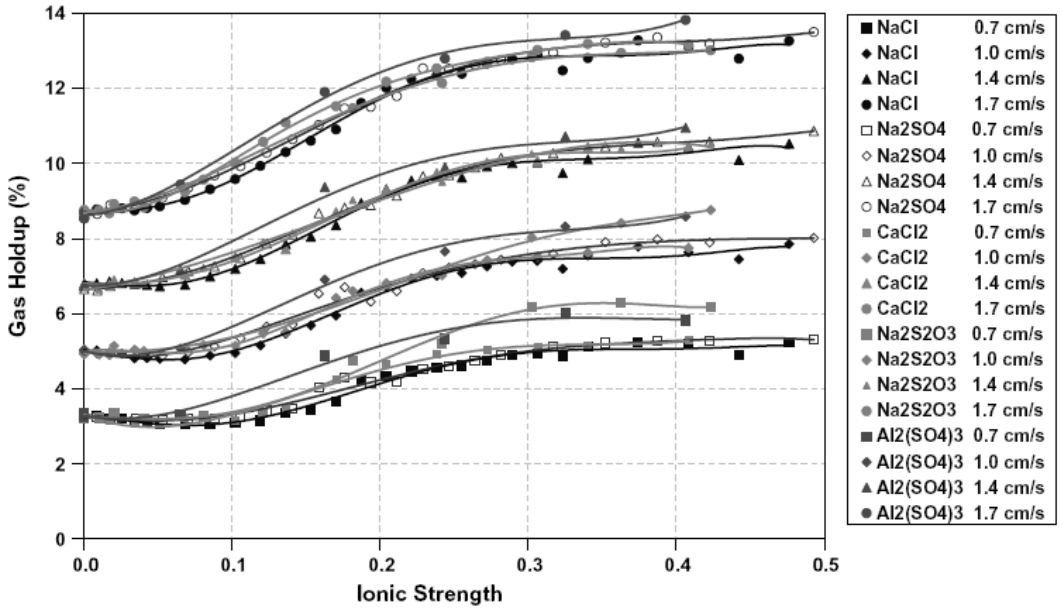

Figure 15: The effects of different salts on gas hold up at different air rates and ionic strengths (Quinn et al, 2007)

Manono et al (2013) measured the effect of ionic strength on bubble size using synthetic process water of different ionic strengths which represent multiples of the strength of typical plant process water as shown in Figure 16. 1SPW, 3SPW, 5SPW, and 10SPW refer to ionic strengths of 0.02, 0.06, 0.1 and 0.19 mol/l respectively, where 1SPW refers to ionic strength of typical plant process water. It can be seen that as the ionic strength increased, the bubble size decreased. It can be seen that compared to the frotherless solution, the 1SPW reduced by bubble size by approximately 0.2 mm and this increased to approximately 0.6mm for the 10SPW.

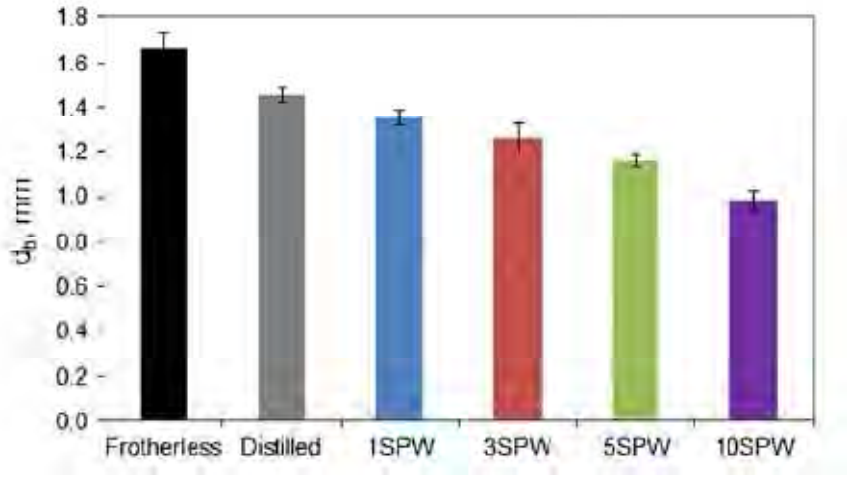

Figure 16: Effect of ionic strength on the sauter mean bubble diameter (Manono et al, 2013)

2.4.7 The importance of bubble size in flotation

Bubble size is an important parameter in PGM flotation. Smaller bubbles are desired to ensure higher probability of particle bubble collisions in the froth. This is due to the stream lines of smaller bubbles that do not hinder the finer particles from making contact. In addition, bubble surface area flux (Sb) is related to the bubble size by the following equation (Gorain et al, 1998):

$$S_b = \frac{6J_g}{d_{32}} \qquad (3)$$

Where: S_b is the bubble surface area flux (m^2/m^2s)

J_g is the superficial gas velocity (m/s)

d_{32} is the Sauter mean bubble size (m)

The bubble surface area flux can also be physically defined as the total surface area of bubbles rising up the cell per unit cross sectional area per unit time (Gorain et al, 1998). Gorain et al. (1997) showed that the flotation rate constant in an industrial flotation cell increases almost linearly with bubble surface area flux. This result was independent of cell impeller type. Hence bubble size plays a very important role in flotation kinetics.

2.4.8 Effect of hydrodynamic parameters on the d_{32}

Gorain et al. (1995) investigated the effects of impeller speed, impeller type and gas rate on the bubble size distribution at different locations in a mechanical cell. The results showed that increasing gas flow rate increased the mean bubble size for all the different impellers running at different speeds. However, the effect of air rate for each impeller was different, implying the different impellers dispersed air differently. In addition, at a constant impeller speed, increasing air rate increased the spread of the bubble size distribution. Furthermore, bubble size distribution varied across the flotation cell and it has been shown that the global average bubble size distribution occurred halfway between the cell rotor and cell wall (Gorain et al, 1995)

Nesset et al. (2007) investigated the effects of hydrodynamic parameters on the d_{32} as well as the effects of frother in a mechanical forced air pilot cell. The effect of frother concentration on the relationship between the d_{32} and the Jg can be seen in Figure 17. This shows that as the frother

concentration increases the almost straight line relationship between d_{32} and Jg shifts downwards. This implied that different concentrations of frother will result in different d_{32} vs. Jg relationships.

Hence for the same frother concentration, an identical impeller type, and speed, measured at exactly the same point, in a bank of cells in series it can be expected that each cell should result in the same relationship between d_{32} and Jg. Furthermore, if this relationship does prove to be true, it can be used to detect if there are problems with cell mechanics as well as if there is enough frother being dosed.

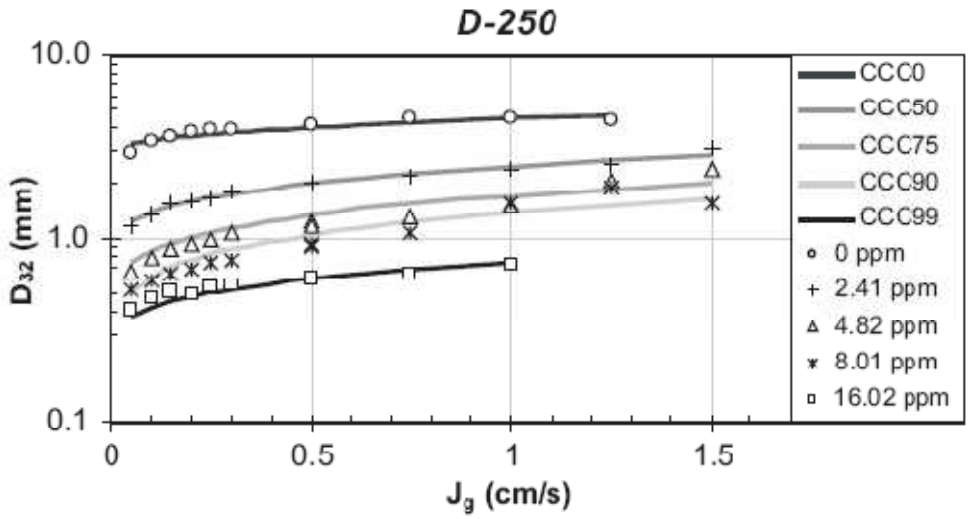

Figure 17: Effect of frother concentration on the relationship between d_{32} and Jg (Nesset et al, 2007)

2.4.9 Bubble size measurement in flotation

This importance of bubble size on flotation performance has prompted the need for measuring bubble size on an industrial scale. Techniques for measuring bubble size have developed and evolved significantly over time. Some of these techniques include: using bubble frequency and total bubble volume in a graduated burette, using conductivity probes, fibre optics, using a tube to suck up a bubble and calculate the bubble size from the equivalent cylindrical volume, using drift flux analysis and using cameras to take photographs and videos (Chen et al, 2001).

Most of these techniques can only be applied on a laboratory scale, which limits the usefulness in full scale industrial flotation plants. The UCT method and the drift flux method have been applied to industrial flotation plants; however they do have drawbacks. The UCT method does not account for bubble segregation during suctioning (Chen et al, 2001); and the drift flux method requires values of the pulp viscosity and density of the particle bubble aggregate, which aren't trivial measurements (Chen et al, 2001).

In addition, measurement of bubble size in industrial scale has been a challenge and the commonly used techniques currently incorporate the use video cameras and image analysis. This has been considered a more credible technique because the photographs of the bubbles consider the entire bubble population (Chen et al, 2001). An early development of such a device was the Bubble Viewer reviewed by Chen et al (2001).

2.4.9.1 Bubble Viewer

Figure 18 is schematic of the Bubble Viewer. The bubble viewer consisted of a viewing chamber attached to a PVC collection tube. Attached to the viewing chamber is a horizontal 2 inch PVC tube which also has a 1 inch PVC socket to allow attachment of the collection tubes. A wire of known diameter is placed diagonally into the viewing chamber at a central plane to allow for focussing of camera and to serve as a reference size for bubble sizing. The bubbles were video recorded; stored

on a video tape on a computer and printed for analysis; and manually determined with an image analysis system (Chen et al, 2001),

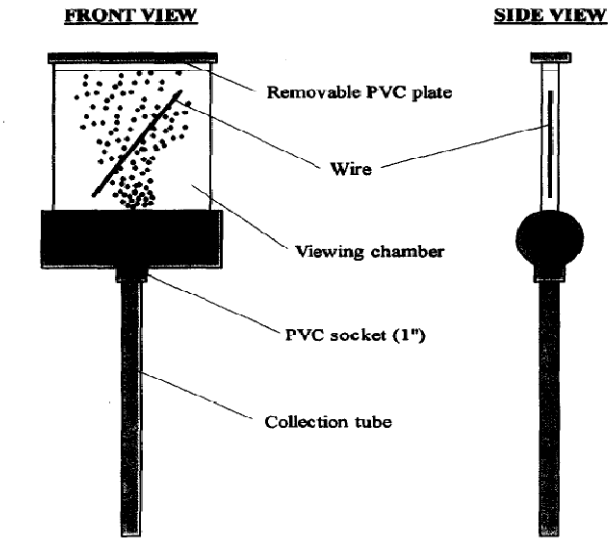

Figure 18: Bubble Viewer schematic (Chen et al, 2001)

The bubble viewer is turned upside down and filled with water together with frother. The camera is then focussed and the bottom of collection tube is blocked with a finger. The sample point on the cell is chosen and the bubble viewer is then quickly turned into its correct vertical position and entered into the cell. Initially large bubbles rise up the collection tube, but a steady flow of bubbles is then achieved. The liquid in the chamber gets cloudy because of bubbles carrying attached particles. There is a 1 minute window for imaging when the liquid remains clear (Chen et al, 2001).

The review indicated that the Bubble Viewer worked well in slurries, and that the device has the potential to be the standard technique for measuring bubble size in industrial flotation cells. There were a few areas of improvement from the device which included: 1) improving the imaging equipment to enlarge bubbles into digitizing images 2) To have an imaging software which automates counting and sizing of bubbles 3) To have illumination in order to increase contrast between bubbles and the background 4) To minimise overlap of bubbles, facilitate cleaning between runs, and to increase the amount of bubbles that stay in focus (Chen et al, 2001)

2.4.9.2 Anglo American Platinum Bubble Sizer

The current device used in practice is the Anglo American Platinum Bubble Sizer. This device has been developed for Anglo American Platinum by Stone Three Technology. It operates on the same principle as the Bubble Viewer but has improved on the shortcomings by design and technological advances.

The unit has the capability of measuring bubble size distributions, superficial gas velocity and suspended solids. It is designed for an industrial scale flotation application. The bubble sizer is a complete unit that is assembled together.

It works by bubbling air through the unit by the displacement of water. The bubbles rise up the collection tubes, enter the viewing pane, and photographs are taken. Frother is added to the water to prevent coalescence in the collection tubes; the amount of frother to be added should be enough to exceed the CCC. There is a water reservoir to allow for a continuous supply of water. In the viewing

pane, there is a white surface with a backlight to allow for the camera to focus. The backlight is powered with a rechargeable battery pack.

The device operates by maintaining an unbroken column of water from deep within the flotation cell. The bubbles rise up the tubes as the water is displaced. The bubbles enter the viewing chamber and with the use of a camera, photographs are taken. The photographs are analysed with image analysing software and the bubble size distribution is determined. In addition, the water reservoir is graduated and the rate at which water is displaced by air can be used to calculate the superficial gas velocity. The device is operated such that a hydraulic pressure correction factor needs to be applied to correct for the pressure difference in the flotation cell and the device. The pressure correction factor (PCF) for bubble size can be defined by equation 4, and for superficial gas velocity it is equation 4:

$$PCF\ (d_{32}) = \sqrt[3]{\frac{P_{atm}+\rho_p g H_p(1-\epsilon_g)-\rho_w g H_w(1-\epsilon_g)}{P_{atm}+\rho_p g H_p(1-\epsilon_g)}}$$

$$PCF\ (Jg) = \frac{P_{atm}+\rho_p g H_p(1-\epsilon_g)-\rho_w g H_w(1-\epsilon_g)}{P_{atm}+\rho_p g H_p(1-\epsilon_g)} \qquad (4)$$

P_{atm} - Atmosphere pressure (kg/m s^2)
ρ_p - pulp density excluding bubbles (kg/m^3)
ρ_w - water density (kg/m^3)
H_p - distance from the pulp surface to the end of J_g probe (m)
H_w - distance from the end measuring mark to the end of J_g probe (m)
g - gravitational factor (m/s^2)
ϵ_g - gas hold-up, which is assumed to be the same inside the probe and in the pulp
J_g - superficial gas velocity in the flotation cell

The parameters H_p and H_w used in equation 4 are measured when the AAPBS is mounted on the flotation cell as is shown on Figure 19. The physical measurements made are the froth depth and the distance from the top of the froth to the union joint. By using these measurements and the dimensions of the AAPBS, H_p and H_w can be determined. There is a difference in pressure between the point at which the bubbles enter the bubble riser tube in the slurry and where measurements are made. Since the measurements made need to represent conditions in the slurry or at the point at which the bubbles enter the bubble riser tube, there needs to be a pressure correction applied. The corrected superificial gas velocity and bubble size can be calculated by multiplying the actual measured made using the AAPBS, and the pressure correction factor. Furthermore the minimum distance of the end of the collection tube should be 30cm below the pulp-froth interface and 30cm above the stator which is shown in Figure 19. This is done to ensure measurements are made in the quiescent zone of the pulp.

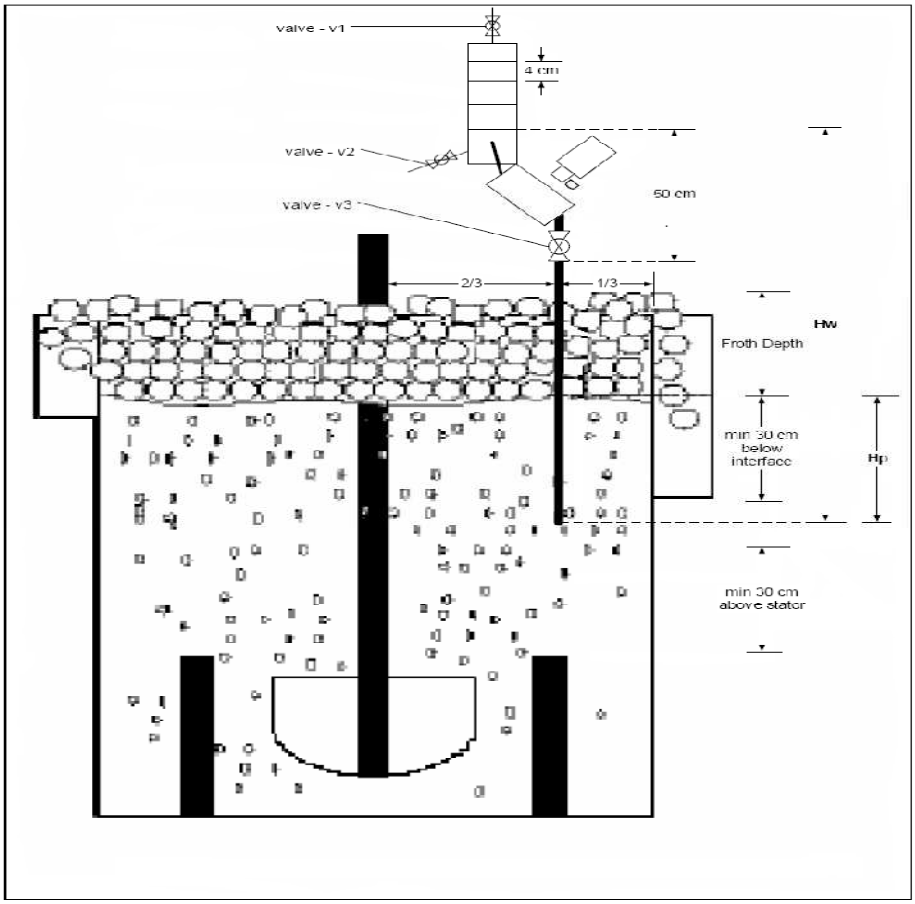

Figure 19: Figure showing positioning of Anglo American Platinum Bubble Sizer (adapted from Anglo American Platinum Bubble Sizer user manual)

Bubble size distribution varies across the flotation cell as shown by Gorain et al (1995). However, it has been shown that the global average bubble size distribution occurred halfway between the cell rotor and cell wall (Gorain et al, 1995). Hence measurements will be carried out in this position of the flotation cell.

2.4.10 Measuring frother concentration in solution

Frother is active in flotation in trace quantities and hence it is used in trace quantities on industrial scale plants. It is critically important that frother is dosed above the CCC to ensure as small bubbles as possible for rapid kinetics and sufficient froth stability. However, determining frother dosage is both a technical decision and an economic one. Overdosing frother to ensure it is above the CCC can also be detrimental in resulting in a very stable froth that doesn't break up easily in the launders, which makes transporting the concentrate difficult. This results in unnecessary spillage, plant instability and excessive reagent costs. In addition, frother overdosage will result in increased entrainment and reduced grade. Hence it is important to dose frother correctly. However in order to decide on a dosage, it is necessary to be able to measure frother concentrations in process streams.

The measurement of frother concentration in process streams hasn't been an easy task over the years. 'For the one hundred years of flotation there has been no convenient, on-site method of determining frother concentration' (Finch *et al*., 2006). This still remains a challenge since flotation reagents are predominantly organic compounds, hence using direct carbon analytical techniques can be challenging. More so, frother is typically used in trace quantities in a plant (measured in ppm)

which also makes measurement difficult. However, there has been a series of techniques that have been tested for measuring frother concentration which include the following:

1) A measurement of the non-adsorbed frother in a laboratory flotation cell by using a total organic carbon analyser (Hadler et al, 2005)
2) The use of gas chromatography to measure frother in industrial scale rougher/scavenger circuits (Tsathouhas et al, 2005)
3) The use of a colorimetric technique to determine the amount of frother in slurries at various industrial sites (Gelinas and Finch, 2007)
4) A non-analytical method by correlating gas hold up with the known CCC (Weber et al, 2003)

2.4.10.1 Total Organic Carbon

Hadler et al. (2005) used a total organic carbon analyser and a UV spectrophotometer to measure the concentration of frother and collector in water in a laboratory flotation cell. The ore and water were analysed with the TOC to measure the amount of carbon present. The UV spectrometry gave an indication of the amount of SIBX present with a known absorbance peak at 310nm. In addition, because SIBX is known to decompose, known solutions of SIBX and water were calibrated with the TOC analyser. Thus, by using the UV spectrophotometer and the TOC analyser, the amount of frother present could be determined. The results showed that a portion of the frother added is adsorbed onto the solids with the addition of SIBX, and the bulk of the frother remains in the pulp phase over time.

2.4.10.2 Gas chromatography

Tsatouhas et al. (2005) used gas chromatography with flame ionisation detection to measure the frother concentration in process streams of two sulphide mineral concentrators. This included a circuit treating copper (circuit A) and another treating copper-lead-zinc (circuit B). Two different frothers were used on circuit A and B which were a mixture of low molecular weight alcohols, aldehydes and esters (circuit A) as well as a triethoxybutane and alcohol mixture and MIBC (circuit B). The measurements involved sampling the feed, concentrates and the tails in both circuits. In addition, flow rates and percentage solids measurements were taken to determine the water flows. The samples were filtered and the aqueous solutions were analysed for frother with gas chromatography. A mass balance was then performed for frother with the water flows and the analytical concentration of frother, obtained from the gas chromatography. The results obtained can be seen in Figure 20.

The results showed that approximately only 4% of the frother leaves in the concentrates, and the bulk of the frother remains in the bulk slurry stream. It was also observed that the frother recoveries to the concentrates were very similar to the water recoveries to the concentrates. Hence reinforcing the notion that frother follows the water stream. In addition, the measurements of the recycled water coming from the tailings thickener as shown in Figure 20 shows that the frother does decompose over time and a smaller amount does recycle back into the plant. However, it is important to quantify this amount of frother returning in the process water as it will affect how much of frother should be dosed in the plant. Overdosing frother is not only expensive but also affects operation of the plant by excessive froth stability. The froth does not break up in the launders and pumping of the concentrate become difficult.

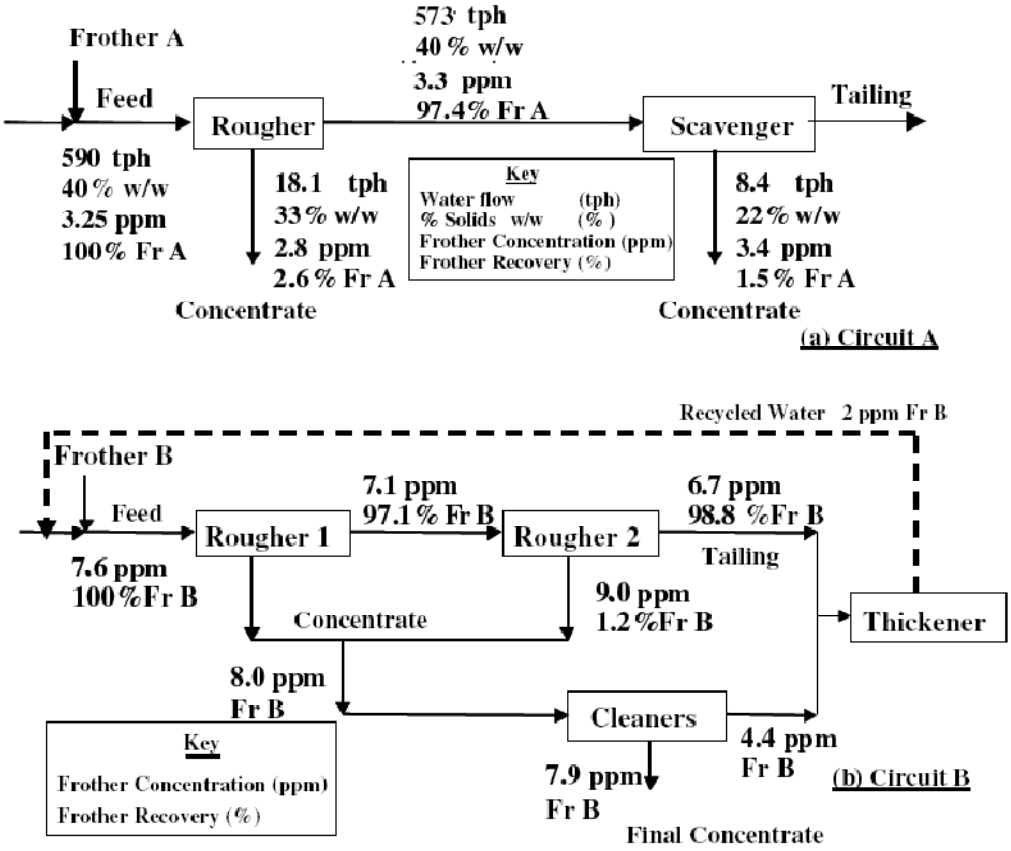

Figure 20: Mass Balance for frother conducted on circuit A and B (Tsotouhas et al, 2006)

2.4.10.3 Colorimetric Technique

The colorimetric technique described by Gelinas and Finch, 2007 uses the Kamarowsky reaction which was originally designed to test methyl isobutyl carbinol (MIBC). This technique was extended to measure other industrial scale frothers, which include MIBC and a polyglycol frother. This technique has been applied to a series of industrial scale circuits. The technique consists of a series of rigorous preparation steps which include: 1) A sample preparation step 2) Reaction step and 3) UV-visible analysis (Gelinas and Finch, 2007).

In the sample preparation step, standards are made with 0.05-0.2 mg of frother per 100 g of water. Similarly process stream samples are decanted and diluted based on estimates of the frother concentration. These samples are then neutralised with dilute sulphuric acid added dropwise to get the pH between 6.5 and 7. Then 20g of sodium chloride per 100ml of water is added to prevent foaming. Then the samples are added to a 250ml separating funnel and two extractions are carried out with 10ml of chloroform. The sample is then rigorously mixed for 2 minutes and the aqueous phase is removed. The bottom phase (organic) is then added to a 50ml separating funnel. Then 10ml of sulphuric acid of concentration 3:1 in water is added and then shaken for 2 minutes. The bottom layer is then transferred to a 25ml sealed vial (Gelinas and Finch, 2007).

In the reaction step, 0.1 ml of 5% salicylaldehyde in a 1:1 solution of acetic acid and water is added to initiate the reaction. The samples are then added into a bath of boiling water and the reaction is stopped after 20 minutes exactly. Then the samples are placed in ice water and only used when doing the colorimetric analysis (Gelinas and Finch, 2007).

Once the sample has reached room temperature, it is removed and added into a 1 ml cell for colorimetric analysis. The UV-visible spectrometer is then used to scan the absorbance spectra. Water is used as a reference (Gelinas and Finch, 2007).

This technique was applied to a rougher/scavenger bank shown in Figure 21. A polyglycol frother was tested and the results showed that the bulk of the frother remained in the tails stream. In addition, the frother concentration in the concentrate streams was similar to the bulk slurry stream.

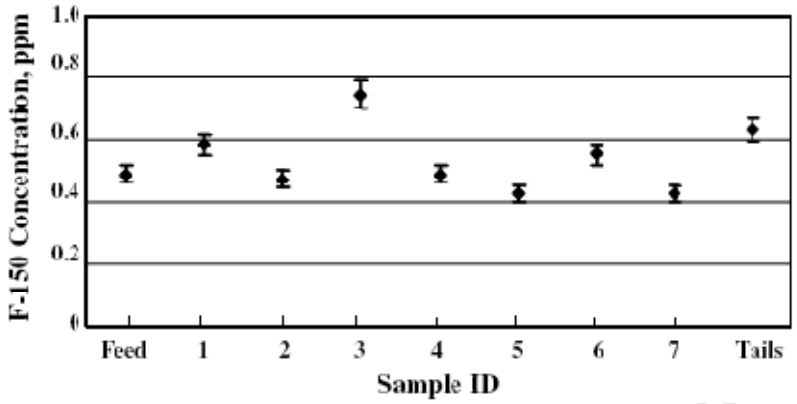

Figure 21: Frother concentration measured with colorimetric technique on a rougher/scavenger bank (Gelinas and Finch, 2007)

2.4.10.4 Correlation of gas hold up with frother concentration

Weber et al. (2003) proposed the use of a “frother concentration meter”. The meter uses the effect of frother on gas hold up to estimate frother concentrations in process streams in a plant. The meter consists of a column of height and diameter 1.6 and 0.12 m, respectively. Air enters into the column via a porous sparger and manometers are used to measure gas hold up.

Known concentrations of frother in water are added to the column at a chosen gas rate and the gas hold up is measured for each concentration. A calibration of frother concentration and gas hold up is generated. A sample of the pulp from a flotation cell is then taken; the water is decanted and added into the column. The gas hold up is then measured and translated into an estimated frother concentration (Weber et al, 2003).

3. Key Questions

3.1 Measuring the CCC with the Anglo American Platinum Bubble Sizer

Can the Anglo American Bubble Sizer (AAPBS) be used to estimate the critical coalescence concentration of frothers on a full scale plant?

3.2 Comparison with literature

How does the measurement of the CCC using the AAPBS compare to measurements and relationships obtained in literature?

3.3 Repeatability and Reproducibility

How repeatable is the measurement and can it be reproduced at different plants using the same frother?

3.4 Estimating frother concentration

Can the technique using the AAPBS be used to estimate frother concentrations in process streams?

3.5 Frother Balance

Can this technique be used to perform a mass balance of frother in a flotation bank and how does this compare to measurements made in literature with other analytical methods of frother concentration measurements?

3.6 Effect of dissolved ions in process water

What effect will the dissolved solids in process water have on reducing bubble size and hence affecting the estimate of frother concentration using the AAPBS?

3.7 Deciding on frother dosages

Can this technique be used for deciding downstream frother dosages and what is the resultant effect on bubble size and flotation performance?

Can the relationship between bubble size and superficial gas velocity in a bank of cells be used as a diagnostic tool to check if enough frother is being dosed?

4. Hypotheses

a. If the critical coalescence concentration can be measured using the AAPBS, then a typical exponential decay curve will be generated in the form, $d_{32} = d_{\lim} + Ae^{-BC_{frother}}$
b. This technique can be extended to estimate the concentration of frother in process streams because the bubble size in the process stream is related to the frother concentration according to the above equation.
c. A frother balance on a flotation bank will indicate that polyglycol type frothers follow the water stream, and that the bulk of the frother remains in the bulk water stream because polyglycol frothers are extremely water soluble.
d. The relationship between superficial gas velocity and bubble size in a bank containing identical flotation cells can be used to check if frother concentration changes down the bank because this relationship is constant for similar bubble generation mechanisms, impeller speeds and frother dosages.

5 Experimental Program

5.1 Investigate techniques to determine the relationship between bubble size and frother concentration on a full scale flotation plant.

The aim of these experiments is to determine a simple and robust technique for measuring the relationship between bubble size and frother concentration which is practical and can be applied in a full scale flotation plant. This technique should produce results which are in agreement with extensive tests performed in literature (Cho and Laskowski, 2002; Finch et al, 2008; Nesset et al, 2006; Nesset et al, 2007; Grau et al, 2005).

Two different techniques for measuring the effect of frother concentration on bubble size will be investigated on a full scale plant. The results obtained from the application of these techniques will be compared to each other and to results obtained in literature. If one of the techniques proves to be successful, it will be tested for different frothers on different plants and on different flotation cells for reproducibility and repeatability. Hence the robustness of the technique will be investigated.

5.2 Investigate a technique to estimate frother concentration in process streams on a full scale flotation plant.

The aim of these experiments is to determine a simple and robust technique for estimating frother concentration in process streams which can be applied in a full scale flotation plant. The results obtained from applying the technique will be compared to results obtained in literature using alternative methods (Gelinas and Finch, 2007; Tsatouhas et al, 2005; Hadler et al. 2005; Weber et al, 2003). Furthermore, this technique will be applied to a rougher bank in two UG2 concentrators, namely Plant B UG2 concentrator and Plant C UG2 concentrator, using the same frother which is Sasfroth 200. Frother Balances will be performed over the rougher banks with the equivalent frother concentration measurements made on process streams in the rougher bank. It is known that ions in solution also affect bubble size but this is only significant at high enough ion concentrations or ionic strength. Hence the process stream aqueous solution ionic strength will be compared with that of literature to determine whether it would significantly affect bubble size and the equivalent frother concentration estimate.

5.3 Investigate the relationship between the Sauter mean bubble diameter and superficial gas velocity in a bank of identical flotation cells in series, and its application in determining frother depletion.

The aim of these experiments is to investigate whether the relationship between the Sauter mean bubble diameter and superficial gas velocity in a flotation bank of identical cells in series is identical for every cell provided the concentration of frother is above the CCC. This will be investigated in the secondary and scavenger cleaner flotation banks at Plant D concentrator.

This relationship will be investigated in a bank that is being fed with sufficient frother. This relationship will then be investigated to detect depletion of frother in a bank that has poor froth structure. The flotation performance of this bank will then be evaluated before and after the addition of frother.

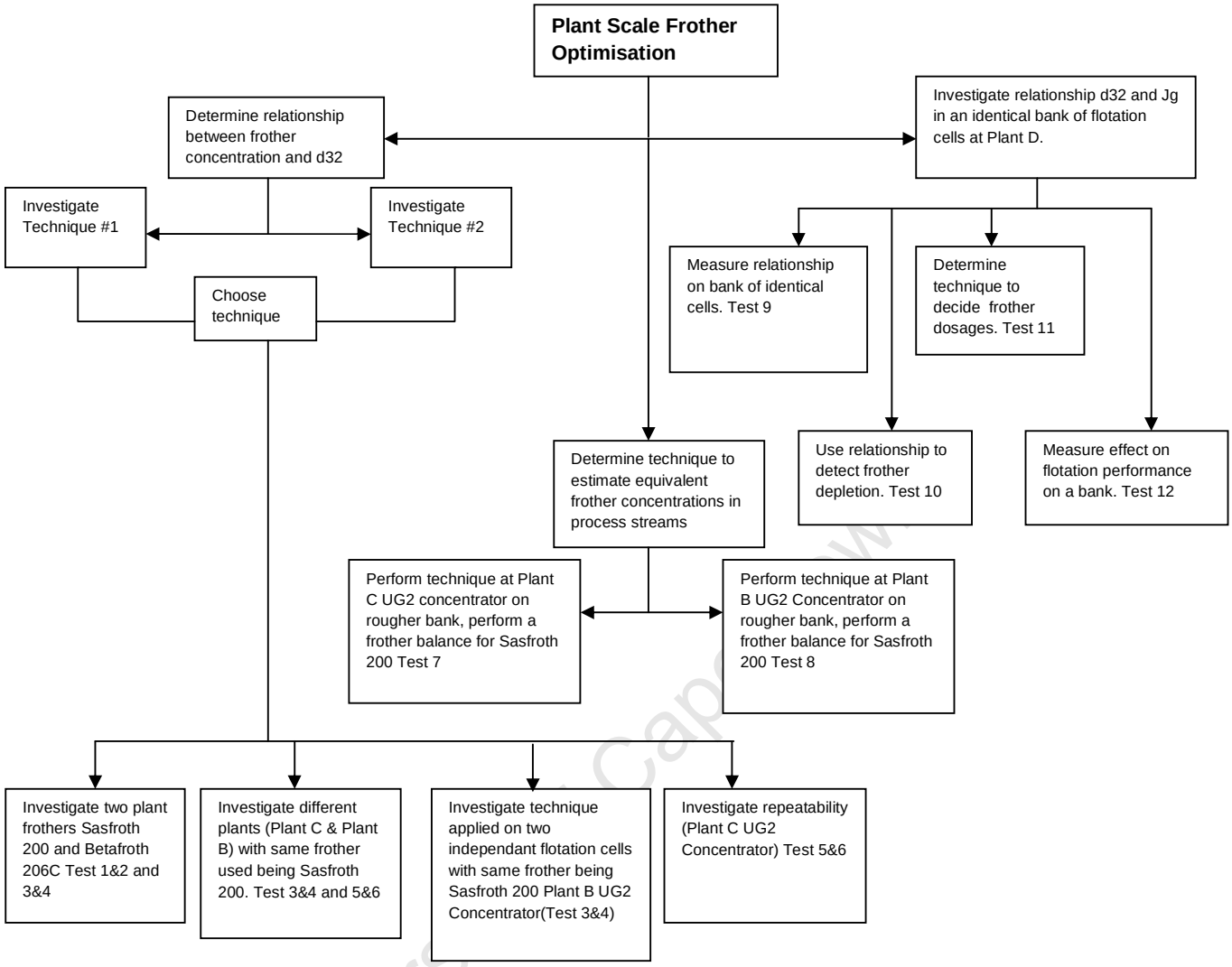

Figure 22: Diagram showing the experimental program

5.4 Experimental Procedure

5.4.1 Using the Anglo American Platinum Bubble Sizer

The Anglo American Platinum Bubble Sizer (AAPBS) was supplied by Stone Three Technology and details regarding assembly are provided in the instruction manual provided by Stone Three. Once assembled, the AAPBS can be mounted on the mentis grating of the flotation cell or on the hand railing around the cell as shown in Figure 23. There are 3 three collection tubes available to the AAPBS which are each 1 metre in length. These are screwed together and air-sealed using o-rings. Depending on the size of the flotation cell 2 or 3 tubes can be used for smaller and larger cells respectively. The collection tubes are then attached to the union joint of the mounted bubble sizer and air sealed with an o-ring. The battery pack is then inserted and connected to the backlight. The digital camera is then adjusted with the brightness, shutter speed and resolution as specified by Stone Three. The camera is then inserted into the camera housing, and the AAPBS is ready for use. Stability of the plant in terms of density and flow entering the cell is important because density affects superficial gas velocity and bubble size, and flow affects froth depth. However, density is a more

important variable than flow. Once the plant is stable with regards to density, measurements can be taken.

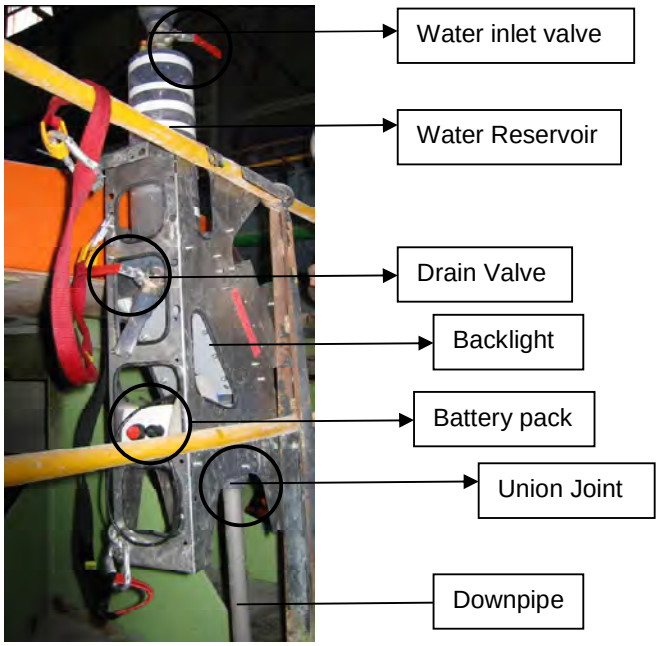

(a) Handrail (b) Mentis Grating

Figure 23: AAPBS mounting options

During a typical superficial gas velocity and bubble size measurement, process water or potable water is dosed with enough frother to surpass the CCC. The drain valve and the valve at the union joint must be closed. This water is then filled into the water reservoir by opening the water inlet valve until it is completely full. The valve at the union joint is then opened, and water will drain into the collection tube whilst air enters the water reservoir. Once there is an unbroken column of water and air in the collection tube, the valve at the union joint is closed and the water reservoir is topped up. The valve at the union joint is then opened. Once there is an unbroken column of water and air rising up the tubes into the water reservoir; measurements can be taken. The air rising up the tubes displaces the water in the reservoir which will indicate the air flow rate. Digital photos are taken for bubble size analysis. The bubbles do not coalesce in the AAPBS because of the frother addition.

There are several measurements that need to be taken which include:

1) Time taken for the air to displace 0.5 litres of water

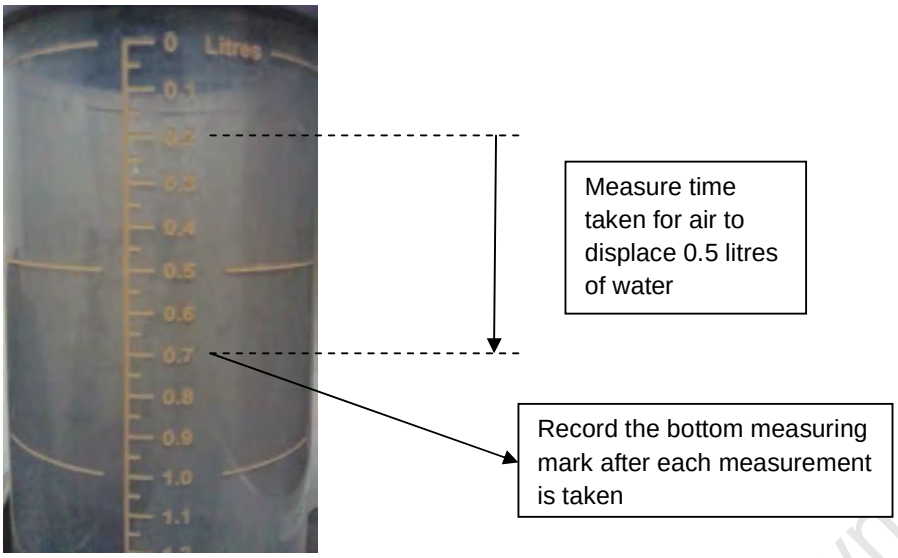

Figure 24: Measuring marks on water reservoir on the AAPB

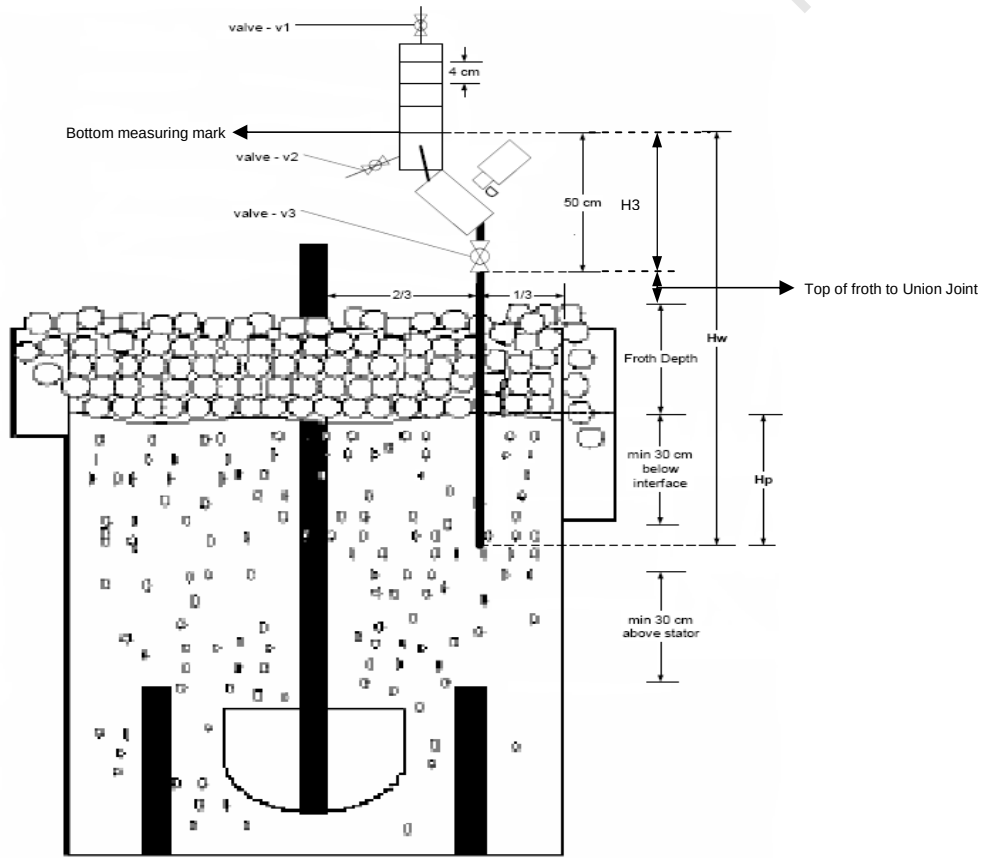

Figure 25: Schematic of AAPBS on flotation cell showing measurements

2) The froth depth was taken with a manual float and measuring tape (Figure 26)

Figure 26: Manual float used in flotation cell

Figure 27: Measuring the froth depth

3) The distance from top of the froth to the union joint was taken with a measuring tape.

Figure 28: Measuring the top of froth to union joint

The bottom measuring mark, the froth depth and the distance from the top of froth to the union joint are measurements used to calculate the pulp height (Hp) and the height of water (Hw) as shown in Figure 25. This was used to calculate the pressure correction factor to account for the differences in hydrostatic head between the bottom of the collection tube and the water reservoir where measurements are made.

For bubble size measurement, the viewing pane was labelled according to the flotation cell name or test being carried out. The camera settings were set according to the AAPBS user manual. The backlight and camera was then turned on and bubble size photos were taken.

Figure 29: Viewing pane of AAPBS

The number of photographs taken depends on the number of bubbles. It was found that 10 photographs would suffice for small bubble sizes and typically 20 photographs for bigger bubble sizes. The photographs were analysed using image analysis software provided by Stone Three.

5.4.2 Determining the relationship between bubble size and frother concentration

The aim of these experiments was to investigate a methodology for establishing the relationship between bubble size and the concentration of frother in an industrial scale flotation plant. There were two techniques that were investigated:

1) The first technique involved adjusting the frother dosage rate into the first rougher cell to target different frother concentrations in the cell and then measuring bubble size at each of the frother concentrations.

2) The second technique involved depleting frother from the first rougher cell; adding known concentrations of frother into the APBS water reservoir and then measuring bubble size at each of these different frother concentrations whilst keeping the air rate constant.

The first rougher cell receives the flotation circuit feed, which is typically depleted of frother. Hence it is the most suitable cell to control frother concentration and hence the most suitable to perform the investigation. Furthermore, tank cells are preferred because of the difficulty in installing the AAPBS

into Wemco cells and Column cells because of their design as well because of better control of air rate in a tank cell.

5.4.2.1 Technique 1: Controlling frother dosage to a cell and measuring bubble size

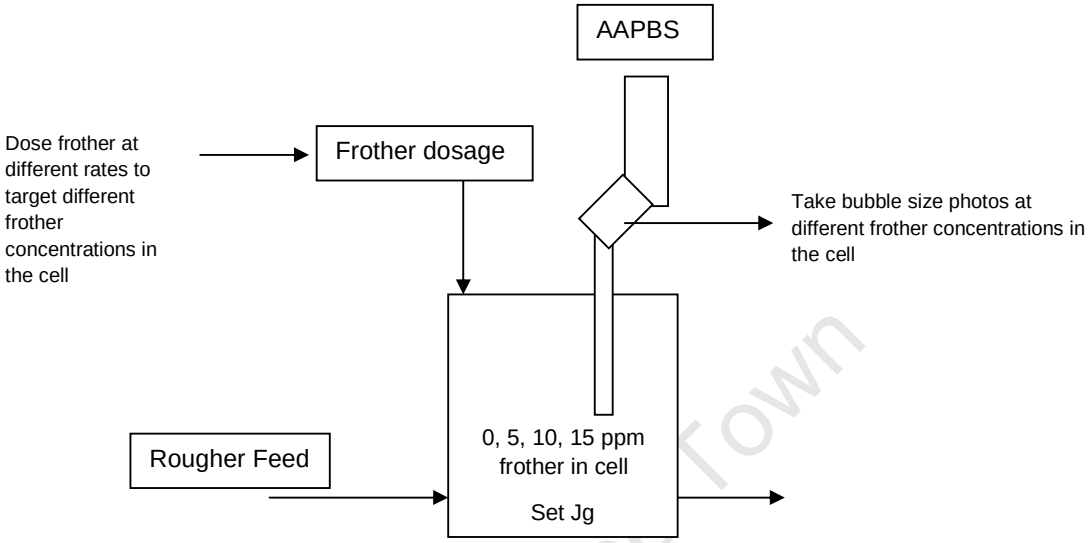

Figure 30: Diagram illustrating experimental set up for using Technique #1 on the first rougher cell

Figure 30 indicates the experimental set up for investigating technique #1. The frother dosage line was on the first rougher cell and was the plant dosage point under normal operation. The first step was calculating the water flow rate in the rougher feed. This was done was using the rougher feed density and the ore feed rate into the circuit. The rougher feed density was used to calculate the percentage solids and the ore feed rate was used to calculate the water flow rate in the rougher feed. The ore feed rate was preferred to the volumetric flow rate in the rougher feed because it is typically a more accurate measurement because it is used for metal accounting purposes.

A reasonable assumption was that the residual frother concentration in the plant water was negligible. The frother dosage rate into the cell was then determined by multiplying the water flow rate into the cell with the test frother concentrations. The test frother concentrations were 0, 5, 10 and 15 ppm. The air rate in the cell was measured and maintained at a constant value for all the tests. For each test, the frother dosage rate was set and the cell was given 30 minutes or 3 cell residence times for the concentration to stabilise in the cell. Thereafter, the AAPBS was set up and bubble size photos were taken. Superficial gas velocity measurements were also taken for each test to check for air rate consistency between tests. The bubble size photos were analysed to calculate the average Sauter mean bubble diameter at each frother concentration tested. A graph of Sauter mean bubble diameter and frother concentration was then plotted.

5.4.2.2 Technique 2: Adding known concentrations of frother to the AAPBS

The aim of these experiments was to investigate a novel technique to determine the relationship between bubble size and frother concentration. Figure 31 shows the experimental set up and procedure for technique 2. It should be noted that this was performed while the plant was in operation. The first step was to deplete the first rougher cell of frother and this was done by bypassing the frother dosage line into the second rougher cell. This allows the first rougher cell to be isolated and

minimises disturbance to the rest of the rougher bank. The first rougher cell was given 30 minutes or 3 cell residence times for the frother to flush out of the cell.

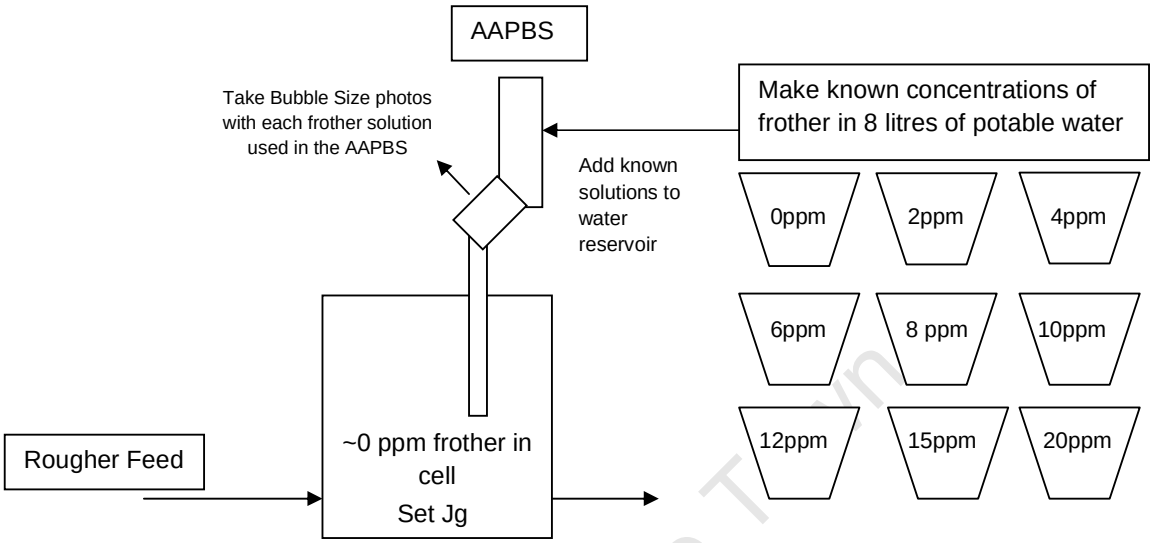

Figure 31: Diagram indicating the experimental set up for using Technique #2 on the first rougher cell

The next step was to make up known concentrations of frother in potable water. This was done by taking a sample of the freshly mixed frother used in the plant at the time. The strength or concentration of the frother in the plant is measured shiftly by the plant personnel using a calibration of frother concentration and refractive index. The refractive index of the frother sample was measured with a refractometer which is shown in Figure 32.

The known concentrations of frother were selected based on the type of frother used and its typical estimate of the CCC in literature. The decay portion of the bubble size vs. frother concentration relationship needs to be well defined in order to fit the exponential decay relationship and to accurately determine the CCC. For example, a polyglycol frother of molecular weight of approximately 200 is typically a strong frother with a CCC in the region of 10 to 15 ppm (Chow and Laskowksi, 2002; Finch et al, 2008; Capucciti and Finch, 2008). Hence a typical range of frother concentrations would be 0, 2, 4, 6, 8, 10, 12, 15, 20, 30, 40 ppm. If the CCC appears to be much higher, then this range can be adapted accordingly.

A sample of the freshly mixed frother on the plant was taken and the strength was measured using a refractometer. By using a calibration curve of refractive index and frother concentration; the frother concentration in the sample taken was measured.

Figure 32: Refractometer used for measuring frother concentration

The volume of frother solution was 8 litres because this is the amount needed to carry out measurement on the AAPBS. This was made up using graduated measuring cylinders shown in Figure 33.

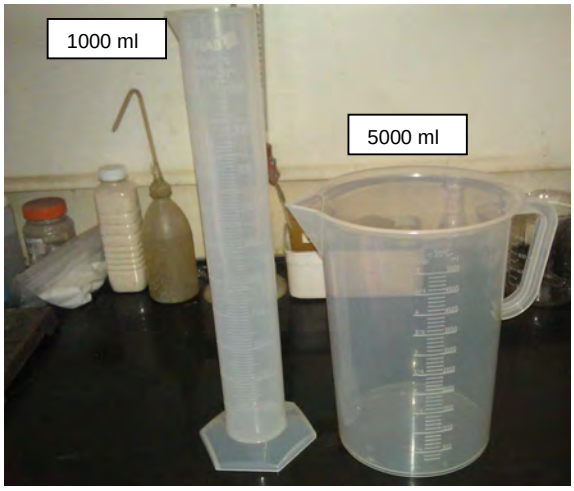

Using a 5 litre and a 1 litre graduated measuring cylinder, 8 litre water aliquots were made in buckets using potable water.

Figure 33: Graduated measuring cylinders used to make up 8 litres of potable water

The concentrations in each bucket were made up by calculating the mass of frother that should be added to 8 litres of water to make up the targeted frother concentrations. Thereafter the volume of frother required was then calculated by dividing the mass of frother required by the concentration of the frother in the sample taken. The volumes of frother required from the frother sample to make up the concentrations in 8 litres of water are small; hence small graduated syringes were used for better accuracy. Figure 34 shows the 1 ml, 2ml and 10ml graduated syringes that were used for making up the frother concentrations.

Graduated syringes were used to measure the frother sample taken as described above. These syringes were also used to make up the frother solutions used in the tests. Three different syringe sizes were used to ensure accuracy of frother addition.

Figure 34: Graduated syringes used for dilution of the frother sample and to make up frother solutions for tests

In some cases the volumes of frother required were too low to be accurately dosed with the syringes. This required further dilution of the frother sample and was done using potable water and measuring cylinders shown in Figure 35.

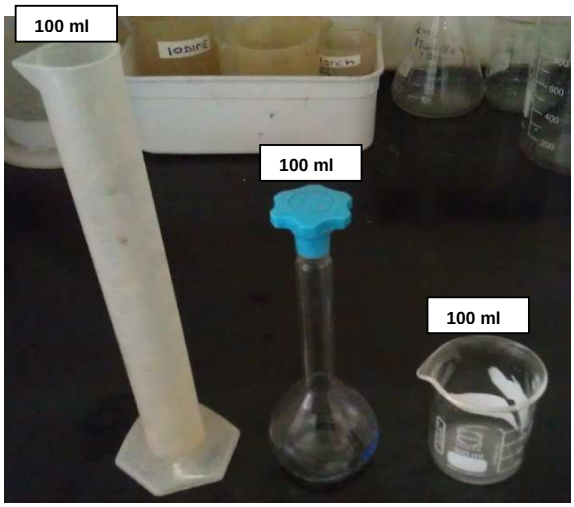

Depending on the concentration of the frother sample, it may require dilution with potable water. This is because the concentrations being tested are very small and when the sample concentration is too high, very small volumes of the sample will be required and this causes measurement inaccuracy.

Figure 35: Pictures of the beaker, measuring cylinder and volumetric flask used for diluting the frother sample

Each known solution was added into the AAPBS and bubble size photos were taken. The operating mechanism of the technique is as follows: Bubbles are generated at the cell rotor in the cell. These bubbles can be assumed to be at a fixed bubble size distribution due to the fixed position of the bubble riser tube in the cell. The bubble riser tube is 3 metres in length and 25 mm in diameter. The long and narrow nature of the tube associates the system to be similar to plug flow. Similarly turbulence and eddies created by the bubbles rising up the tubes also improve the mixing system. As these bubbles pass through the solutions at different concentrations of frother; the bubbles will coalesce to different degrees as is known to occur in literature, and the resultant bubble size distributions will be measured by taking camera images at the viewing pane of the AAPBS. The air rate in the cell was kept constant throughout the measurements. The bubble size photos were then analysed and the average sauter mean bubble diameter was determined for each condition. A graph of sauter mean bubble diameter and frother concentration was then plotted.

5.4.3 Measuring an equivalent frother concentration (EFC) in process streams and performing a frother balance

The aim of these experiments was to determine a methodology to estimate frother concentrations in the process streams of a plant. This estimate of frother concentration was based on comparing the effect of the process stream solution on Sauter mean bubble size compared to a known frother solution. In effect, using the CCC curve generated in 5.4.2 as a calibration curve. Furthermore, this data was used to perform a mass balance for frother across a flotation bank.

The first step in the procedure was to determine the relationship between frother concentration and bubble size for the frother used on the plant. This was done by following the procedure described in 5.4.2.2. The next step was to perform a survey of a flotation bank and it was decided to use the rougher bank. The survey was carried out over at least an hour with five sampling increments.

In the case of water soluble polyglycol frothers, which are used for PGM flotation it can be assumed that the bulk of the frother remains in the water component of the process stream (Gelinas and Finch, 2007; Tsatouhas et al, 2005; Hadler et al. 2005). Hence a water balance across the circuit was required to perform a frother balance. The survey involved sampling of the feed, concentrates and tails. In addition, mass flow rates of each of concentrate streams were taken. The volume of sample taken was enough to perform bubble size measurements using the AAPBS.

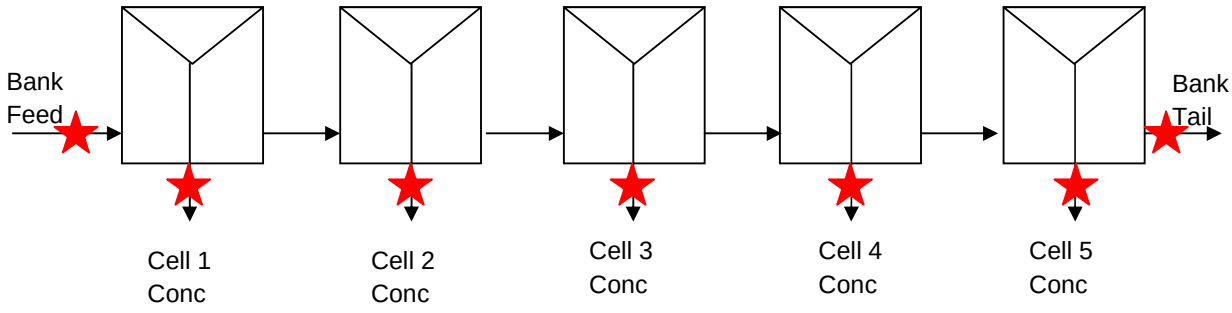

Figure 36: Sampling points indicated on a typical rougher bank

After the survey, wet masses of the samples were taken. The samples were then filtered and care was taken to ensure that the filtrate from each sample was not contaminated with wash water. Hence the filtrate from each sample was used as wash water for the same sample. The filtrate for each sample was then labelled and stored in buckets.

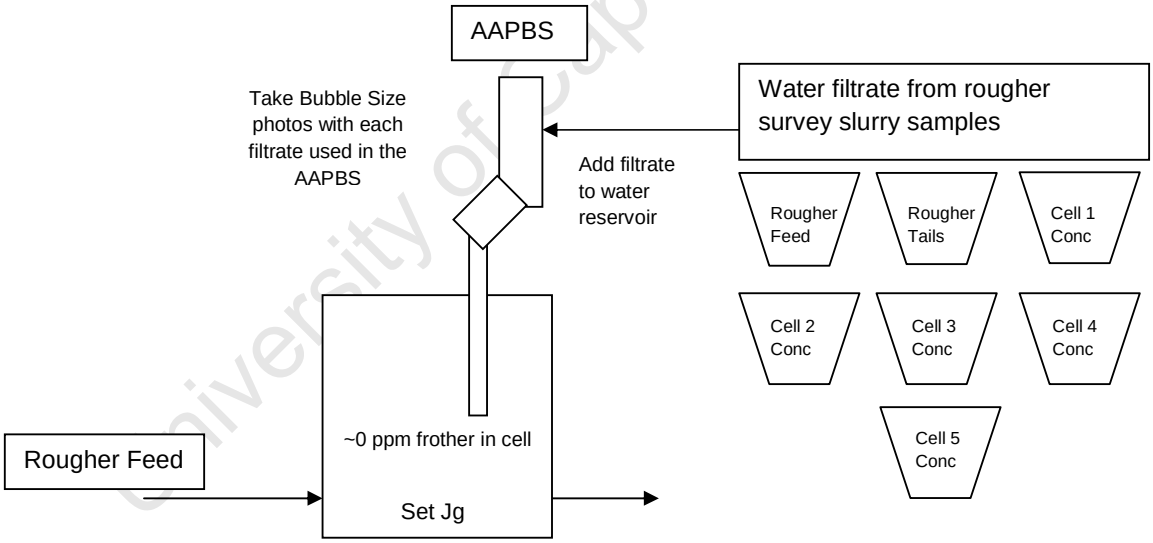

Figure 37: Experimental Setup on first rougher cell for measuring bubble size using process stream water samples

The bubble size of each filtrate was measured using the AAPBS according to the method described in 5.4.2.2. The procedure in 5.4.2.2 takes known solutions of frother and measures the effect on bubble size. In the case of the process stream sample filtrates, the AAPBS was used to determine the bubble size of the process streams as shown in Figure 37. The equivalent frother concentration (EFC) of the process streams was then determined by comparing the effect of the process stream water solutions on bubble size with the effect of the known concentrations of frother on bubble size. The EFC can be defined as the concentration of frother which has the same effect on bubble coalescence as the process stream aqueous solution. This was done using the bubble size measurement from the process stream aqueous solution and the bubble size vs. frother concentration relationship, to find the frother concentration gives the same effect on that bubble size.

However, in order to accurately estimate this equivalent frother concentration, the bubble size measured should be in the decay portion of the bubble size vs. frother concentration relationship. Hence the filtered solutions were diluted with potable water (which had zero frother concentration) before the bubble size was measured. This was because the concentrations of frother in these process streams were already outside the decay portion of the curve. The dilution ratios used were chosen based on an initial guess of the equivalent frother concentration in the stream but the measurements were often repeated if the dilution ratios were too low. The dilution ratios were then multiplied by the measured equivalent frother concentrations to get the actual equivalent frother concentrations.

5.4.4 Determining the relationship between Sauter Mean Bubble Diameter and Superficial Gas Velocity in a bank of identical flotation cells

Three different air rates were chosen for each cell on the plant scada and superficial gas velocity and bubble size measurements were carried out as described in 5.4.1. Graphs of Sauter mean bubble diameter and superficial gas velocity were plotted.

5.4.5 Experimental Error

There were different sources of error for different parts of the experiments. For making up the frother concentrations in solution there is measurement inaccuracy which could affect the bubble size measurement, similarly when measuring the bubble size with the AAPBS there will be error. It can be expected that the largest error would come from instabilities in the plant. However, the errors were estimated using measurement error in the measuring devices like syringes and measuring cylinders. Similarly there was error in bubble size measurement using the AAPBS. The effect of these errors on the measurements was estimated using propagation of error.

Error when making up frother concentrations:

There were four sources of error which included the error in measuring the frother concentration using the refractometer, the error when diluting the frother sample, the error when making up 8 litres of water, and the error when adding frother into the 8 litres of water to make up the frother concentration.

1) Measuring frother concentration in sample:

The error here will be due to the accuracy of the refractometer, the refractometer accuracy is reported by manufacturer as 0.2%. Hence the error in the frother concentration will be calculated based on the relationship between frother concentration (C_f) and refractive index (RI).

If the Cf = f(RI) which was Cf = 12xRI obtained from the plant personnel, then propagation of error onto Cf will be (Napier-Munn, 2010) where δ_i refers to the maximum error in variable i.

$$\delta_{Cf} = \left(\frac{dCf}{dRI}\right) \quad \delta_{RI} \qquad (4)$$

$$\delta_{Cf} = 12 \times 0.2\% * 17 = 0.408\, ppm \qquad (5)$$

Hence for a frother sample concentration of 200 g/l, the % error will be approximately 0.408/200 ~ 0.2%.

2) Diluting the frother concentration:

The error here will be measurement inaccuracy associated with the syringes used to measure the volumes of frother and water required.

For example: to dilute 200 g/l of frother to 50 g/l, this will require adding 25 ml of frother solution to 75 ml of water.

By using an 10 ml syringe to do this, the accuracy of the 10 ml syringe can be taken as the half the division on either side of the smallest unit in the 10 ml syringe which was +/- 0.25 ml.

Adding 25 ml of frother will require 2 and a half syringe fulls which means using the syringe three times, at each time the accuracy is +/- 0.25 ml. Hence the total error will be +/- 0.75 ml. This translates to a relative error of +/- 3%.

Similarly adding 75ml of water will require 7 and a half syringe fulls which translates to an error of +/- 2 ml. The error in the total volume will be 2ml+0.75 ml which is 2.75ml.

Using propagation of error for the diluted concentration, where V_f and Vtot are the volumes of frother and the total volume respectively, and Dc_f is the diluted frother concentration:

$$Dc_f = \frac{Cf \times V_f}{V_{tot}} \quad (6)$$

$$\delta Dc_f = \frac{dDc_f}{dCf} \times \delta Cf + \frac{dDc_f}{dV_f} \times \delta V_f + \frac{dDc_f}{dV_{tot}} \times \delta V_{tot} \quad (7)$$

$$\frac{dDc_f}{dCf} = \frac{V_f}{V_{tot}} \qquad \frac{dDc_f}{dV_f} = \frac{Cf}{V_{tot}} \qquad \frac{dDc_f}{dV_{tot}} = -\frac{Cf \times V_f}{{V_{tot}}^2} \quad (8)$$

Hence the error in measurement of the diluted frother concentration will be:

$$\delta Dc_f = \frac{25}{100} \times 0.2\% * 200 + \frac{200}{100} \times 3\%25 + \frac{-200 \times 25}{100^2} \times 2.75\% * 100 = 0.225 g/l \quad (9)$$

Hence for a diluted frother concentration of 50 g/l, the relative error will be 0.225/50~0.45%.

3) Making up 8 litres of water:

Similarly, using measurement inaccuracy associated with the measuring jugs and cylinders.

To make up 8 litres, one 5 litre jug full and three 1 litre cylinder fulls were used which implies using the jug once and the cylinder three times.

Similarly the accuracy of the 5 litre measuring jug was determined as +/-50 ml and the 1 litre measuring cylinder was determined as +/- 5 ml. Hence for an 8 litre measurement the inaccuracy is 8 litres +/- 65 ml. This gives a relative error of +/- 0.8%.

4) Dosing the diluted frother into the 8 litres of water to make up frother concentration

The error here is similarly due to error in using the syringe, the syringe used was a 1 ml syringe which had an accuracy of +/- 0.005 ml.

For example to make 5 ppm or mg/l of frother in 8 litres of water, this requires 0.8 ml of frother at a concentration of 50 g/l. Dosing 0.8 ml will result in an error of +/- 0.005 ml which is equivalent to a relative error of 0.625%.

Using propagation of error, where V_w and V_{Dcf} are the volumes of the water and diluted frother concentrations respectively, and mC_f is the made up frother concentration, the made up frother concentration can be calculated from:

$$mC_f = \frac{Dc_f \times V_{Dc_f}}{V_w} \quad (10)$$

Similarly, using equations 7, 8, 9 and 10, the propagation of error onto the made up frother concentration was calculated as:

$$\delta Dc_f = \left(\frac{0.8}{8000} \times 0.45\% * 50 + \frac{50}{8000} \times 0.625\% \times 0.8 + \frac{-50 \times 0.8}{8000^2} \times 0.8\% * 8000\right) \times \frac{1000mg}{g} = 0.014mg/l \quad (11)$$

Hence for a frother concentration of 5mg/l or 5 ppm, the error is approximately 0.28%.

Propagation of error when measuring the sauter mean bubble diameter at each frother concentration

The error in making up the frother concentration will result in error in the resulting bubble size measurement. This error can be estimated by using propagation of error, and by using the mathematical relationship between sauter mean bubble diameter and frother concentration described by Comley et al (2002) as shown by equation 1.

Similarly to equation 4, the propagation of error onto the sauter mean bubble diameter can be calculated using equation 1, where A and B is taken to be 2.88 and -0.29 respectively:

$$\frac{d_{d_{32}}}{d_{Cf}} = -2.88 \times 0.29 \times e^{-0.29Cf} \quad (12)$$

$$\delta_{d_{32}} = \frac{d_{d_{32}}}{d_{Cf}} \times \delta C_f \quad (13)$$

It can be seen that $\frac{d_{d_{32}}}{d_{Cf}}$ is dependant on the frother concentration, hence the error in the bubble size measurement will be a maximum at zero frother concentration and a minimum at higher frother concentrations. Hence taking by taking the error at a frother concentration of 5 ppm, the error in measurement of the bubble size will be approximately 0.08mm. At 5 ppm, the bubble size would be 1.77mm and this translates to a relative error of 4.4%. Table 2 shows the error estimates at various frother concentrations. A maximum allowable error of 10% was used to also consider plant instability.

Table 2: Table indicating error estimates in bubble size at different frother concentrations

Frother Concentration, ppm	Bubble Size, mm	Relative error %
20	1.1	0.1
10	1.25	1.5
5	1.77	4.4
2	2.71	6.9

Measuring Bubble Size using the AAPBS

The error associated here investigated was the precision of the bubble size measurement, this was done by taking multiple photos at a given air rate. The variation in bubble size can be attributed to variance in the cell air rate, because the solution used in the AAPBS was mixed and the bubbles rising up in the tubes of AAPBS will also enhance mixing of the solution, hence the solution can be considered to be homogeneous and bubble size variance will not be a result of inadequate mixing of frother in the AAPBS.

The sauter mean bubble diameter was obtained for each photo and the standard deviation of the sauter mean bubble diameter was used as an indication of the precision. Table 3 shows the number of bubbles and sauter mean bubble diameter measured in each photograph taken. The total number of bubbles analysed for all the photographs were 5191. The average sauter mean bubble diameter was approximately 1.78mm with a standard deviation of 0.15mm. If it can be considered that each photo is asample of the population; then there are 18 samples of the population. By using the central limit theorem, this translates to a standard error of approximately 0.03mm. This translates to a relative standard error of ~ 2%.

Table 3: Summary of bubble size measurements at a frother concentration of 6ppm in AAPBS

Photo no.	Number of bubbles	Sauter Mean bubble diameter (mm)
1	312	1.702
2	311	1.716
3	292	1.676
4	277	1.693
5	227	1.858
6	300	1.678
7	274	1.883
8	209	2.184
9	300	1.714
10	282	2.084
11	321	1.619
12	337	1.577
13	283	1.806
14	327	1.813
15	286	1.695
16	278	1.695
17	309	1.743
18	266	1.864
Total	5191	

Using bubble size to estimate an equivalent frother concentration from the relationship between sauter mean bubble diameter and frother concentration.

The error in the bubble size measurement as shown above can be taken to be approximately 2%. Hence there will be error in reading off the frother concentration. The relationship between frother concentration and bubble size can be rewritten using the equation 1 to the form, where A and B are taken be 2.88 and -0.29:

$$C_f = \frac{\ln\left(\frac{d_{32}-1.1}{2.88}\right)}{-0.29} \qquad (14)$$

$$\frac{dC_f}{dd_{32}} = \frac{1}{-0.29}\left(\frac{1}{d_{32}-1.1}\right) \qquad (15)$$

$$\sigma^2_{EFC} = \sqrt{\left(\frac{dC_f}{dd_{32}}\right)^2 \sigma^2_{d_{32}}} \qquad (16)$$

Similarly, $\frac{dC_f}{dd_{32}}$ is dependant on the sauter mean bubble diameter and which will affect the error measurement. As the d_{32} increases, $\frac{dC_f}{dd_{32}}$ decreases and the error decreases. Hence at a d_{32} of 2mm,

the EFC will be 4 ppm and the error in the EFC will be 0.38 ppm which is approximately 10%. Similarly for a d_{32} of 3mm, the EFC will be 1.43 ppm and the error in the EFC is 0.18 ppm which is equivalent to approximately 12%. If the d_{32} is lower and close to flat portion of the curve, the error escalates, hence for example at a d_{32} of 1.2 mm, the EFC will be 11.5ppm and the error is 3.44 ppm which is equivalent to 30%. Hence measurements of d_{32} were targeted to be in the decay portion of the curve where the bubble size ranged from 2-3 mm which translates to an error of 10-12%.

6 Results

6.1 Relationship between Sauter Mean Bubble Diameter and frother concentration

6.1.1 Technique #1: Controlling frother dosage to a cell and measuring bubble size

Technique 1 involved dosing frother into the first rougher cell at different rates. The first rougher cell was a 70 m^3 Outokumpu forced air mechanical cell. The frother used was Betafroth 206C which is a polyglycol type frother of which the actual composition is unknown. The dosage rates of frother were set to achieve different concentrations of frother in cell. The assumption was that there was negligible frother concentration in the rougher feed water. At each concentration of frother, the bubble size in the cell was measured using the AAPBS using the procedure described in 5.4.1. This experiment was carried out at Plant A treating UG2 ore.

Table 2 shows a summary of the operating conditions at each of the different frother concentrations. The solids feed rate was relatively constant, as was the rougher feed density. From these the water volumetric flow rate was calculated in order to dose the correct frother dosage. Superficial gas velocity varied somewhat and this would be expected to affect the bubble size. Increasing air flow rate would result in increasing bubble size (Gorain et al, 1995) but the extent of this effect would depend on cell characteristics. In this study, the bubble size did, indeed, increase with increasing air flow rate, except in the case of the 0.8 cm/s air flow rate, which showed anomalous behaviour in that it exhibited the largest bubble size.

Table 4: Summary of operating conditions and results for Technique #1

Frother (Betafroth 206C) concentration	Solids feed rate (t/h)	Rougher feed density (t/m^3)	Rougher Feed Flow Rate (m^3/h)	Superficial Gas Velocity (cm/s)	Sauter Mean Bubble Diameter (mm)
0 ppm	294	1.33	656	0.91	0.80
5.4 ppm	328	1.37	654	0.96	0.84
10.3 ppm	333	1.38	646	0.80	0.93
14.6 ppm	299	1.34	647	0.87	0.75

Figure 38 shows the Sauter mean bubble diameter as a function of the concentration of frother feeding the first rougher cell. The Sauter mean bubble diameter shows no correlation with frother concentration. Furthermore, the bubble size at zero frother dosage was already very small for mechanically agitated flotation cells (Gorain et al, 1995). Hence the initial assumption of negligible frother concentration in the rougher feed water may have been inaccurate.

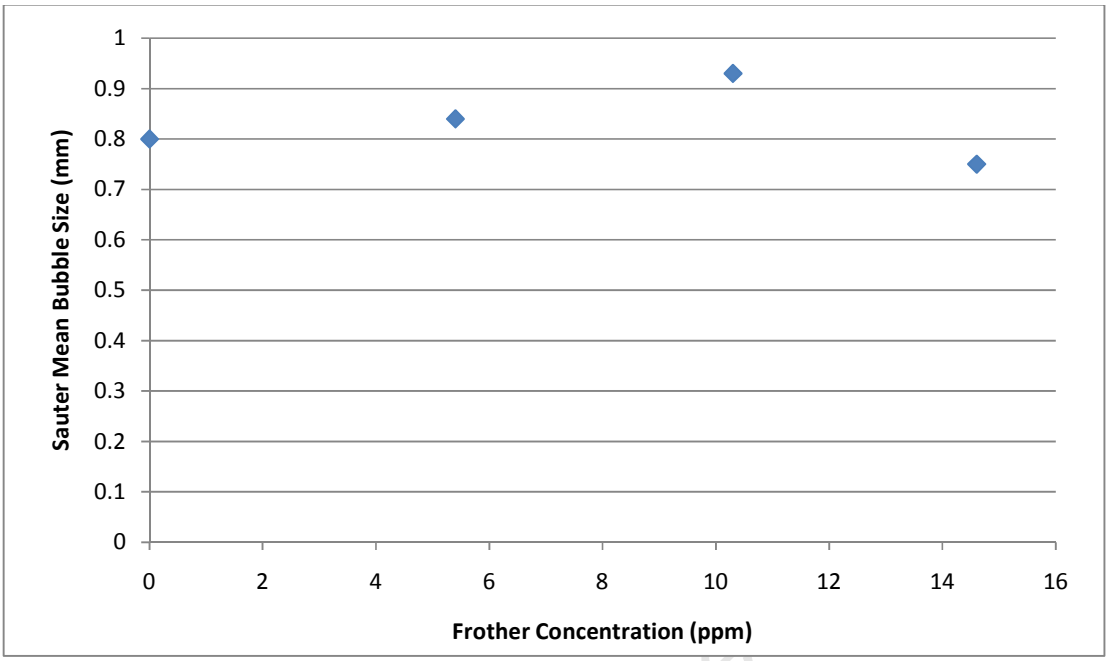

Figure 38: Sauter Mean Bubble Diameter vs. Betafroth 206C concentration for technique 1

Figure 39 shows the bubble size distributions (BSD) at the different frother concentrations. The bubble distributions are unimodal. The BSD at 0 and 5.4 ppm are identical, as are those for 10.3 and 14.6 ppm. The BSD for the higher frother concentrations were slightly wider than the BSD for the low frother concentrations. This is anomalous because higher frother concentrations should narrow the bubble size distribution by preventing bubble coalescence as shown by Nesset et al, 2006. In addition, the air flow rates are lower at the higher frother dosages which should have narrowed the BSD (Gorain et al, 1995; Nesset et al, 2007) Furthermore, the bubble size distributions are unimodal and in the 2 phase air/water system, it was shown by Nesset et al, 2006 that the bubble size distribution approaches unimodal as the frother concentration approaches the CCC. This implies that there could have been significant residual frother concentration in the rougher feed.

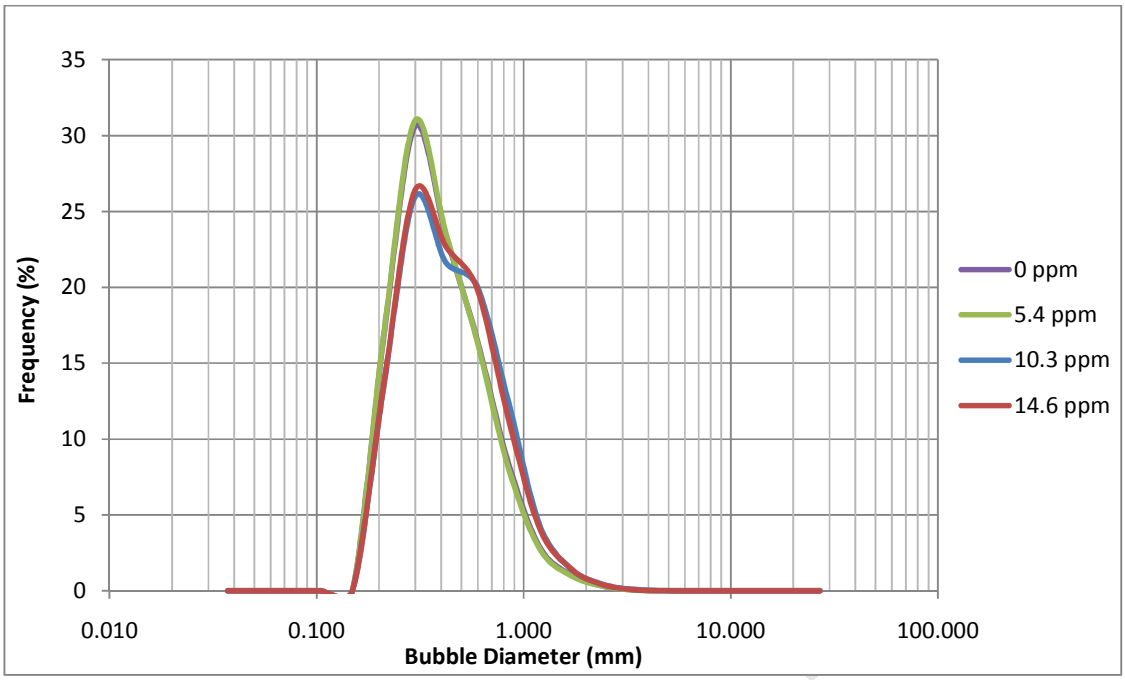

Figure 39: Bubble size distributions obtained for the different Betafroth 206C concentrations in the rougher feed

6.1.2 Technique #2: Adding known concentrations of frother to the AAPBS

Technique 2 involved by-passing frother from the first rougher cell into the second rougher cell in order to deplete the first rougher cell of frother. The first rougher cell was a 70 m^3 Outokumpu forced air mechanical cell. The frother used was Betafroth 206C. Different concentrations of frother were made in 8 litres of potable water. Each solution was added into the AAPBS and the bubble size was measured at each frother concentration. The cell operating conditions were kept constant, and this included keeping the air rate constant.

Table 5 shows the summary of the frother concentrations and bubble sizes measured using this technique (test 1). This experiment was carried out at Plant A. The superficial gas velocities were relatively constant for the test. At zero frother concentration the bubble size is relatively big and is similar to the bubble sizes measured by Nesset et al, (2006, 2007); Finch et al 2008; Cho and Laskowski, 2002; Grau et al 2005 with no frother present. There is a dramatic decrease in the bubble size as the frother is increased from 0 to 10ppm; it drops from 4.23 to 1 mm. It can also be seen that any further increase in frother concentration above 10ppm had very little reduction on the bubble size. This resembles the exponential decay relationship of bubble size and frother concentration described by Comley et al, 2002; Finch et al, 2008; Nesset et al 2006, 2007; Cho and Laskowksi, 2002, Grau et al, 2005. The experimental data points were then fitted to the exponential decay equation described by Comley et al, 2002 and Nesset et al, 2006 (Figure 40). The fitted Sauter mean bubble diameters are very close to the experimental results. However, the frother concentrations tested were outside the decay portion of the relationship. Hence the test was repeated with additional lower frother concentration data points to define the decay portion of the relationship, (test 2) shown in Table 6.

Table 5: Summary of Results and operating conditions for applying technique 2 with Betafroth 206C called Test 1.

Betafroth 206C Frother Concentration (ppm)	Experimental Sauter Mean Bubble Diameter (mm)	Fitted Sauter Mean Bubble Diameter (mm) $d_{32} = 0.98 + 3.25e^{-0.5C_{frother}}$	Superficial Gas Velocity (cm/s)
0	4.230	4.230	0.89
10	0.999	1.000	0.89
15	0.991	0.981	0.88
20	0.965	0.980	0.92
30	0.986	0.980	0.93

Table 6 shows the summary of results by repeating the measurement in test 1 but at concentrations less than 10 ppm in order to define the decay portion of the relationship between Sauter mean bubble diameter and frother concentration. The air rate was constant at 0.9 ± 0.02 cm/s. The results show the same trend as in test 1. However, it can be seen that the decrease in bubble size with increasing frother concentration is more gradual now with the lower frother concentration data points. Hence the decay portion of the relationship is more clearly defined.

The initial bubble size at zero frother concentration for test 1 and test 2 were 4.23 and 3.33 mm respectively. This difference in bubble size could be due to slightly different air rates, or difference in the bubble size distribution at the point of measurement due to change in cell characteristics between test 1 and test 2 which were conducted on different days. However, bubble sizes at high frother concentrations for test 1 and test 2 are similar at approximately 1mm. These numbers again agree with the findings of Nesset et al, 2006 for measurements using a forced air mechanical flotation cell. Similarly to test 1, the exponential decay relationship described by Comley et al, 2002 and Nesset et al, 2006 was fitted to the experimental data for test 2 resulting in an excellent fit.

Table 6: Summary of Results for repeating the experiments at with lower frother concentrations to define the decay portion of the relationship with Betafroth 206C called Test 2.

Betafroth 206C concentration (ppm)	Sauter Mean Bubble Diameter (mm)	Fitted Sauter Mean Bubble Diameter (mm) $d_{32} = 1.02 + 2.3e^{-0.33C_{frother}}$
0	3.33	3.33
2.1	2.18	2.19
4.2	1.64	1.61
6.3	1.30	1.32
8.4	1.18	1.18
15.8	1.06	1.04
50	1.01	1.03

Figure 40 shows the graphs of the Sauter mean bubble diameter and frother concentration for test 1 and 2. The graphs contain the experimental data indicated by points and the fitted model indicated by the broken lines. Both the graphs for test 1 and test 2 are in agreement with the relationship between bubble size and frother concentration described by Cho and Laskowksi (2002); Grau et al, 2005; Nesset et al (2006, 2007); Finch et al, 2008; Comley et al, 2002. These graphs very closely resemble the graphs generated by Nesset et al, 2006 for the different frothers performed in a forced air mechanical cell. It can been seen in Figure 40 that experimental data points for test 1 and additional

lower concentration data points for test 2 are in very good agreement. Furthermore the data points appear to exist on a common line. This is also the case for the fitted models for test 1 and test 2. The method described by Grau et al (2005) was used to estimate the CCC by the inflection point or the intersection of the horizontal asymptote with the sloped line approximating the curve at lower frother concentrations. The fit of the sloped line at low frother concentrations was generally poor and the line which was due to the bubble size at zero frother concentration which skewed the fit. Hence it was decided to exclude this data point in the fit of the sloped line which is consistent with Grau et al (2005). This is shown in Figure 40 below, where the CCC for test 2 was approximated to be approximately 8 ppm. The CCC for test 1 was not approximated because of a lack of data points at low frother concentrations.

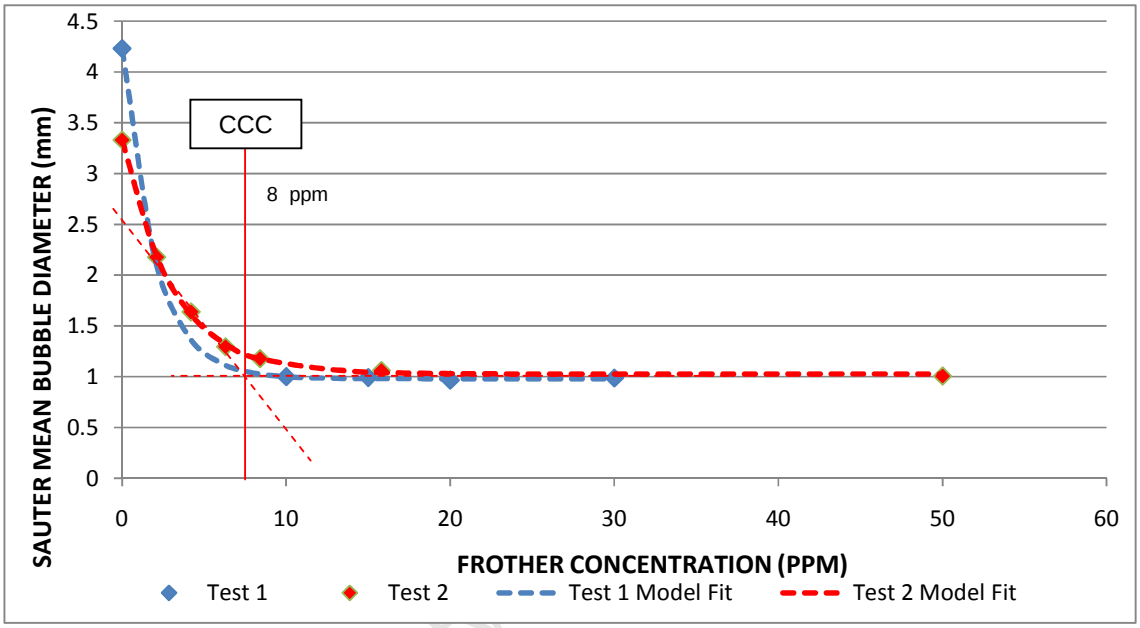

Figure 40: Graphs of Sauter Mean Bubble Diameter and Betafroth 206C frother concentration at Plant A for test 1 and 2.

Figure 41 shows the bubble size (number) frequency distributions at different concentrations of Betafroth 206C for test 2. It can be seen that at zero frother concentration, the bubble size distribution is bi modal and wide. There are a large proportion of 3.5 mm and 0.30 mm bubbles initially. Hence there is a distribution of coarse and fine bubbles which is in agreement with Nesset et al (2006). As the frother concentration increases the bubble size distributions become narrower and finer. Furthermore, the bubble size distributions approach a unimodal distribution. This is an identical result obtained by Nesset et al (2006) when performing similar measurements on a mechanically forced air pilot cell in an air/water system. Furthermore, the results are in agreement with the coalescence mechanisms described by Finch et al (2008). Finch et al (2008) showed that during coalescence there is formation of larger bubbles and finer bubbles which break up after coalescence. Hence the initial distribution with zero frother will be bimodal. It was also shown that the addition of frother prevented coalescence, and this can be seen with bubble size distributions in Figure 41 becoming narrower and finer as the frother concentration is increased.

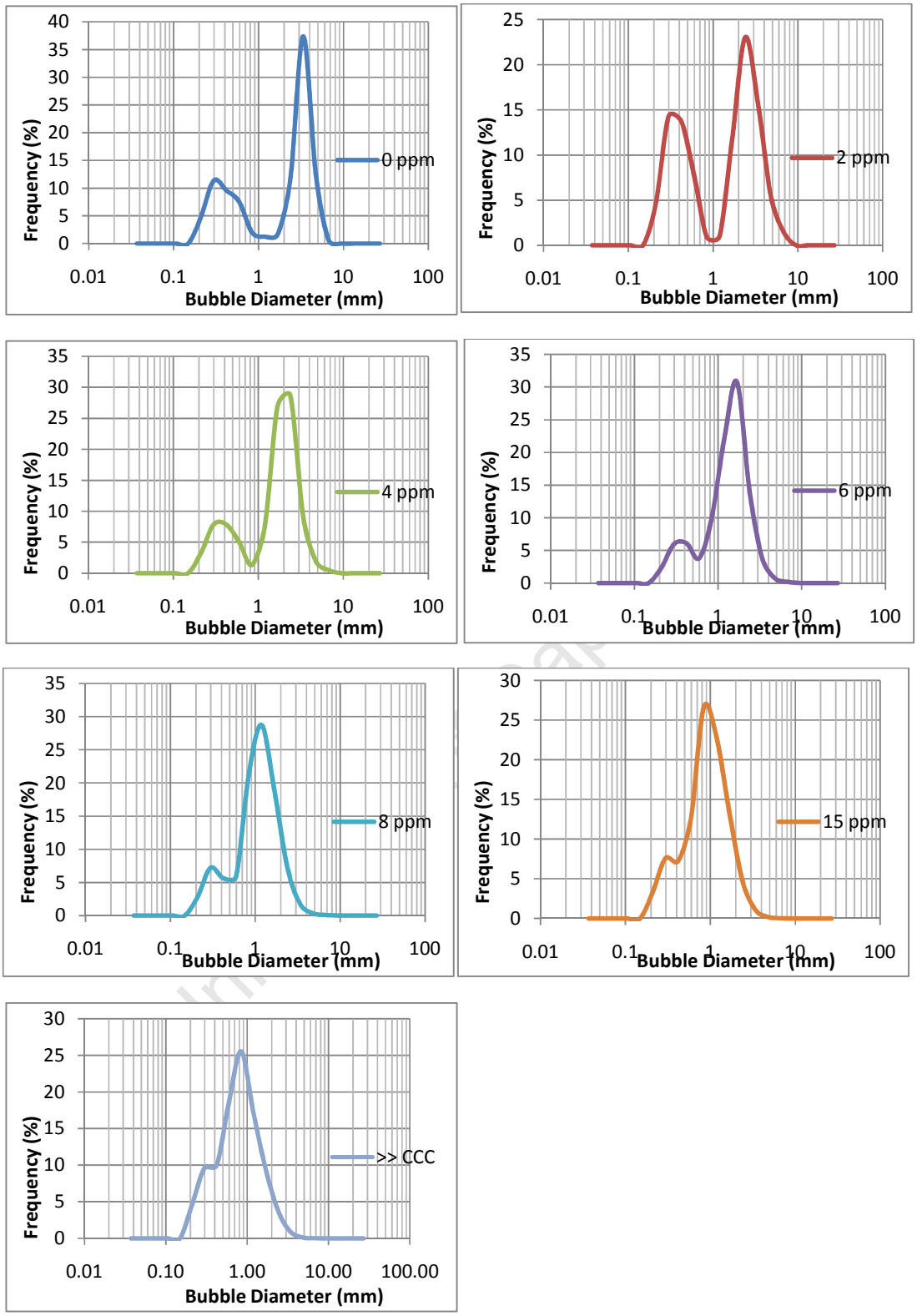

Figure 41: Bubble Size Distributions for different Betafroth 206C frother concentrations for test 2

6.1.3 Selection between technique 1 and 2 for determining relationship between bubble size and frother concentration.

It can be seen that technique 2 has resulted in much more positive results compared to technique 1. The results for technique 2 are in agreement with the findings in literature (Cho and Laskowksi 2002; Grau et al, 2005; Nesset et al (2006, 2007); Finch et al, 2008). Hence technique 2 was chosen as the better method. In addition technique 2 has the added advantage of having minimum disruption on the plant process. Technique 1 requires the alteration of frother dosage to the entire bank, which would affect the grades and recoveries. Technique 2 will hereafter be referred to as "the method".

6.1.4 Reproducibility of the method on two similar rougher cells

Technique 2 was applied to a different frother (Sasfroth 200) and was performed on a different plant (Plant B UG2 Concentrator) treating UG2 ore. The first rougher cell, which was used for the measurements, was a 70 m^3 Outokumpu forced air mechanical cell. Sasfroth 200 is a polyglycol type of frother of average molecular weight of approximately 200 g/mol. Plant B UG2 Concentrator operates with two parallel rougher banks. This provided an opportunity to investigate the effect of different cell characteristics on the measurements by repeating test 3 using the first rougher cell of the parallel bank. The rougher cells are of the same size and type being 70 m^3 Outokumpu forced air mechanical cells. However, the cell internals will not be identical due to differences in wear rates and maintenance schedules. Hence gas dispersion and bubble size distribution generated by the impeller and stator will be slightly different compared to test 3.

Table 7 shows a summary of the results obtained by applying technique 2 to a different frother called Sasfroth 200 which is also a polyglycol type like Betafroth 206C. The results show a similar relationship as observed for Betafroth 206C. At zero frother concentration, the bubble size is large at 3.9mm and decreases to 1.1 mm at high frother concentrations. The relationship obtained is are very similar to that obtained in test 1 and 2 with Betafroth 206C which agrees with Nesset et al (2006). Nesset et al (2006) tested five different frothers using a mechanical forced air cell and showed that the exponential decay relationship between bubble size and frother concentration applied to all five frothers. However the different frothers reduced bubble size differently which can be seen in Figure 10.

Table 7: Summary of results for performing technique 2 with Sasfroth 200 at Plant B UG2 Concentrator called test 3.

Sasfroth 200 Concentration (ppm)	**Experimental Sauter mean bubble diameter (mm)**	**Fitted Sauter mean bubble diameter (mm)** $d_{32} = 1.08 + 2.76e^{-0.26C_{frother}}$
0	3.91	3.86
2	2.58	2.74
4	2.13	2.07
6	1.78	1.67
8	1.55	1.43
10	1.16	1.29
12	1.12	1.20
15	1.08	1.14
20	1.10	1.10
40	1.08	1.08

Table 8 shows the summary of the results for investigating the application of technique 2 using a flotation cell with slightly different cell characteristics and bubble size distributions (test 4). The results show the same exponential decay relationship and as the frother concentration increases the bubble size decreases from 3 to 1.15 mm. The initial bubble size at zero frother concentration for test 3 and 4 were 3.9 and 3 mm respectively. This could be attributed to a different bubble size distribution generated in the cells for test 3 and 4.

Table 8: Summary of Results for applying technique 2 with the first rougher cell of the parallel rougher bank at Plant B UG2 Concentrator in order to investigate the effect of different cell characteristics (test 4).

Sasfroth 200 Concentration (ppm)	Experimental Sauter mean bubble diameter (mm)	Fitted Sauter mean bubble diameter (mm) $d_{32} = 1.15 + 1.95e^{-0.23C_{frother}}$
0	3.04	3.09
3	2.27	2.13
6	1.65	1.64
9	1.31	1.40
12	1.16	1.27
15	1.15	1.21

Figure 42 shows the graphs of the Sauter mean bubble diameter and frother concentration for tests 3 and 4. The experimental data is plotted as points and the fitted model is shown as a broken line. Both fitted graphs for test 3 and 4 fit the experimental data well. There is a difference in the initial bubble size at zero frother concentration between test 3 and 4. However, most of the experimental data points for test 3 and 4 overlap each other and appear to lie on a common line. The graphs yield an identical CCC of approximately 10 ppm for both test 3 and 4 respectively. Hence it can be see that the results for test 3 and 4 are almost identical. This could be due to both rougher cells either having identical conditions which is unlikely. It is likely that the bubble size distributions entering the AAPBS would be different which can be seen in Figure 43 and Figure 44 which could be due to different cell internals due difference in wear rates of the impeller and stator. The results imply that technique 2 is reproducible and is able to generate the same result with different flotation cells of the same size.

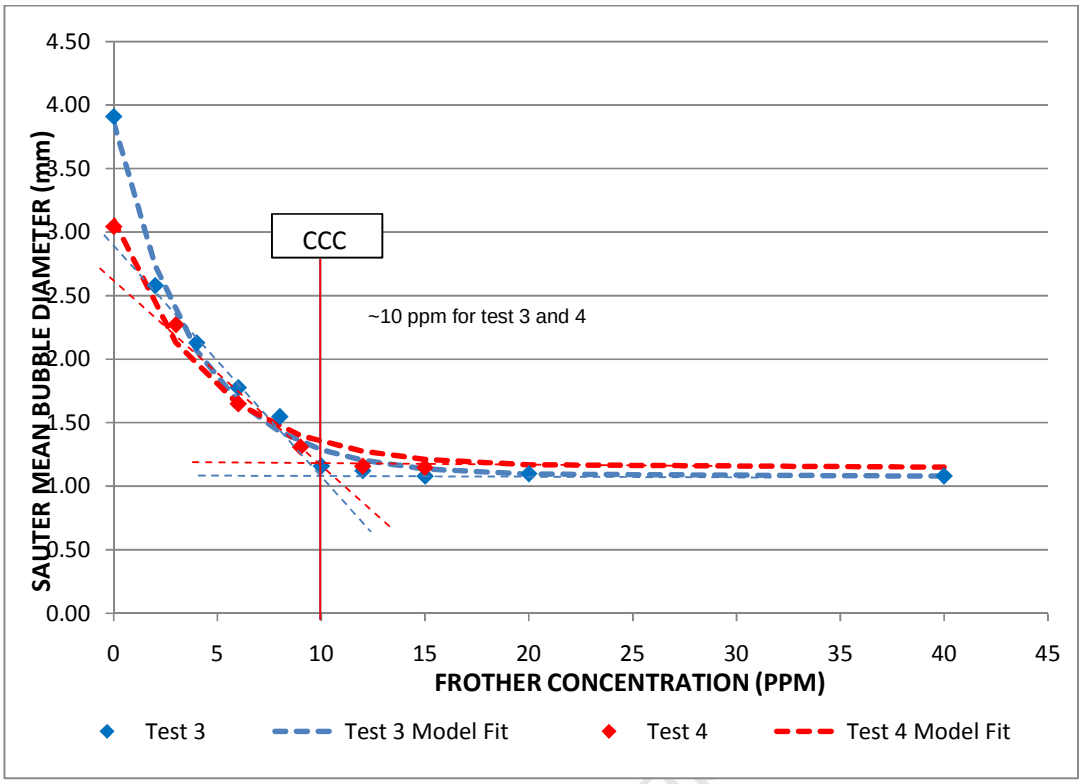

Figure 42: Sauter Mean Bubble Diameter vs. frother concentration for test 3 and 4 with Sasfroth 200 at Plant B UG2 Concentrator

Figure 43 shows the bubble size (number) frequency distribution at different frother concentrations for test 3. At zero frother concentration the bubble size distribution is bi modal with an almost equally large proportion of coarse and fine bubbles. The coarse and fine bubble sizes were approximately 3 and 0.28 mm. This is similar to the result obtained for test 2 and it is in agreement with results obtained by Nesset et al (2006). As the frother concentration increases the bubble size distribution gets narrower and finer and approaches a unimodal distribution at high frother concentrations which is in agreement with Nesset et al (2006). Furthermore, at a concentration of greater than 15 ppm, the bubble size distribution is unimodal and does not change with any further increase in frother concentration. An explanation for this would be that increasing frother concentration reduces the degree of bubble coalescence. Hence there is a reduction in coarse bubbles and fine bubbles which are products of bubble coalescence (Finch et al, 2008). Coalescence reduces to a minimum and the bubble size distribution approaches a unimodal distribution generated at the cell impeller (Cho and Laskowski, 2002). Hence any further increase in frother concentration has little or no effect on the bubble size distribution.

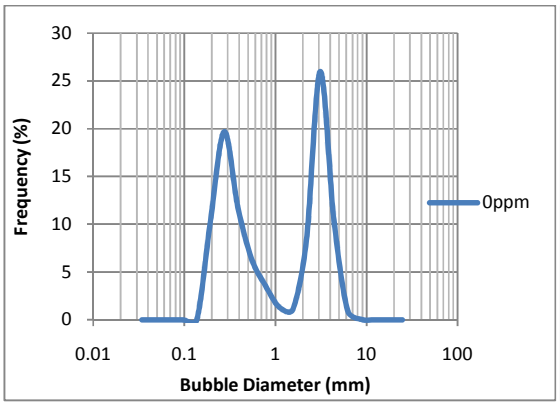
Frequency (%)
30
25
20
15
10
5
0
0.01
0.1
1
10
100
Bubble Diameter (mm)
0ppm

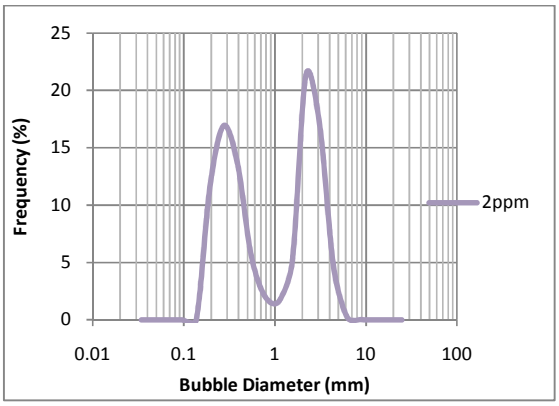
Frequency (%)
25
20
15
10
5
0
0.01
0.1
1
10
100
Bubble Diameter (mm)
2ppm

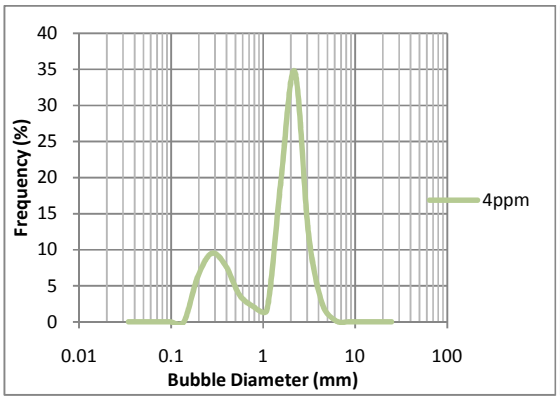
Frequency (%)
40
35
30
25
20
15
10
5
0
0.01
0.1
1
10
100
Bubble Diameter (mm)
4ppm

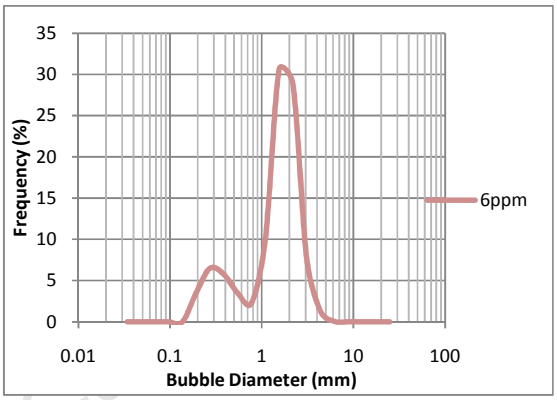
Frequency (%)
35
30
25
20
15
10
5
0
0.01
0.1
1
10
100
Bubble Diameter (mm)
6ppm

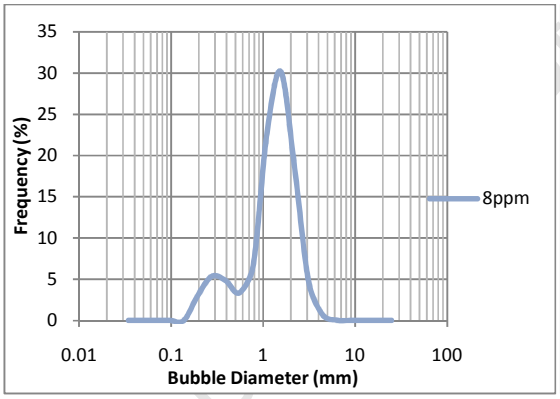
Frequency (%)
35
30
25
20
15
10
5
0
0.01
0.1
1
10
100
Bubble Diameter (mm)
8ppm

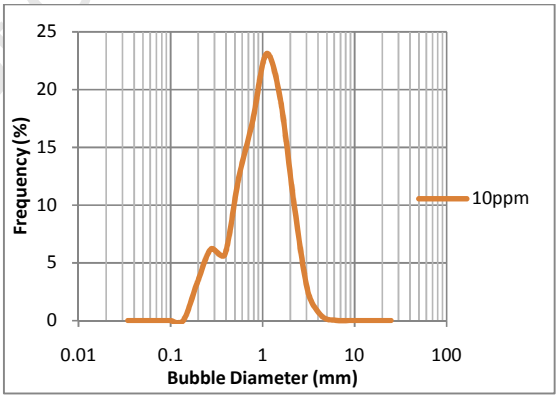
Frequency (%)
25
20
15
10
5
0
0.01
0.1
1
10
100
Bubble Diameter (mm)
10ppm

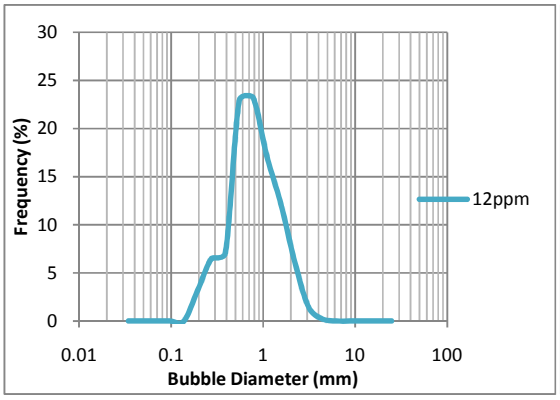
Frequency (%)
30
25
20
15
10
5
0
0.01
0.1
1
10
100
Bubble Diameter (mm)
12ppm

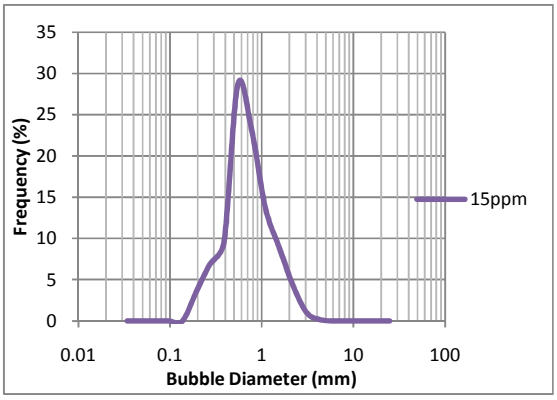
Frequency (%)
35
30
25
20
15
10
5
0
0.01
0.1
1
10
100
Bubble Diameter (mm)
15ppm

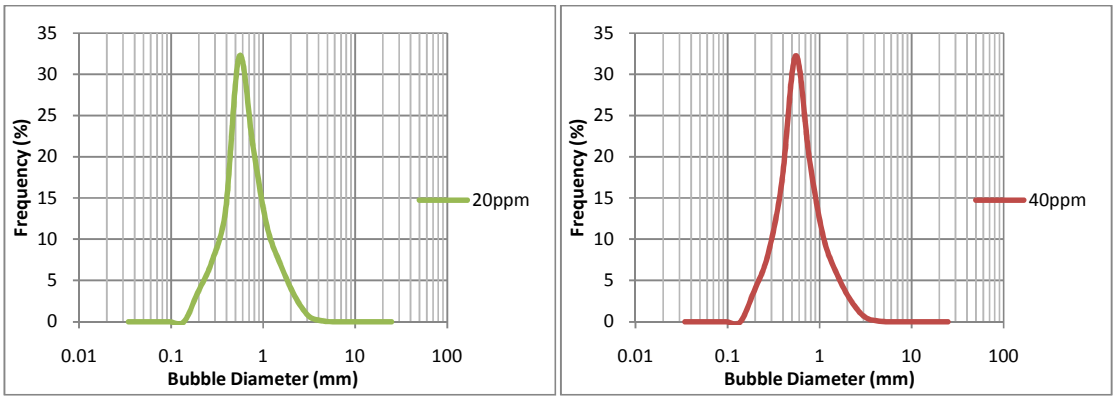

Figure 43: Test 3 bubble size frequecy distributions at different Sasfroth 200 concentrations

Figure 44 shows the bubble size frequency distributions at different frother concentrations for test 4. In Figure 44 at zero frother concentration, a bimodal distribution can be seen however with a much higher proportion of coarser bubbles than finer bubbles. The coarse bubbles and fine bubble sizes were predominantly 2.2 and 0.28 mm. As the frother concentration increased, the proportion of coarser bubbles decreased, the bubble size distribution became narrower and finer and approached a unimodal distribution at approximately 15ppm.

By comparing the bubble size distribution at zero frother concentration to test 3 it can be seen that there was a smaller proportion of fine bubbles in test 4. This could be due to a smaller degree of coalescence as the coarse bubble size was also smaller compared to test 3, which was 3.9mm (Finch et al, 2008). A smaller degree of coalescence is associated with the presence of frother. Hence it is possible that there may have been some residual frother in the rougher cell which influenced the results. This could have been due to spillage containing frother finding its way into the rougher feed. In addition, there could have been a difference the gas dispersion mechanisms because of differences in the wear of the stator and impeller between the two cells.

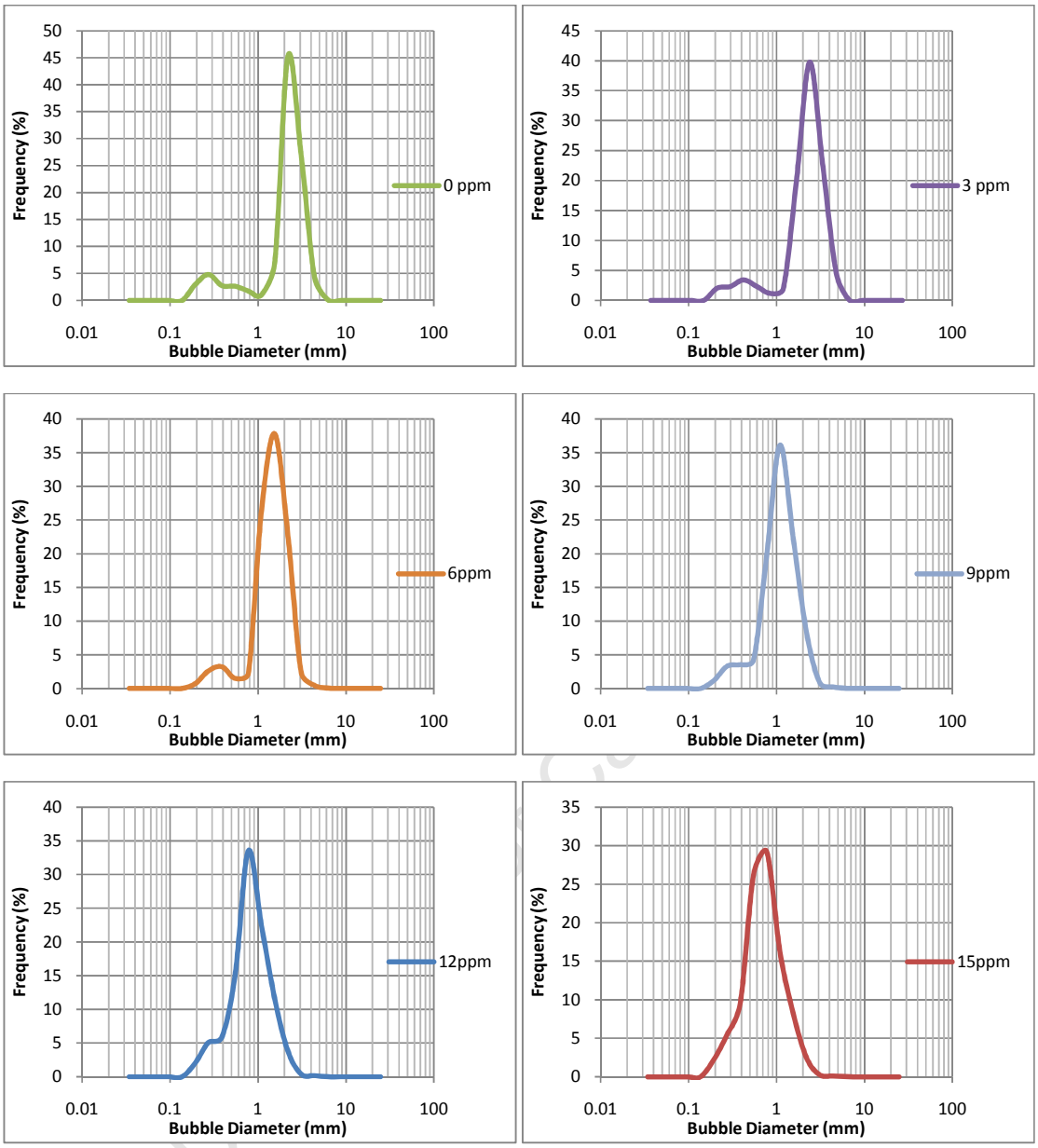

Figure 44: Test 4 bubble size frequency distributions at different Sasfroth 200 concentrations.

6.1.5 Comparison of two different polyglycol frothers, namely Betafroth 206C and Sasfroth 200

Figure 45 shows a comparison of the relationship for Betafroth 206C and Sasfroth 200, and the exponential decay relationship is clearly observed for both frothers. Both frothers have been reported by their manufacturers to have a molecular weight of approximately 200 g/mol. Sasfroth 200 contains a mixture of polyglycol ethers, and alcohols which can be seen in Table 9 below. However, the compositions or mixture of betafroth 206C is unspecified and cannot be used for comparison.

In Figure 45, it can be seen that both frothers show a similar relationship with the graph for betafroth 206C occurring slightly below that of Sasfroth 200. Hence it can be seen the Betafroth 206C had a stronger effect on reducing bubble size. Furthermore the CCC for Betafroth 206C and Sasfroth 200

was approximately 8 and 10 ppm respectively which is outside an experimental error of 10%, and is considered to be significantly different. Hence it appears that Betafroth 206C is a stronger frother than Sasfroth 200.

Table 9: Composition of Sasfroth 200 (taken from MSDS for Hitech Chemicals)

Components	2-[2-(2-butoxyethoxy)ethoxy]ethanol; TEGBE, triethylen glycol monobutyl ether; butoxytriethylene glycol	>= 70 < 80%
	2-(2-butoxyethoxy)ethanol; diethylene glycol monobutyl ether	>= 12.5 < 20 %
	3,6,9,12-Tetraoxahexadecan-1-ol	>= 20 <= 30%

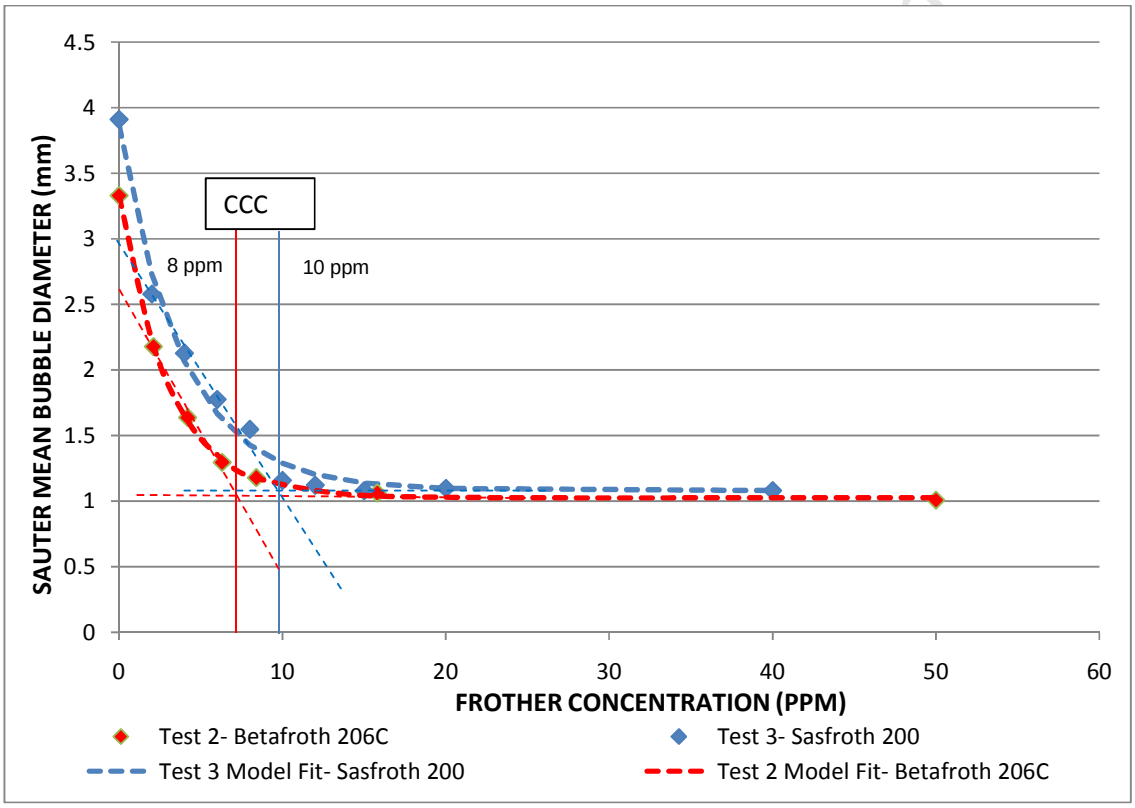

Figure 45: Comparison between the relationship between Sauter mean bubble diameter and frother concentration for Betafroth 206C and Sasfroth 200

6.1.6 Comparison of the method using the same frother but different cells and sites

Technique 2 was applied in a different cell size, which was a smaller 50 m^3 Outokumpu forced air mechanical cell compared to the 70 m^3 rougher cell used in all the previous tests. The frother tested was Sasfroth 200 which is used by the plant in the process.

The difference in cell size will have a significant difference in the cell characteristics such as gas dispersion and bubble size generation. It will be useful to compare the results of applying this technique for the same frother but on different cell sizes. This is important because it will provide an

indication of the robustness of the application of technique 2 on different plants, which will likely have different cell sizes. These results can be compared with Tests 3 and 4.

Furthermore, two tests were performed on the same rougher cell on different days; which will provide an indication of the effect of different plant operating conditions.

Table 10 and Table 11 show the summary of results for investigating the application of technique 2 in a smaller (50 m^3) rougher cell at Plant C UG2 concentrator (Test 5 and Test 6). Both Test 5 and Test 6 show the exponential decay relationship seen in the previous runs. The fitted model also fits the experimental data well. There is a difference in the bubble size at higher frother concentrations, which is 1.04 and 0.9 for Test 5 and Test 6, respectively. However, for both Test 5 and Test 6 at a frother concentration of 15 ppm and more there is very little change in the bubble size.

Table 10: Summary of results for application of technique 2 in a smaller 50 m^3 forced air mechanical cell at Plant C UG2 concentrator for Sasfroth 200 (Test 5).

Frother Concentration (ppm)	Experimental Sauter mean bubble diameter (mm)	Fitted Sauter mean bubble diameter (mm) $d_{32} = 1.08 + 2.89e^{-0.29C_{frother}}$
0	4.10	3.97
2	2.38	2.71
4	2.07	2.00
6	1.75	1.60
8	1.52	1.37
12	1.24	1.17
15	1.09	1.12
20	1.08	1.09
25	1.09	1.08
30	1.09	1.08
40	1.04	1.08

Table 11: Summary of results for repeated test of technique 2 in smaller 50 m3 forced air mechanical cell at Plant C UG2 concentrator for Sasfroth 200 (Test 6).

Frother Concentration (ppm)	Experimental Sauter mean bubble diameter	Fitted Sauter mean bubble diameter (mm) $d_{32} = 0.9 + 2.43e^{-0.2C_{frother}}$
0	3.4	3.3
2	2.3	2.5
4	2.0	2.0
6	1.7	1.6
8	1.5	1.4
10	1.2	1.2
12	1.0	1.1
15	0.9	1.0
20	0.9	0.9
30	0.9	0.9
50	0.9	0.9

Figure 46 shows the graphs of the relationship between bubble size and frother concentration for Test 5 and Test 6 which were done at Plant C UG2 concentrator on a smaller 50 m^3 Outokumpu forced air mechanical cell. There is an excellent fit between the fitted lines and experimental data points for Test 5 and Test 6. The data points for Tests 5 and 6 overlap each other and are almost identical in the lower frother concentration region. However, there is a slight difference in the limiting bubble diameter at the higher frother concentrations which is approximately a 0.2mm difference. This could have been due to a difference in the air rates with possibly a slightly higher air rate for Test 5 which elevated the limiting bubble size. The CCC95 obtained for test 5 and test 6 were approximately 10.5 and 12 ppm respectively. It can be seen that the slope approximating the curve at lower frother concentrations for both test 5 and 6 are similar, however it is the difference in the asymptote which results in a different CCC for test 5 and 6.

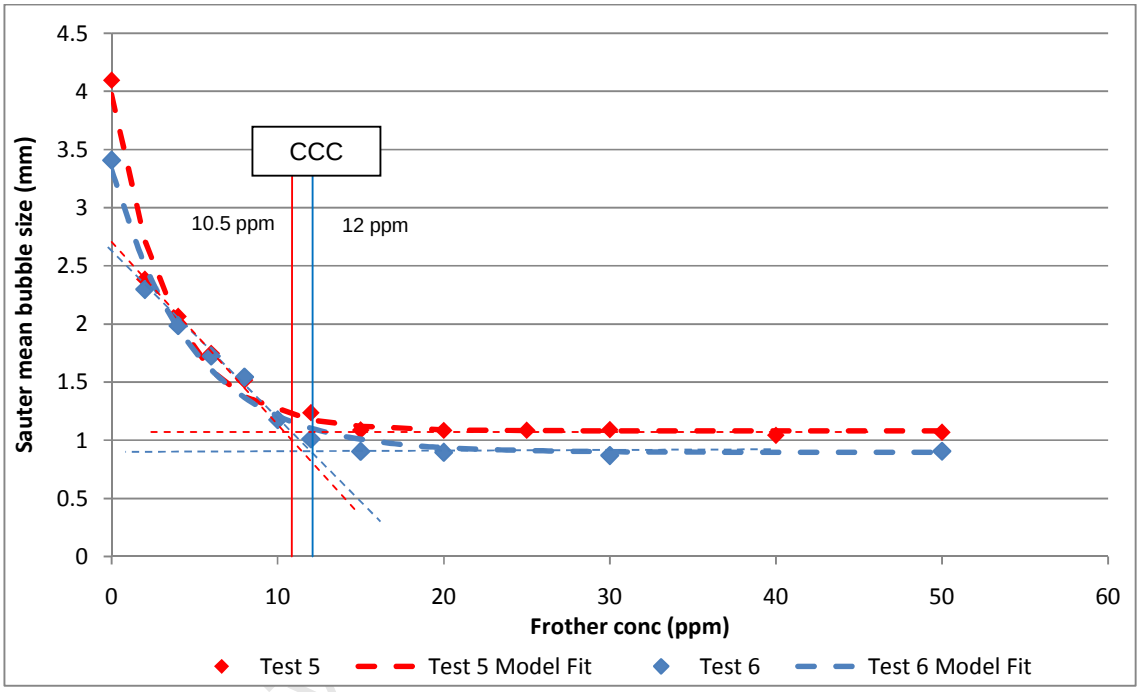

Figure 46: Sauter Mean Bubble Diameter vs. frother concentration for Tests 5 and 6 with Sasfroth 200 at Plant C UG2 concentrator performed in a smaller 50 m^3 forced air mechanical flotation cell.

Figure 47 and Figure 48 show the bubble size frequency distributions for Tests 5 and 6 respectively. These bubble size distributions are similar to those obtained for Tests 3 and 4. Similarly the bubble size distributions are bimodal at zero frother concentration and as the frother concentration increases the distribution gets narrower and the bubble size becomes smaller. The bubble size distribution for both tests approaches a unimodal distribution at a frother concentration of 15ppm and any further increase in frother concentration does not significantly change the distribution.

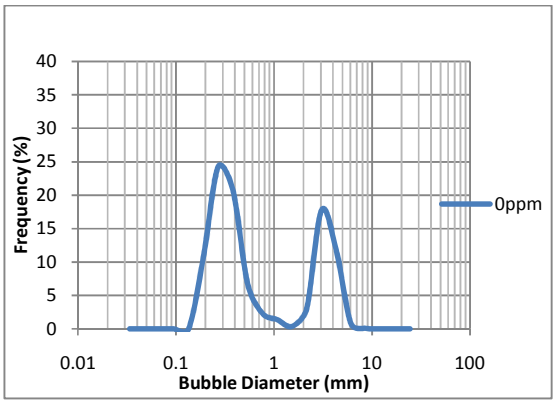
Frequency (%)
40
35
30
25
20
15
10
5
0
0.01
0.1
1
10
100
Bubble Diameter (mm)
0ppm

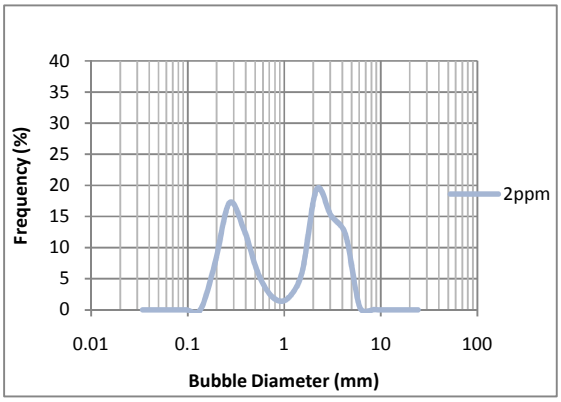
Frequency (%)
40
35
30
25
20
15
10
5
0
0.01
0.1
1
10
100
Bubble Diameter (mm)
2ppm

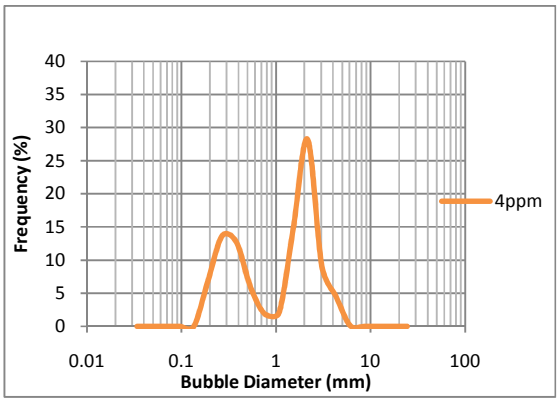
Frequency (%)
40
35
30
25
20
15
10
5
0
0.01
0.1
1
10
100
Bubble Diameter (mm)
4ppm

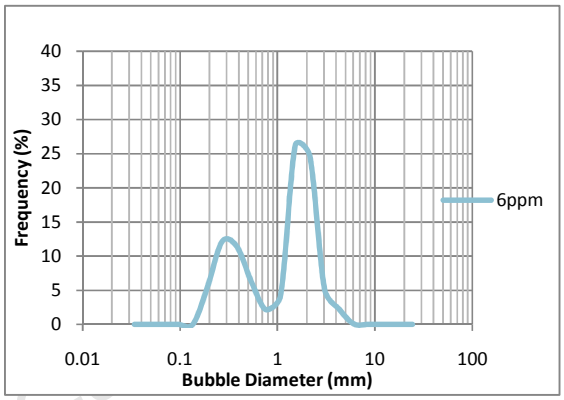
Frequency (%)
40
35
30
25
20
15
10
5
0
0.01
0.1
1
10
100
Bubble Diameter (mm)
6ppm

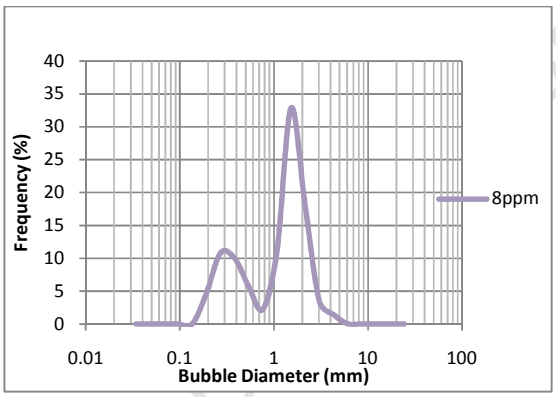
Frequency (%)
40
35
30
25
20
15
10
5
0
0.01
0.1
1
10
100
Bubble Diameter (mm)
8ppm

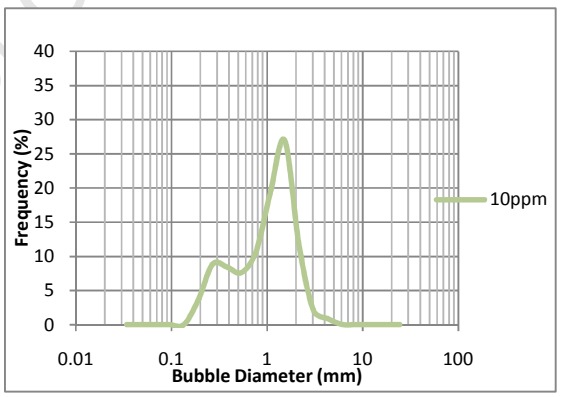
Frequency (%)
40
35
30
25
20
15
10
5
0
0.01
0.1
1
10
100
Bubble Diameter (mm)
10ppm

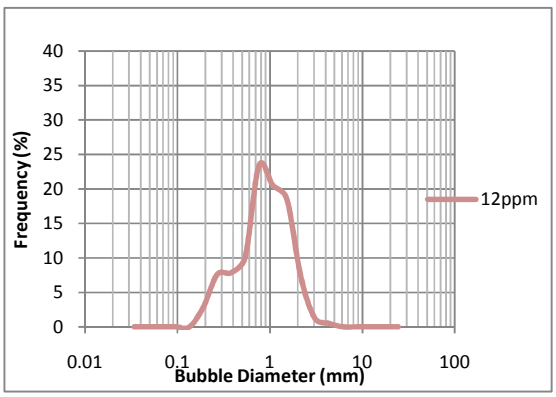
Frequency (%)
40
35
30
25
20
15
10
5
0
0.01
0.1
1
10
100
Bubble Diameter (mm)
12ppm

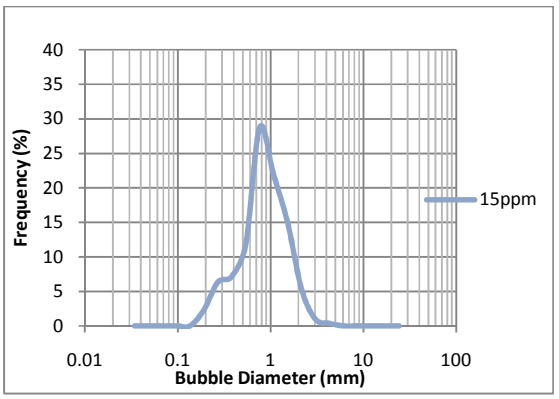
Frequency (%)
40
35
30
25
20
15
10
5
0
0.01
0.1
1
10
100
Bubble Diameter (mm)
15ppm

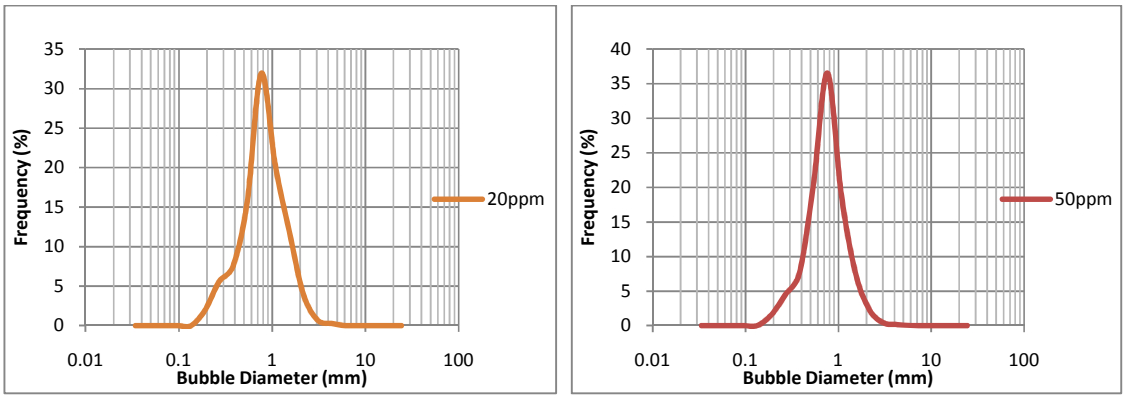

Figure 47: Test 5 Bubble size distributions for different Sasfroth 200 concentrations

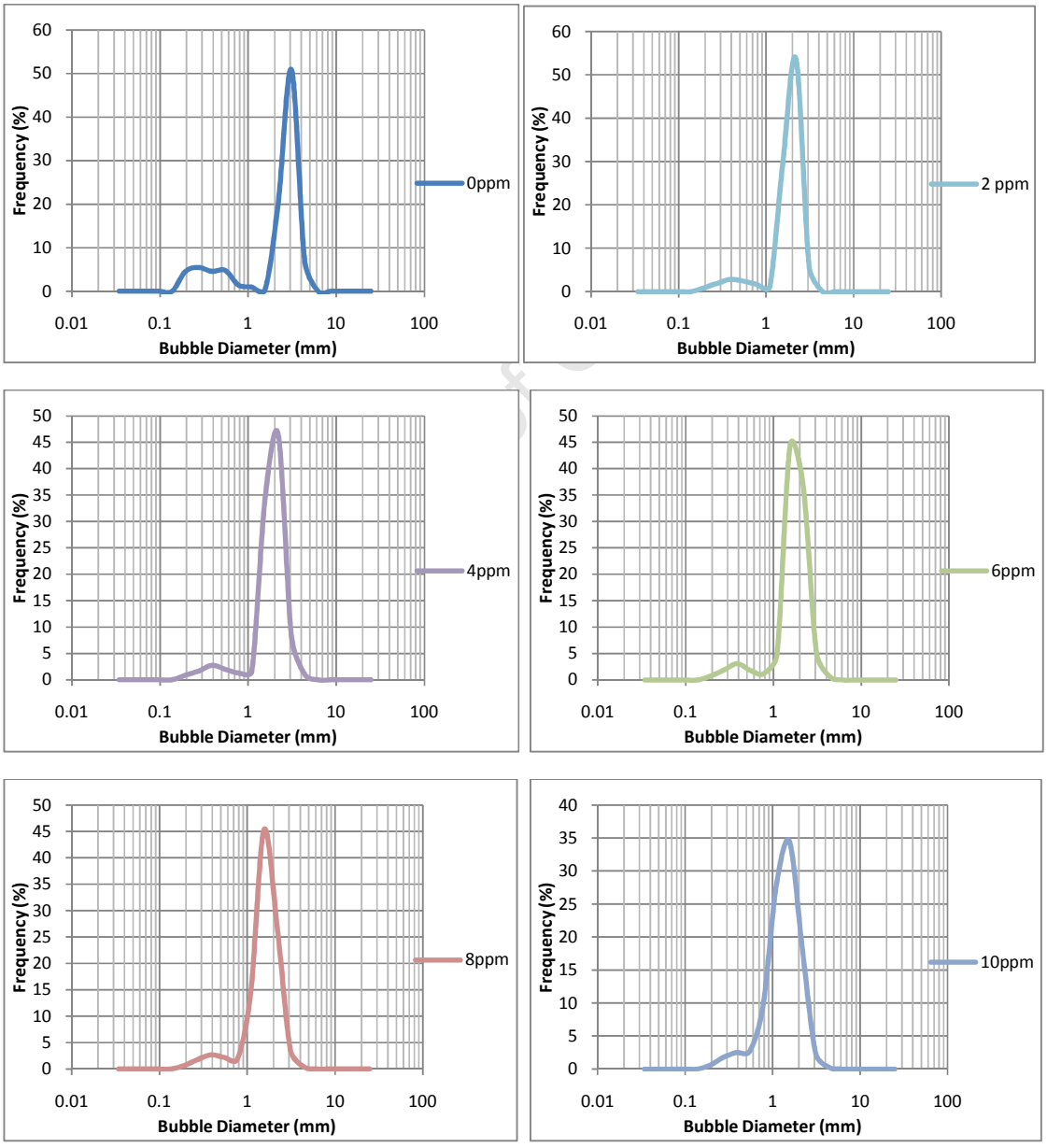

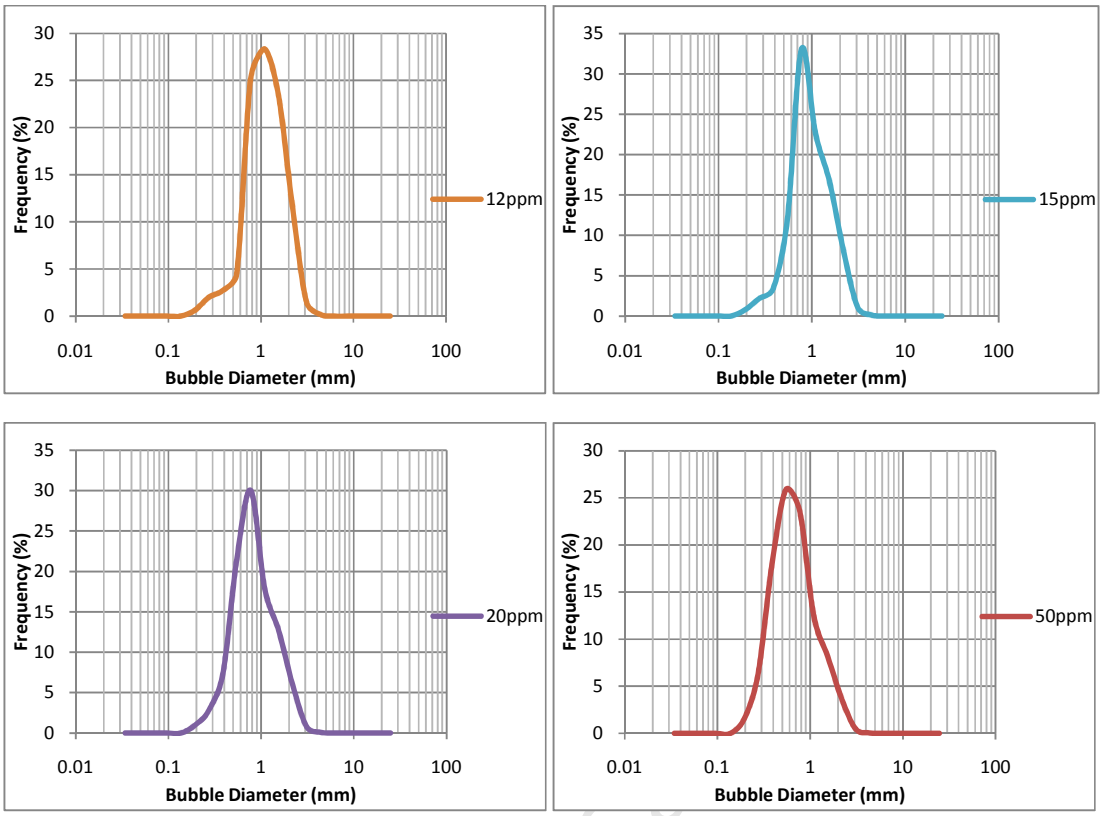

Figure 48: Test 6 Bubble size distributions for different Sasfroth 200 concentrations

Figure 49 shows a comparison of the all the graphs of Sauter mean bubble diameter and frother concentration for Sasfroth 200 which was established on different cells, different cell sizes, different plants and at different times. It can be seen that the data points overlap each other and all the data points appear to lie on a common line which describes the relationship between frother concentration and bubble size. The average CCC was 10.6 ppm with a relative standard error of 4.4% which is within 10% experimental error. Hence technique 2 is robust, repeatable and reproducible on different plants, cell sizes and cell characteristics for mechanical forced air cells. Similarly this finding also agrees with the findings of Grau et al (2005) in which the CCC for a given frother could be treated as a material constant. Grau et al (2005) found that the measurement of the CCC for a given frother was the same when using different bubble generating devices. Furthermore, this result was obtained by operating the cells at similar air rates which were in the region of 0.7-0.9 cm/s for all the tests.

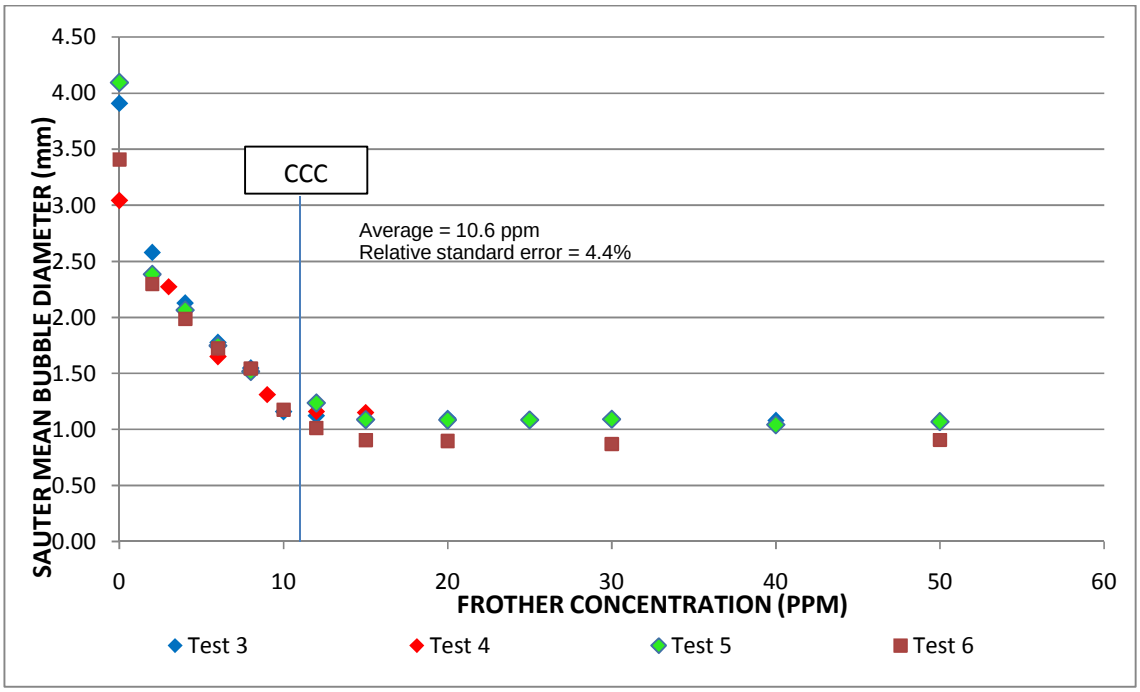

Figure 49: Comparison of tests 3-6 for Sasfroth 200 on different plants, cell charateristics, cell sizes and times

6.2 Estimating frother concentrations in process streams and performing a frother balance

This section shows the results for estimating frother concentrations in solution in flotation and using these estimates to perform a frother balance across the flotation bank. The frother concentrations were estimated using the technique described in 5.4.2 by using the effect of frother on bubble coalescence as a proxy for frother concentration.

The tests were performed on the rougher banks at Plant B UG2 Concentrator and Plant C UG2 concentrator. Both of these plants use Sasfroth 200 in the process. For each test a full rougher bank survey was completed over a period of an hour. Samples were taken of the feed, concentrates and tails of the bank. Flow rates of the concentrates were also taken. A matrix mass balance was performed for each survey. The equivalent frother concentrations were included as assays in the mass balance, and an assumption made was that frother did not adsorb onto solids but remained in solution with the water stream.

6.2.1 Frother balance for Plant C UG2 concentrator

Figure 50 shows the process flow diagram of the rougher bank at Plant C UG2 concentrator. There is a total of six rougher cells and frother was fed at the beginning of the bank at 14 g/t based on the solids feed rate to the roughers, which was equivalent to approximately 10 ppm. The bank was sampled for an hour. The sampling points are indicated with the red stars. Flow rates were also taken of all the cell concentrates. Mass percentage solids were measured for all the streams, and together with flow rates, a water balance across the bank was established. The equivalent frother concentration in each stream was then estimated using the technique described in 5.4.2. By using the equivalent frother concentration and water flow rates; a frother balance across the bank was established.

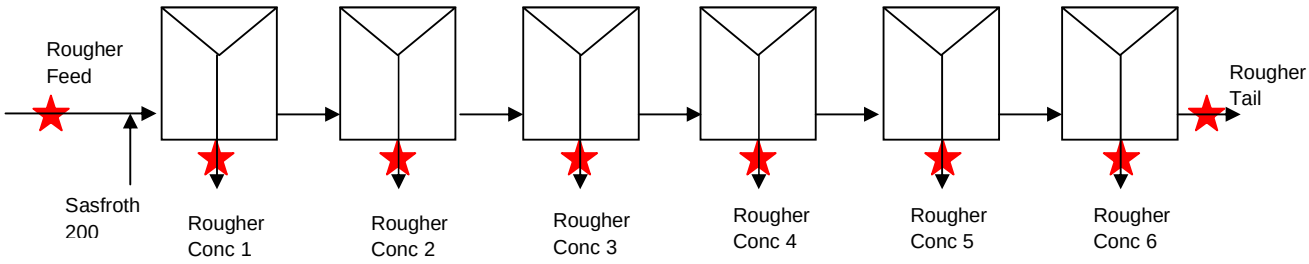

Figure 50: Process Flow Diagram of Rougher Bank at Plant C UG2 concentrator. Stars indicate the sampling points.

Table 12 shows the results for the measurements of the equivalent frother concentrations for each sampled stream. The dilution ratios used for each stream are also shown. For all the concentrates a dilution ratio of 1:5 was used. This is diluting one part of the process stream water filtrate with five parts of potable water which is equivalent to a dilution factor of 6. The rougher feed could not be measured due to insufficient sample; however the process water was taken as an estimate of the equivalent frother concentration (EFC) of the rougher feed before frother addition.

After dilution, the effect of each process stream filtrate on bubble coalescence is shown in the measured Sauter mean bubble diameter column in Table 12. This was then translated into an equivalent frother concentration (EFC) using the model fit equation for the relationship between Sasfroth 200 concentration and Sauter mean bubble diameter by rewriting the equation to solve for frother concentration as shown in equation 17 and 18. Figure 51 shows the relationship between Sauter mean bubble diameter and Sasfroth 200 concentration which was used to calculate the EFC.

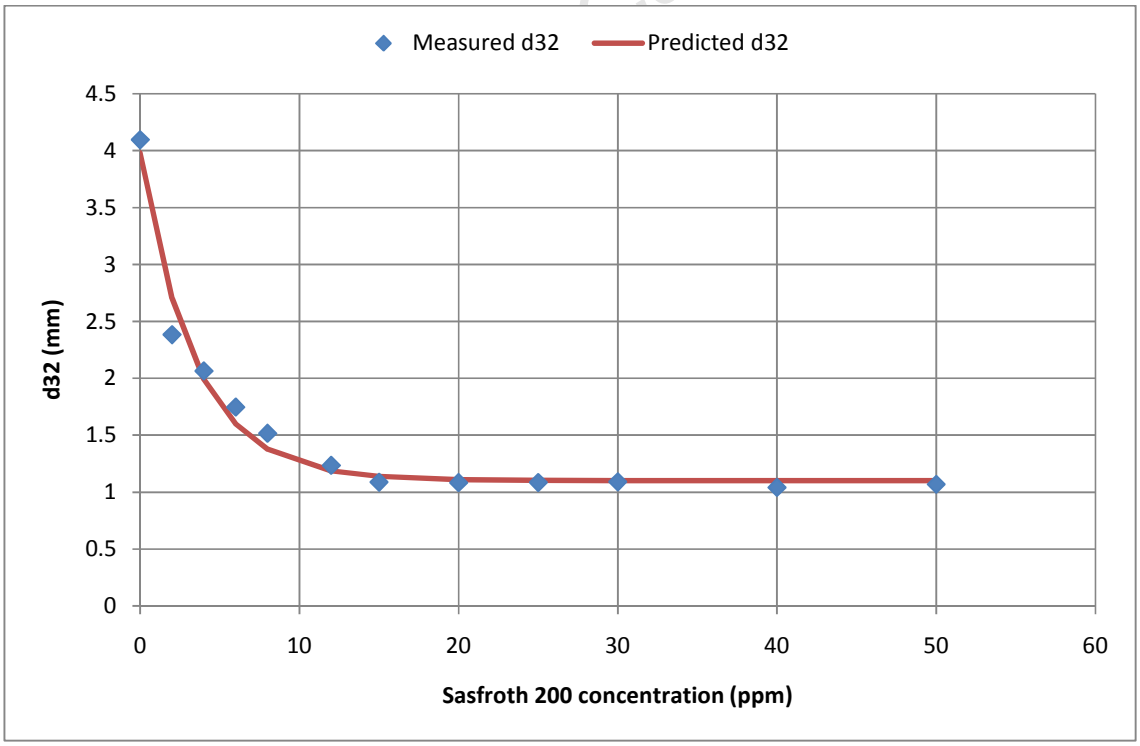

Figure 51: Relationship between Sauter mean bubble diameter and Sasfroth 200 concentration used to calculate the EFC at Plant C UG2 concentrator.

The relationship shown in Figure 51 can also be defined by equation 17 below:

$$d_{32} = 1.1 + 2.88e^{-0.29C_{frother}} \qquad (17)$$

Furthermore, the EFC can be calculated by rearranging the above equation to solve for frother concentration as shown by equation 18 below:

$$EFC_{Sasfroth\,200} = \frac{\ln\left(\frac{d_{32}-1.1}{2.88}\right)}{-0.29} \qquad (18)$$

The calculated EFC using the above equations for the diluted streams is shown in the diluted EFC column of Table 12. Thereafter by multiplying this concentration with the dilution factor, the actual EFC was calculated as shown in the EFC column in Table 12. Table 9 shows that there was a residual frother concentration in the process water which was approximately 3ppm which is in agreement with Tsatouhas et al. (2005). Tsatouhas et al (2005) used gas chromatography to measure the frother concentration in the recycle water in a plant and found that a small portion of frother recycles back into the process. The rougher tails EFC was calculated using 2 different dilution ratios for the process stream filtrate. The dilution ratios used for the rougher tails were 1:1 and 1:5 and each resulted in an EFC of 10.8 and 12.5 respectively. These are relatively close to each other within 15% which is good considering errors in extrapolation. The EFC for the first rougher concentrate was higher at 23 ppm compared to the rest of the bank which was approximately 15 ppm. The elevation in the EFC in rougher concentrate 1 could have been a result of the fresh frother being fed into the first rougher cell. Some of the fresh frother could have short circuited into the concentrate.

Table 12: Summary of measurements of the equivalent frother concentrations of Sasfroth 200 in the process streams for the rougher bank at Plant C UG2 concentrator.

Process Stream	Dilution Factor (Dilution Ratio)	Measured Bubble Size	Diluted Equivalent Frother Concentration, ppm	Equivalent frother concentration, ppm
Process Water	1	2.30	3.0	3.0
Rougher Tails	2 (1:1)	1.70	5.4	10.8
	6 (1:5)	2.66	2.1	12.5
Rougher Conc 1	6 (1:5)	2.02	3.9	23.4
Rougher Conc 2	6 (1:5)	2.31	3.0	17.8
Rougher Conc 3	6 (1:5)	2.46	2.6	15.4
Rougher Conc 4	6 (1:5)	2.46	2.6	15.4
Rougher Conc 5	6 (1:5)	2.53	2.4	14.4
Rougher Conc 6	6 (1:5)	2.48	2.5	15.1

Table 13 shows the mass balance results for the EFC of the measured process streams for the rougher bank at Plant C UG2 concentrator. Table 13 shows that there is little adjustment between the measured and balanced data. The results show little change in the EFC between the rougher feed and tail which implies the bulk of the frother remains in the bulk water stream. Polyglycol frothers are very water soluble and it is typical for the bulk of water soluble frothers to remain in the bulk water stream (Gelinas and Finch, 2007; Hadler et al, 2005; Tsatouhas et al. 2005).

From Table 13 it can be seen that the EFC concentrations in the rougher concentrates and rougher tails are close to the CCC for Sasfroth 200, which is 15 ppm. These streams typically feed into

cleaner and scavenger flotation banks. This implies that the feed to the cleaners and scavengers possibly don't need a significantly large amount of frother.

Table 13: Mass Balance results for EFC of Sasfoth 200 for rougher bank at Plant C UG2 concentrator. Mass Balance performed using the matrix method in Microsoft excel

Process Stream	Balanced EFC (ppm)	Measured EFC (ppm)
Rougher Tail	11.92	11.7
Rougher Feed (after frother addition)	12.75	-
Rougher Conc 1	23.37	23.37
Rougher Conc 2	17.81	17.80
Rougher Conc 3	15.39	15.39
Rougher Conc 4	15.38	15.37
Rougher Conc 5	14.39	14.39
Rougher Conc 6	15.10	15.10

Figure 52 shows the balanced EFC concentrations in the process streams of the rougher bank. It can be seen that the EFC of the concentrates are slightly higher than the rougher feed EFC but generally have a concentration similar to the bulk slurry stream. The initial jump in the frother concentration in rougher first concentrate was described above.

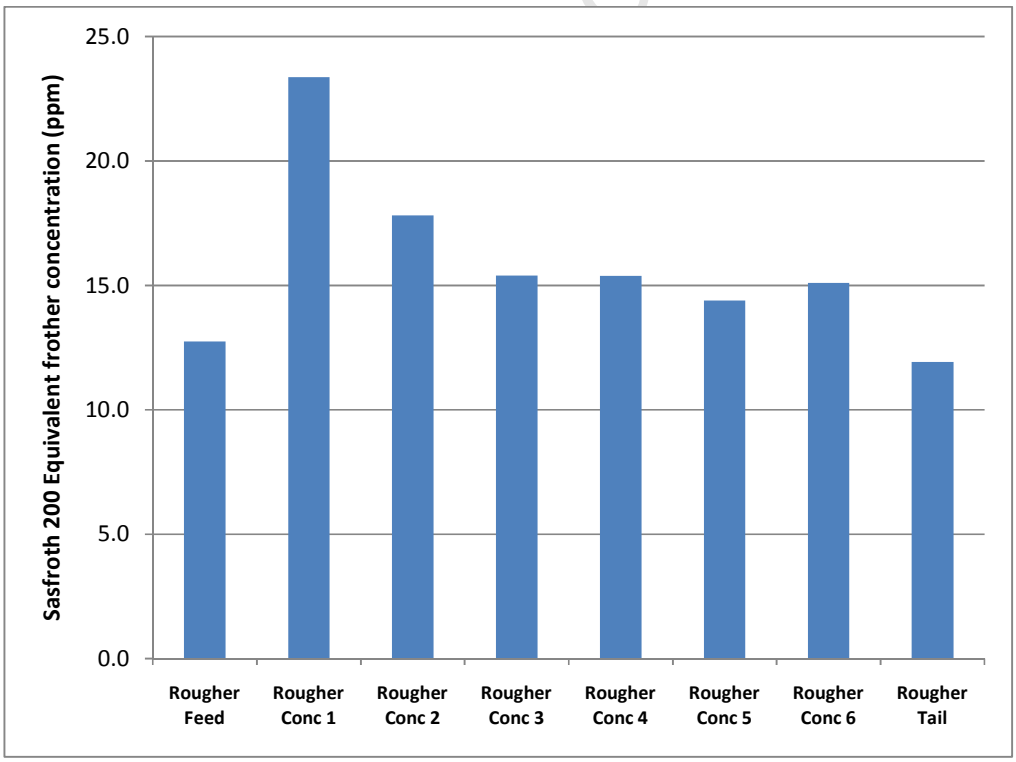

Figure 52: Balanced EFC of Sasfroth 200 in the process streams of the rougher bank from mass balance for Plant C UG2 concentrator.

Figure 53 shows a graph of frother recovery to concentrate and water recovery to concentrate which was obtained from the mass balance data. The relationship is linear and can be fitted with a straight line passing through the origin. The fit is very good with an R^2 value of 0.98. Hence it can be seen that the recovery of frother is strongly dependant on the recovery of water. Furthermore, the frother recoveries obtained are similar to the water recoveries which were also observed by Tsatouhas et al (2005). This further shows that polyglycol frothers which are water soluble preferentially remain in the water phase.

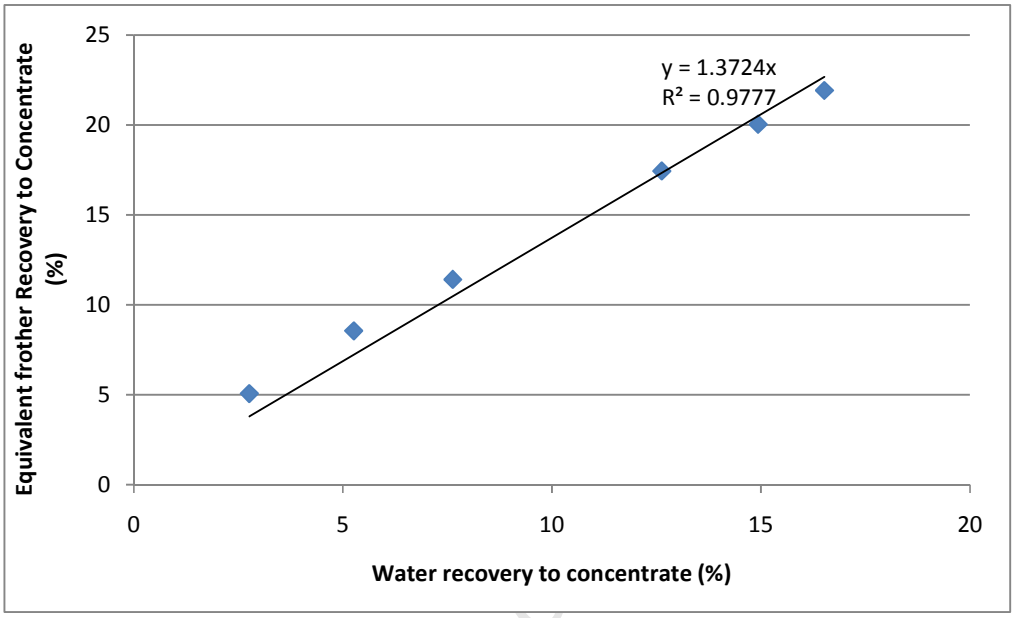

Figure 53: Equivalent Sasfroth 200 recovery to concentrate vs. water recovery to concentrate

6.2.2 Measurement of dissolved ions in the process streams and inferred effect on bubble size

In a process plant, the process water contains dissolved ions. It has been shown that ions also affect bubble size and gas hold up at high molar concentrations (Quinn et al, 2007). It was shown that 0.4M NaCl had the same effect on bubble size that 10ppm of MIBC frother. Hence measurements of the ionic content in water of the process streams in the rougher bank at Plant C UG2 concentrator were done. These measurements were done separately from the above survey, but are assumed to be relatively constant. Table 14 shows the molar concentrations of the different ions in solution and the pH of the water in the different process streams in the rougher bank. The pH of all the process streams where slightly basic. It can be expected that there will be more than the four ions present in solution, and the ionic strength will be at least equal to the number calculated in Table 14 below of approximately 0.03 mol/l. In the process water it is likely that there are organic molecules due to degradation of reagents like collector and depressant which may influence the results. However, the effect on bubble coalescence and bubble size can be strongly related to frother.

Table 14: Ionic content of the process stream water filtrate on the rougher bank

		Cl^-	SO_4^{2-}	Ca^{2+}	Mg^{2+}	Ionic strength
	pH at 25 C	mol/l	mol/l	mol/l	mol/l	(mol/l)
Rougher Feed	8.39	0.01	0.004	0.003	0.005	0.031
Rougher Conc 1	7.52	0.01	0.004	0.002	0.005	0.027
Rougher Conc 2	7.36	0.01	0.004	0.002	0.005	0.027
Rougher Conc 3	7.26	0.01	0.004	0.002	0.005	0.027
Rougher Conc 4	7.35	0.01	0.005	0.002	0.005	0.029
Rougher Conc 6	7.35	0.01	0.004	0.002	0.005	0.027
Rougher Tail	7.38	0.01	0.004	0.002	0.005	0.027

6.2.3 Frother balance for Plant B UG2 Concentrator

Figure 54 shows the process flow diagram of the rougher banks at Plant B UG2 Concentrator. There are 2 parallel banks with five cells in each bank. The rougher bank was surveyed for an hour. The sampling points are indicated with red stars. Flow rates were taken for all the rougher concentrates. Mass percentage solids were measured for every sampled stream and together with flow rates a water balance was established for the bank. The equivalent frother concentration in each stream was then estimated using the technique described in 5.4.2. By using the equivalent frother concentrations and water flow rates; a frother balance across the bank was established. Fresh frother was dosed at the feed of each bank at a rate of 5 g/t based on the rougher feed solids flow rate. This was equivalent to a concentration of 10ppm in the rougher feed to each bank.

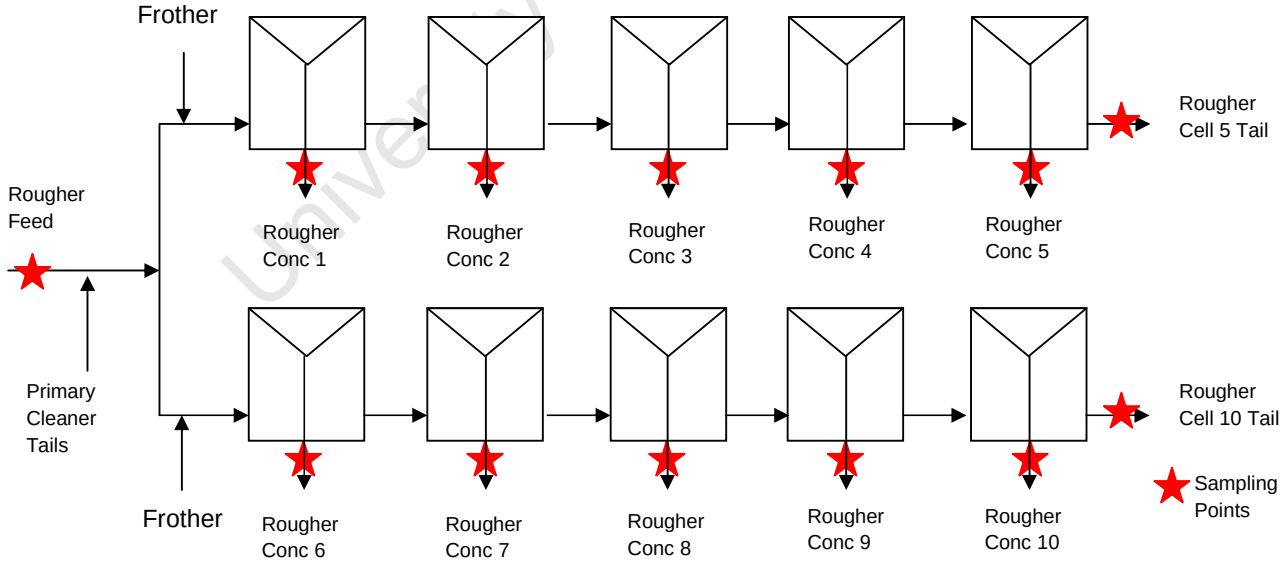

Figure 54: Rougher Bank process flow diagram at Plant B UG2 Concentrator. Red stars indicate sampling points

Figure 55 shows the relationship between Sauter mean bubble diameter and frother concentration used to determine the EFC for each of the above process streams.

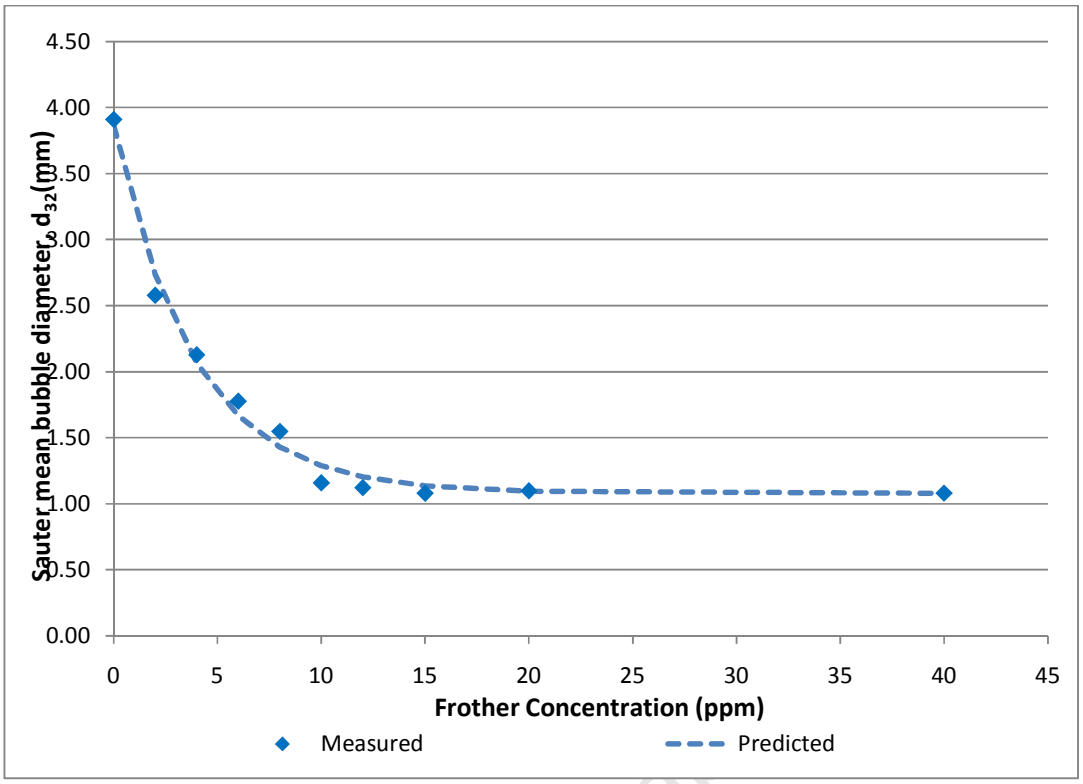

Figure 55: Relationship between Sauter mean bubble diameter and Sasfroth 200 frother concentration, used to calculate the EFC.

Similarly the relationship in Figure 55 can described using the equation 17 and the EFC can be determined by rewriting the equation to solve for the frother concentration as shown by equation 18.

Table 15 shows the results for the raw measurements of the equivalent frother concentrations (EFC) for each sampled stream. Multiple dilution ratios were tested for the rougher feed and some of the rougher concentrates. This was done to check whether the measurements were reproducible at different dilution ratios. The measurements of the rougher feed, rougher concentrates 2, 3, 4 and 7 were reproducible at the different dilution ratios. The EFC at different dilution ratios for rougher concentrate 2 was different because the bubble size at dilution ratio of 1:5 which was 1.12mm was too small. This bubble size was in the flat portion of the curve and not the decay portion which resulted in an inaccurate measurement, which was therefore discarded.

The rougher feed EFC displayed is the EFC before the addition of frother and before the primary cleaner tails. This measurement was relatively high at 20 ppm before frother addition implying a high residual frother concentration. The EFC for the rougher concentrates are also high which follows the rougher feed. Hence it is possible that the concentration of residual frother in the rougher feed was high, possibly due to pumping of spillage containing frother into the rougher feed sump.

Table 15: Measurements of the equivalent frother concentrations in the process streams for the rougher bank at Plant B UG2 Concentrator.

Process Stream	Dilution Factor/ (Dilution Ratio)	Measured Sauter Mean Bubble Diameter (mm)	Diluted Equivalent Frother Concentration (ppm)	Equivalent frother concentration (ppm)
Rougher Feed	1.6 (0.6:1)	1.2	12.1	19.4
	13 (1:12)	2.91	1.6	20.9
Rougher Cell 5 Tail	6 (1:5)	2.05	4.1	24.4
Rougher Cell 10 Tail	6 (1:5)	2.07	4.0	24.0
Rougher Conc 1	6 (1:5)	1.47	7.6	45.6
Rougher Conc 2	6 (1:5)	1.12	16.3	97.6
	9 (1:8)	1.84	5.0	45.0
Rougher Conc 3	6 (1:5)	1.40	8.3	50.0
	9 (1:8)	1.87	4.8	43.5
Rougher Conc 4	6 (1:5)	1.59	6.5	39.2
	8 (1:8)	1.86	4.9	39.3
Rougher Conc 5	6 (1:5)	1.86	4.9	29.5
Rougher Conc 6	6 (1:5)	1.79	5.3	31.6
Rougher Conc 7	6 (1:5)	1.91	4.7	28
	8 (1:7)	2.12	3.8	30.2
Rougher Conc 8	6 (1:5)	1.83	5.1	30.5
Rougher Conc 9	6 (1:5)	1.97	4.4	26.3
Rougher Conc 10	6 (1:5)	1.94	4.5	27.1

Table 16 shows the mass balance results for the EFC for the rougher bank at Plant B UG2 Concentrator. It can be seen that the adjustments to the measured data on the rougher concentrates were small. However, there was a significant adjustment made to both the rougher cell 5 and 10 tail stream. This was expected because these samples were difficult to take for each bank and was taken at the drain valve of the cell.

Table 16: Mass Balance Results for EFC for rougher bank at Plant B UG2 Concentrator

Process Stream	Measured EFC (ppm)	Balanced EFC (ppm)
Rougher feed into each bank after frother addition	-	30.9
Rougher Cell 5 Tail	24.4	30.1
Rougher Cell 10 Tail	24.02	31.2
Rougher Conc 1	45.6	45.9
Rougher Conc 2	45.0	45.4
Rougher Conc 3	46.8	47.2
Rougher Conc 4	39.2	39.6
Rougher Conc 5	29.5	29.7
Rougher Conc 6	31.6	31.8
Rougher Conc 7	29.1	29.4
Rougher Conc 8	30.5	30.9
Rougher Conc 9	26.3	26.5
Rougher Conc 10	27.1	27.4

Figure 56 shows the EFC for the rougher feed, concentrates and tails obtained from the mass balance. It can be seen that the EFC for the rougher concentrates 1-4 are higher than the other concentrates. This could be attributed to different cell operating conditions such as air and levels. The remaining concentrates are similar to the bulk water streams indicated by the rougher feed and tails. The EFC of the rougher feed and tails streams were similar, implying that the bulk of the frother remains in the bulk water stream which was also observed by (Gelinas and Finch, 2007; Hadler et al, 2005; Tsatouhas et al. 2005).

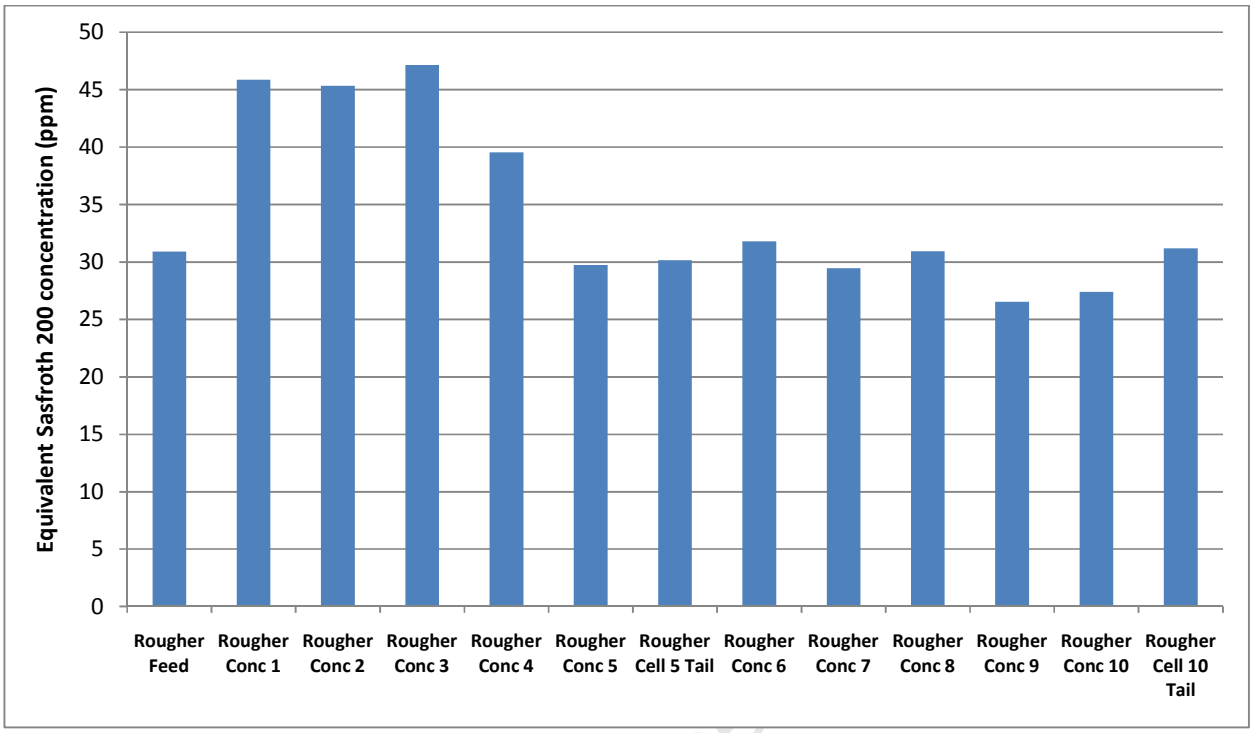

Figure 56: Equivalent Sasfroth 200 concentrations in process streams for Plant B UG2 concentratorroughers.

Figure 57 shows the cumulative equivalent Sasfroth 200 concentrations against the cumulative water recovery for the individual rougher banks and the combined rougher banks. It can be seen that the relationships fitted straight lines passing through the origin with excellent fits. The R^2 values for all three graphs were greater than 0.98. Furthermore, the frother recoveries are similar to the water recoveries which were observed by Tsatouhas et al (2005) which indicate that the frother moves with the water phase. It can be seen that the straight line relationship for rougher cells 1-5 was higher than that of rougher cells 6-10. This again could be due to the different operating conditions such as air and level of the cells which are indicated by the difference in cumulative water recoveries between both banks down the bank.

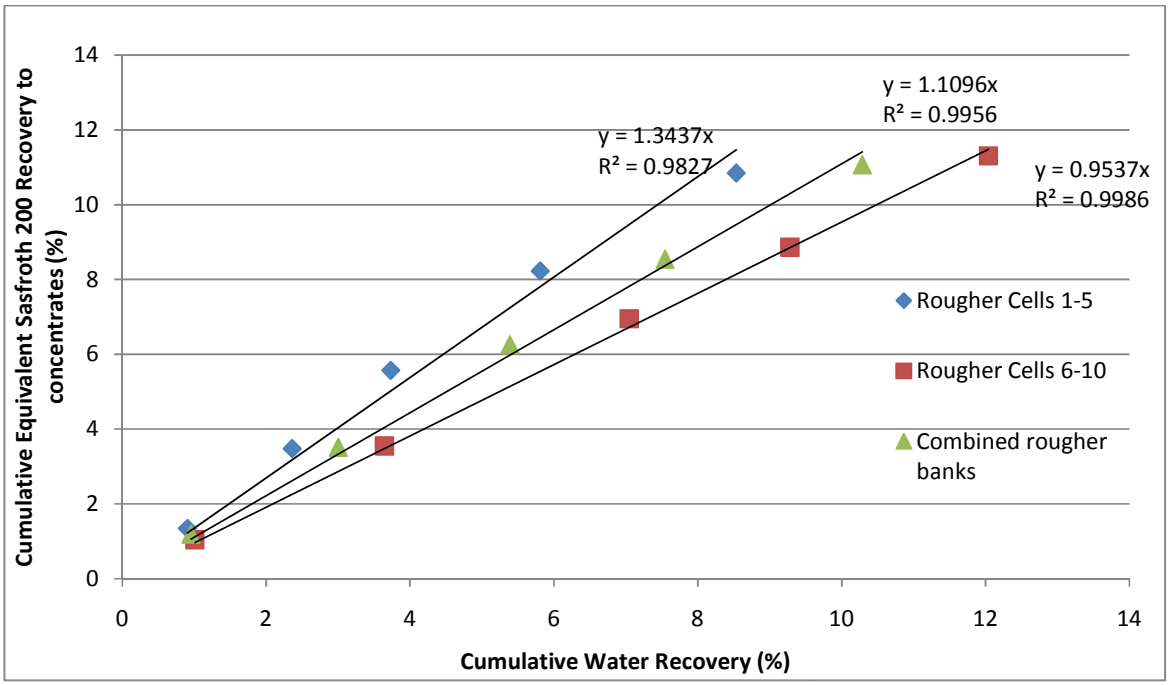

Figure 57: Cumulative equivalent sasfroth 200 recovery to concentrate vs. cumulative water recovery to concentrate for Plant B UG2 Concentrator down the rougher banks (combined).

.

6.3 Using the relationship between Sauter mean bubble diameter and superficial gas velocity to detect frother depletion in a flotation bank of identical cells

This was investigated in the cleaner circuit at Plant D concentrator. Plant D concentrator treats Platreef ore. Platreef ore contains larger amounts of base metals and alteration silicate minerals than the UG2 and Merensky reefs. The frother used in the process is Betafroth 206 which is a polyglycol type frother. It was assumed that effects of Betafroth 206C and 206 would be similar. Hence measurements of the CCC for Betafroth 206C were used as a reference for the effect of Betafroth 206 on bubble size.

Figure 58 shows the relationship between Sauter mean bubble diameter and superficial gas velocity for the first four cells in series in the secondary cleaner bank at Plant D concentrator. This cleaner bank was being fed with frother, which was of sufficient dosage to be in excess of the CCC. The graphs show that, generally, all the data points lie on a common line, which was the initial hypothesis. Hence this technique was then applied to detect depletion of frother in a bank which showed poor froth stability. This was the cleaner scavenger bank which did not receive any frother.

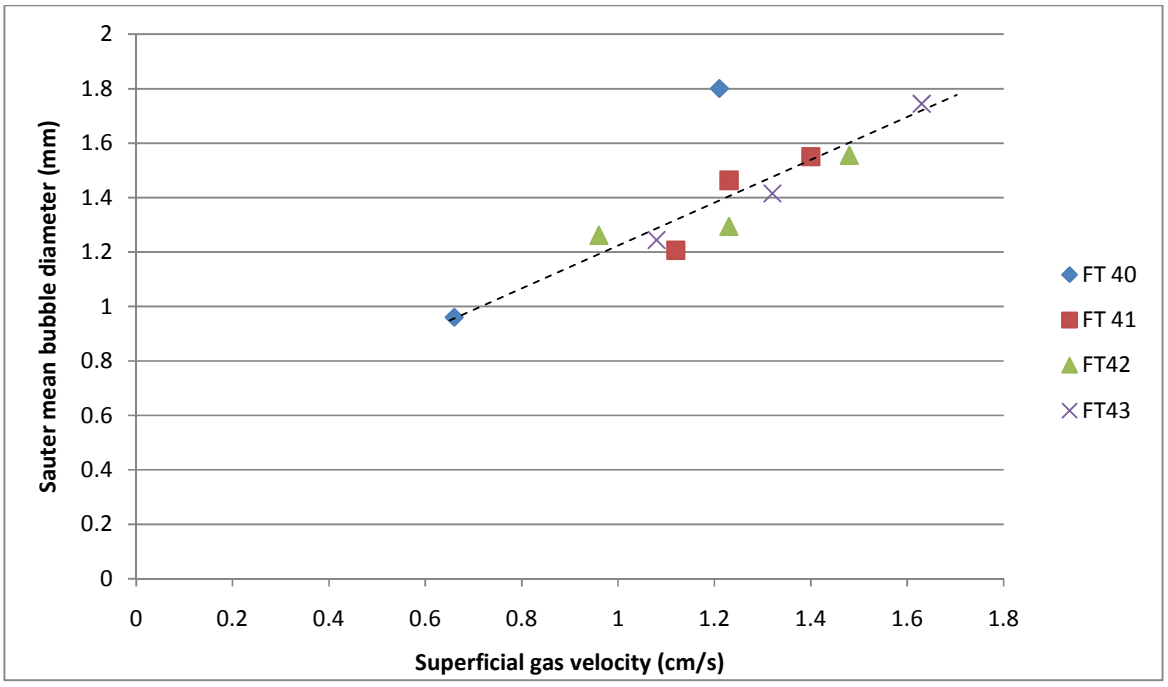

Figure 58: Graph of Sauter mean bubble diameter and superficial gas velocity for the first four cells in series in a secondary cleaner bank.

Figure 59 shows the Sauter mean bubble diameter and superficial gas velocity relationship for the 6 identical cells in series in a cleaner scavenger bank at Plant D concentrator which showed poor froth stability. There was no frother being added to this bank. The last few cells on the cleaner scavenger bank showed poor froth stability and struggled to pull mass under normal operation. The results showed that the relationships for FT59 and FT60 lie on the same straight line. However the relationships for cells FT61-64 continue to shift upwards. This implies that down the bank, for a given

superficial gas velocity the bubble sizes were increasing. Furthermore this could not be attributed to a mechanical problem on the cells because it is unlikely that all four cells would have the same problem simultaneously. Hence in conjunction with the poor froth stability, this was a sign of frother depletion in the bank.

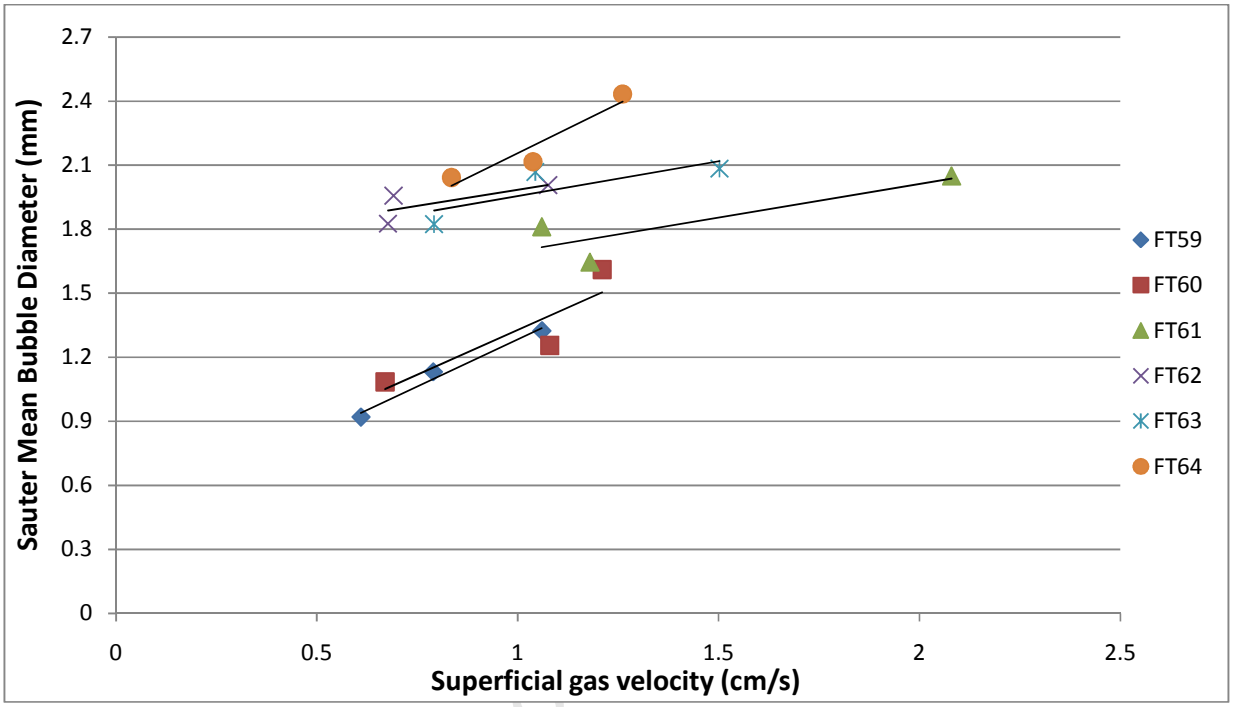

Figure 59: Graph of Sauter mean bubble diameter and superficial gas velocity for 6 cells in series in a cleaner scavenger bank where no frother was added.

The first two cells in the cleaner scavenger bank had good froth stability and were pulling mass. They did not show signs of frother depletion. However from FT 61-64 there were clear signs of frother depletion. Hence it was decided to dose frother on FT61. The frother dosage rate for the bank was determined by calculating the water flow in the feed to the bank and the targeted frother concentration. It was decided however to gradually increase the frother dosage rate and monitor the change in bubble size in the last cleaner scavenger cell at a fixed air rate.

Figure 60 shows the effect of increasing the frother dosage rate on the bubble size in FT64 measured as a function of time. The frother dosage rate was increased at regular intervals and the visual impact on the froth phase was also monitored. It can be seen that the bubble size decreased as the frother dosage rate was increased, which was expected. The frother dosage rate chosen was 3.84 kg/hr which translates to a target concentration of approximately 15ppm. At this dosage rate, the froth structure on the cells improved dramatically and the bubble size measured at this dosage rate was considered small enough.

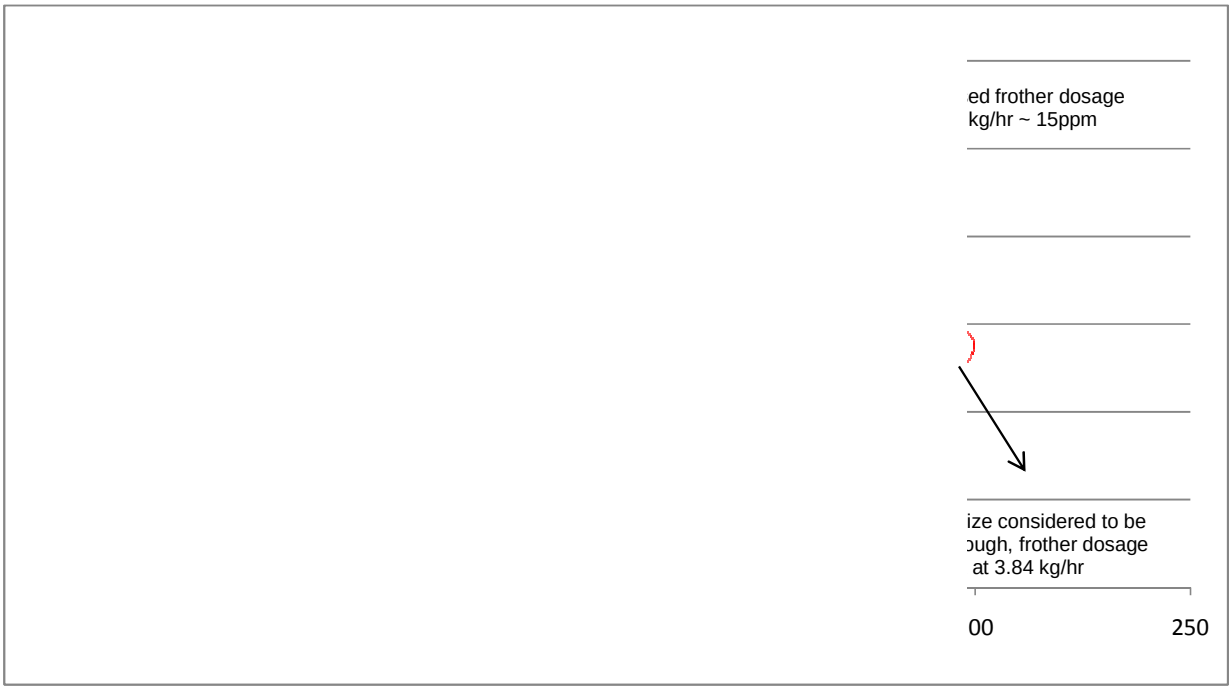

Figure 60: Graph showing the Sauter mean bubble diameter over time in the last cleaner scavenger cell as the frother dosage was increased at different intervals.

Once the frother dosage rate was established and set, the relationship between Sauter mean bubble diameter and superficial gas velocity was measured again on the cleaner scavenger bank to investigate the effect with the addition of frother. Figure 61 shows the relationships between Sauter mean bubble diameter and superficial gas velocity for the cells in the cleaner scavenger bank after the addition of frother. It can be seen that all the data points are now on the same straight line. Hence this indicates that the frother concentration in the bank was now greater than or equal to the CCC.

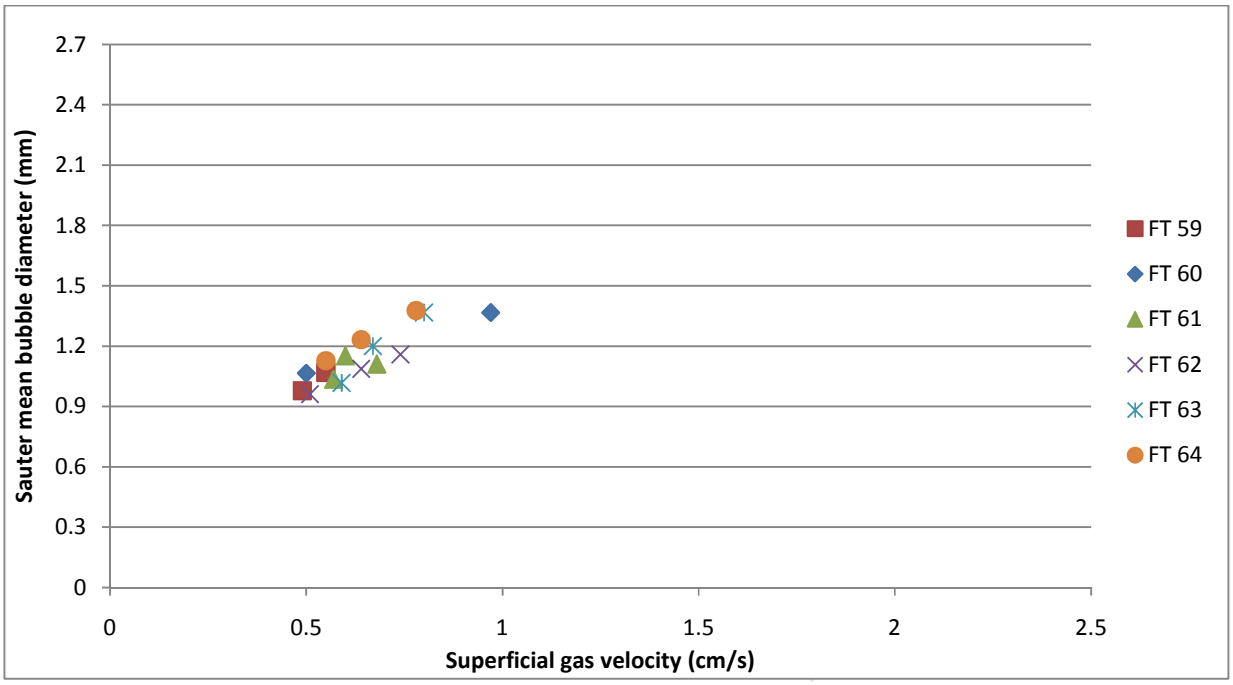

Figure 61: Graph of Sauter mean bubble diameter and superficial gas velocity for the same cleaner scavenger bank after frother was added on FT 61.

6.4 Survey Results for Cleaner Scavenger Bank at Plant D concentrator

The effect of dosing additional frother in Section 0 on the overall flotation performance of the bank was investigated by performing a survey before and after the frother addition. These surveys were performed over an hour and on the same day to allow a comparison to be made.

Figure 62 shows the process flow diagram of the cleaner scavenger bank at Plant D concentrator. The fresh feed to the cleaner scavenger bank is the tail from the secondary cleaners. This is the last cleaner stage in the process. Depressant and collector were the only reagents being dosed at the feed of the bank. The bank operates by recycling the last four concentrates to the feed and sending the first two concentrates to the final plant concentrate. The sampling points are indicated with red stars and the frother dosage point is indicated on the diagram.

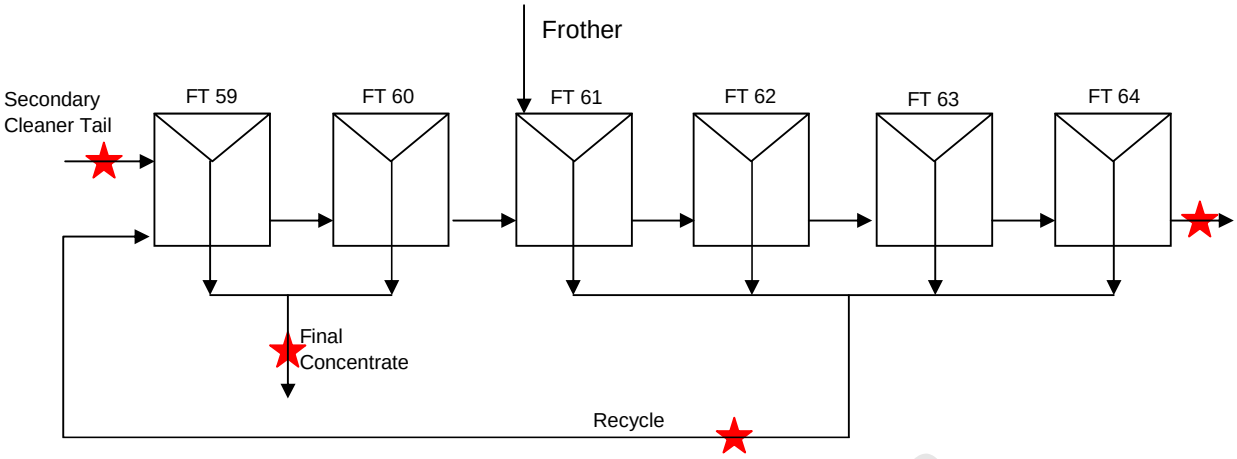

Figure 62: Process flow diagram of the Cleaner Scavenger bank showing the sampling points and the frother addition point

Figure 63 shows the normalised copper, nickel and 4E PGM grade for both surveys called S1 and S2. S1 or survey 1 is the "as found" (without frother) condition and S2 or survey 2 is the condition where frother was dosed on FT61. The copper and nickel grades were determined using an energy dispersive XRF. Figure 63 shows a slight decrease in normalised copper grade from 1 to 0.92%, but a significant increase in the normalised nickel grade from 1 to 1.36 %. 4E PGM grade refers to the combined grade of platinum, palldium, rhodium and gold which is determined by fire assay with lead sulphide collection. Similarly there is a significant increase in the normalised 4E PGM grade from 1 to 1.31 g/t.

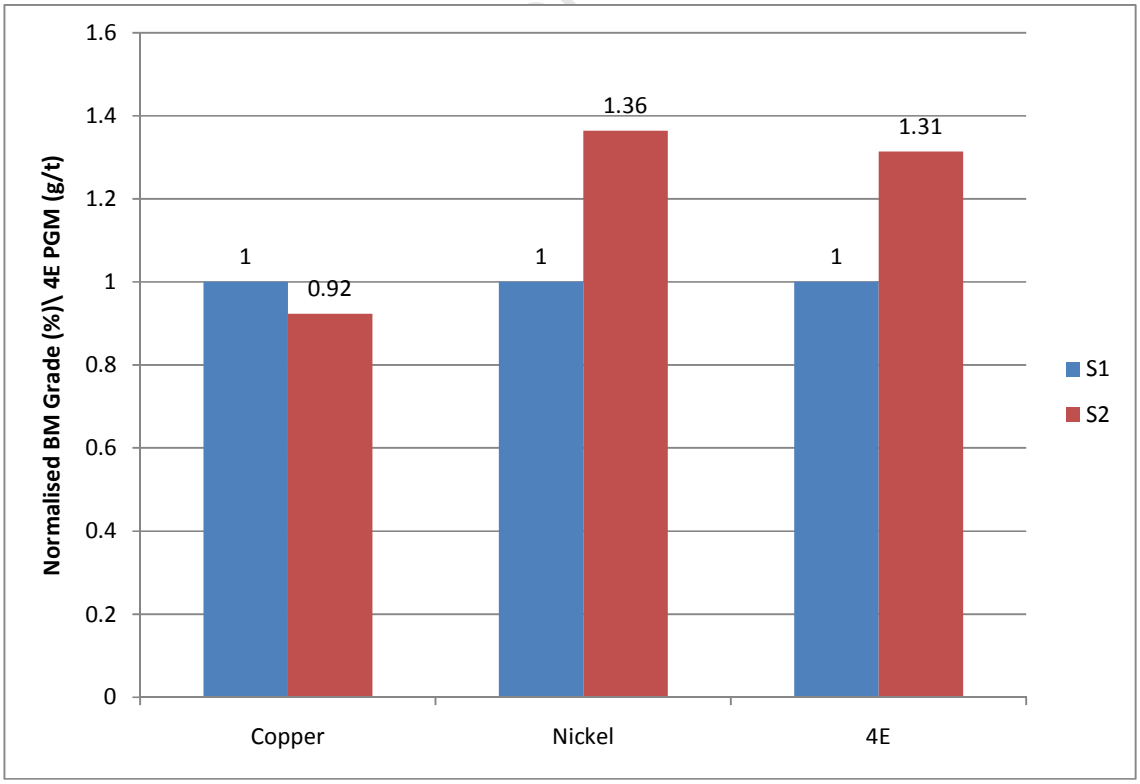

Figure 63: Comparison of the normalised copper, nickel and 4E grade for survey 1 (no frother) and survey 2 (with frother) on the final concentrate of the cleaner scavenger bank.

Figure 64 shows a comparison of the solids flow rate of the final concentrate leaving the cleaner scavengers before and after frother addition. It can be seen that there was a significant increase in the solids flow rate from 4.46 to 5.56 tph. It should be mentioned that for survey 1 the cleaner scavenger bank could not exceed this solids flow rate because of poor froth stability. However, after the addition of frother the froth stability improved and the flotation cells were able to pull more concentrate which resulted in an increase in the solids flow rate.

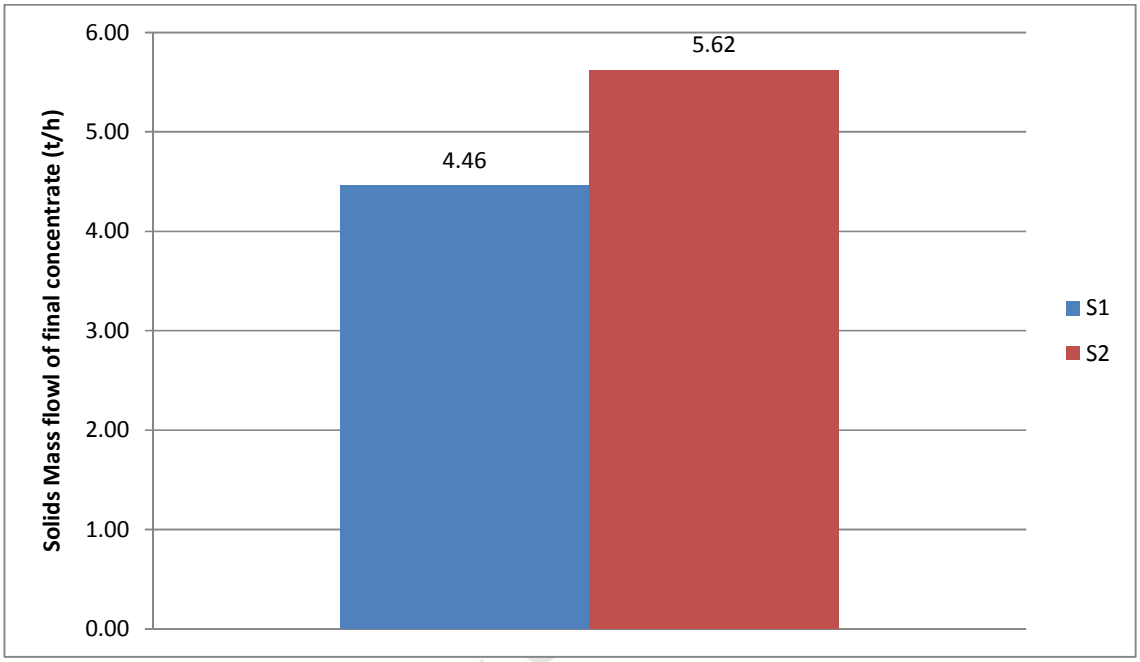

Figure 64: Comparison of the solids flow rate for surveys 1 and 2 of the final concentrate leaving the cleaner scavenger bank before and after frother addition respectively.

Figure 65 shows the bank recoveries for copper, nickel and Platinum Group Metals (PGMs). It can be seen that the addition of frother resulted in a significant improvement in recovery of base metals and PGMs. The recoveries of nickel and PGMs had a two-fold increase. There was also a significant increase in copper but not as dramatic as nickel and PGMs. This can be expected because copper floats as chalcopyrite which is considered a fast floater; hence the bulk of the copper would have been recovered in the previous cleaning stages. The increases in recoveries also came at an increased grade which implies that there was an upward shift in the grade/recovery relationship for the bank for nickel and PGMs.

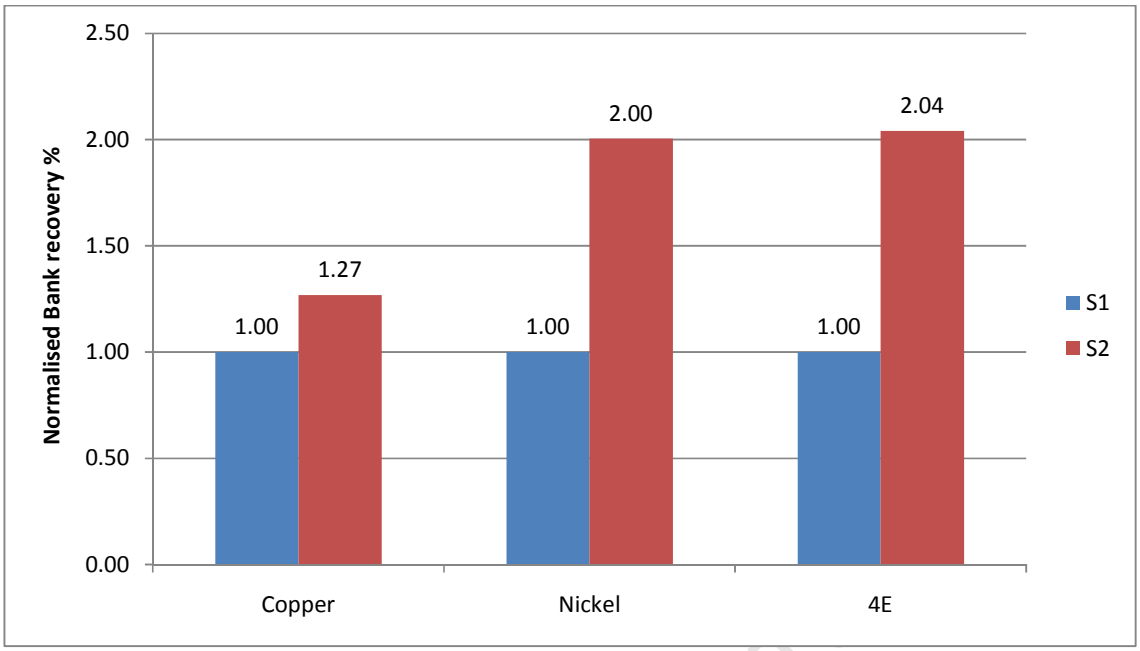

Figure 65: Comparison of the normalised bank recoveries for base metals and PGMs between survey 1 and 2 for the Cleaner Scavengers before and after frother addition respectively.

7 Discussion

7.1 Technique for determining the relationship between Sauter mean bubble diameter and frother concentration

There are different techniques and experimental setups in literature for determining the relationship between Sauter mean bubble diameter and frother concentration in laboratory/pilot scale (Cho and Laskowski, 2002; Finch et al, 2008; Nesset et al, 2006; Nesset et al, 2007; Grau et al, 2005).

Cho and Laskowski (2002) performed measurements using a single hole and three hole sparger as well as in a Leeds cell. These measurements were made in a two phase air/water system. Bubble size measurements were conducted with the different spargers in a 3 litre plexiglass tank at different aqueous concentrations of frother in the tank. Bubbles were generated at the sparger, and a coalescence funnel was used to allow the bubbles to collide after generation. The bubbles generated coalesced differently based on the concentration of frother in the plexiglass tank. The resulting bubble size was then measured with the UCT bubble sizer. In the open top Leeds cell, bubbles collided frequently because of the stirring action and turbulence created at the impeller. Similarly the bubbles coalesced differently based on the different concentrations of frother in the Leeds cell, and the resulting bubble size was measured using the UCT bubble sizer. Hence, the system consisted of a bubble generation device, a mechanism of bubble contact, a water/frother aqueous environment, and a bubble size measurement device.

Nesset et al (2006, 2007) performed measurements in a 0.8 m^3 Metso pilot cell as shown in Figure 8. The cell was fitted with gas velocity and gas hold up probes. Bubble size measurements were performed with the Bubble Viewer which used image analysis. The operation of the Bubble Viewer is described in 2.4.9.1. Measurements were carried out in a two phase air/water system. Montreal tap water was used in the cell and frother was dosed into the cell to achieve different concentrations. The frother was conditioning in the cell for 10 minutes without air addition before measurements were made. In this experimental set up, a mechanical cell was used to generate bubbles, the turbulence created by the cell mechanism allowed for bubble contact in a water/ frother aqueous environment and the bubble viewer was used as the bubble measurement device.

Cho and Laskowski (2002), Grau et al (2005) and Nesset et al (2006, 2007) have successfully demonstrated and established the above mentioned experimental apparatus and procedure for a laboratory scale/pilot scale application. However, the practical application of such in a plant environment is a challenge. The very nature and role of the plant metallurgist on a plant makes it impractical to set up and maintain such an experimental apparatus as mentioned above, let alone justify the costs. However, there are a few tools available, one such tool is the AAPBS.

7.1.1 Technique 1

Technique 1 was applied to Plant A which was using Betafroth 206C as the plant frother. Betafroth 206C is a polyglycol type frother of molecular weight of approximately 200g/mol.

Technique 1 involved dosing frother at different rates into the first rougher cell. The frother dosage rates were set to achieve different frother concentrations in the cell. The assumption made was that the frother concentration in the rougher feed was negligible. The actual dosage rates were determined by calculating the water flow rate into the first rougher cell using volumetric flow and density. The bubble size was measured in the cell at each frother concentration. Figure 66 shows the experimental

setup for technique 1. This experimental set up is similar to the setup described by Nesset et al (2006, 2007), however there are differences. The system is three phase, there is a mixture of solids, water and air. The cell is an actual operational industrial cell in a flotation plant and is subject to process operating conditions. The experimental setup does have a bubble generating mechanism which is the cell rotor/stator mechanism. Bubble-bubble contact occurs in the turbulent impeller region. The hydraulic environment however is not two phase, there is water, solids and air. It was assumed that the presence of solids would not significantly affect the coalescence mechanism. It was expected that at different concentrations in the cell, the bubbles would coalesce to different degrees in the turbulent zone and the resulting bubble size in the quiescent zone would be measured by the AAPBS.

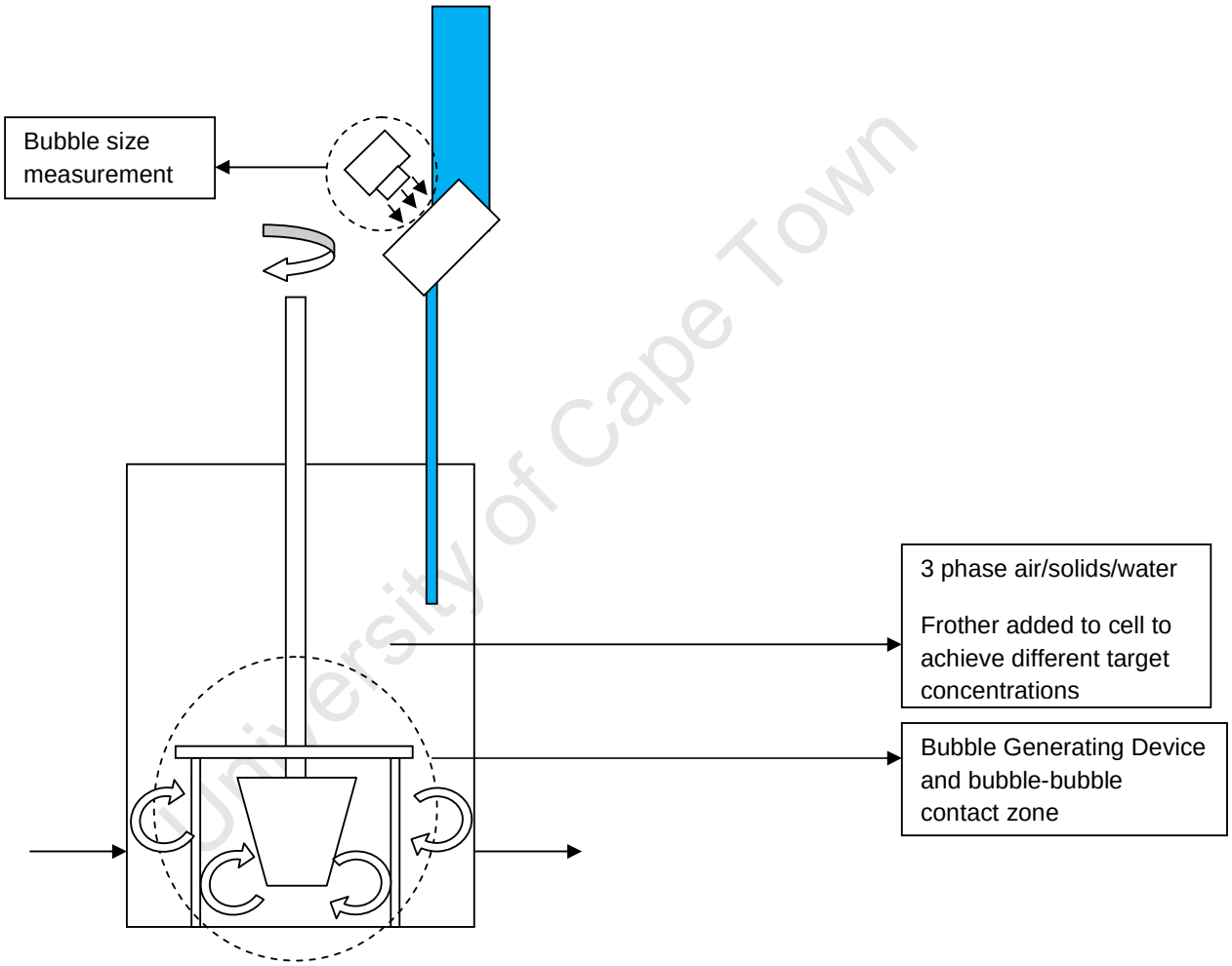

Figure 66: Experimental set up for technique 1

The results are shown in Table 4, Figure 38 and Figure 39. The results obtained do not display the relationship between bubble size and frother concentration observed by (Cho and Laskowski, 2002; Nesset et al, 2006, 2007; Grau et al, 2005, Finch et al, 2008). In fact there is no correlation between the bubble size and frother concentration. The rougher feed flow rate and density were relatively constant. However, there was a change in the superficial gas velocity between the runs which is known to affect the bubble size (Gorain et al, 1995). There was a trend with the bubble size increasing as the superficial gas velocity increased, except at an air rate of 0.8 cm/s which resulted in the largest bubble size which was anomalous.

The bubble size at zero frother concentration was already small compared to typical measurements in mechanically agitated cells (Gorain et al, 1995). Similarly the bubble size distributions were unimodal at the low frother concentrations which is a characteristic typical of high frother concentrations in excess of the CCC. This implies that the initial assumption of negligible frother concentration in the rougher feed may have been incorrect. There could have been residual frother coming from sources of spillage in the process. This is not uncommon in flotation plants.

Furthermore applying this technique on a full scale plant adds a significant amount of process instability. The frother dosage to the entire rougher has to be changed and this will affect the entire rougher flotation circuit. Applying this technique takes a considerable amount of time to complete and this will result in prolonged instability in the circuit which will negatively affect the process. Thus, this technique was rejected in favour of technique 2.

7.1.2 Technique 2

The experimental set up for technique 2 is shown in Figure 67. The experimental setup shows the experimental conditions are in fact similar to the conditions for the experiments conducted by (Cho and Laskowski, 2002; Grau et al, 2005; Nesset et al (2006, 2007) as discussed below.

Technique 2 is applied to the plant under normal operation. It involves depleting the first rougher cell of frother by sending the frother into the second cell. This isolates the first rougher cell and allows the rest of the bank to operate as normal. The first rougher cell is used purely as a bubble generating device. Air is blown into the cell; the rotor and stator shear and disperse the air into fine bubbles. The AAPBS is mounted in the cell in the quiescent zone of the cell and is kept at a fixed location, this is important because the bubble size distribution is different at different points in the cell (Gorain et al, 1995). The AAPBS consists of a 5 litre water reservoir and 3 metre long tubes which are immersed in the rougher cell and the predominant phases are air and water. The AAPBS does receive a small portion of particles attached to air bubbles but this is minimal. Hence, the environment is an air-water system. Different concentrations of frother were made in 8 litres of tap water and were added to the water reservoir of the AAPBS. Hence the environment is a water/frother aqueous solution. The bubbles enter the bubble riser tube from the cell. The tube has a diameter of approximately 25 mm, which is narrow and this allows for bubble-bubble collision and contact. Bubble-bubble contact and coalescence is known to occur in the AAPBS and it has been recommended by the manufacturer that sufficient frother should be added to preserve the bubble size distribution received from the cell. The tube is 3 metres in length and considering that superficial gas velocities were in the order of 1cm/s, this should be enough time for bubble-bubble contact. Furthermore, the long and narrow dimensions of the tube simulate a “plug flow” type of environment which implies good axial and radial mixing. The bubbles coalesce and interact differently based on the different concentrations of frother in solution. Thereafter the bubbles pass through the viewing pane and images were taken of the bubbles for analysis. Hence the experimental setup for technique 2 very closely resembled the experimental conditions required for the experiments conducted by Cho and Laskowski (2002) and Nesset et al (2006, 2007). There is a bubble generating device, a bubble contact zone, water/frother solution, and bubble size measurement. Furthermore, it should be mentioned that this technique is simple to use. Many concentrator plants have the AAPBS and it would require one or a maximum of two people to perform this technique.

It is important to note that air rate was kept constant on scada but a plant environment is not as well controlled as a laboratory or pilot scale because of many variables which affect the air rate. These variables include but are not limited to blower pressures, instrument air for control, air controller tuning, change in air temperature and maintenance of equipment. Hence the relationship for the bubble size and frother concentration were not reported at a specific air rate but a range which was kept as far as possible to between 0.7-0.9 cm/s for all the tests.

It is clear that technique 2 uses two phase air/water environment to perform measurements of bubble coalescence, and this environment is different from a operational flotation cell which operates in a three phase air/water/solids environment. Other factors may affect coalescence such as the ionic content of the process water as well as the solids concentration in the cell. The effect of ionic strength will be discussed later in the discussion. Both the presence of ions and solids will reduce bubble coalescence hence it could imply that less frother will be required to achieve a target bubble size in the flotation cell.

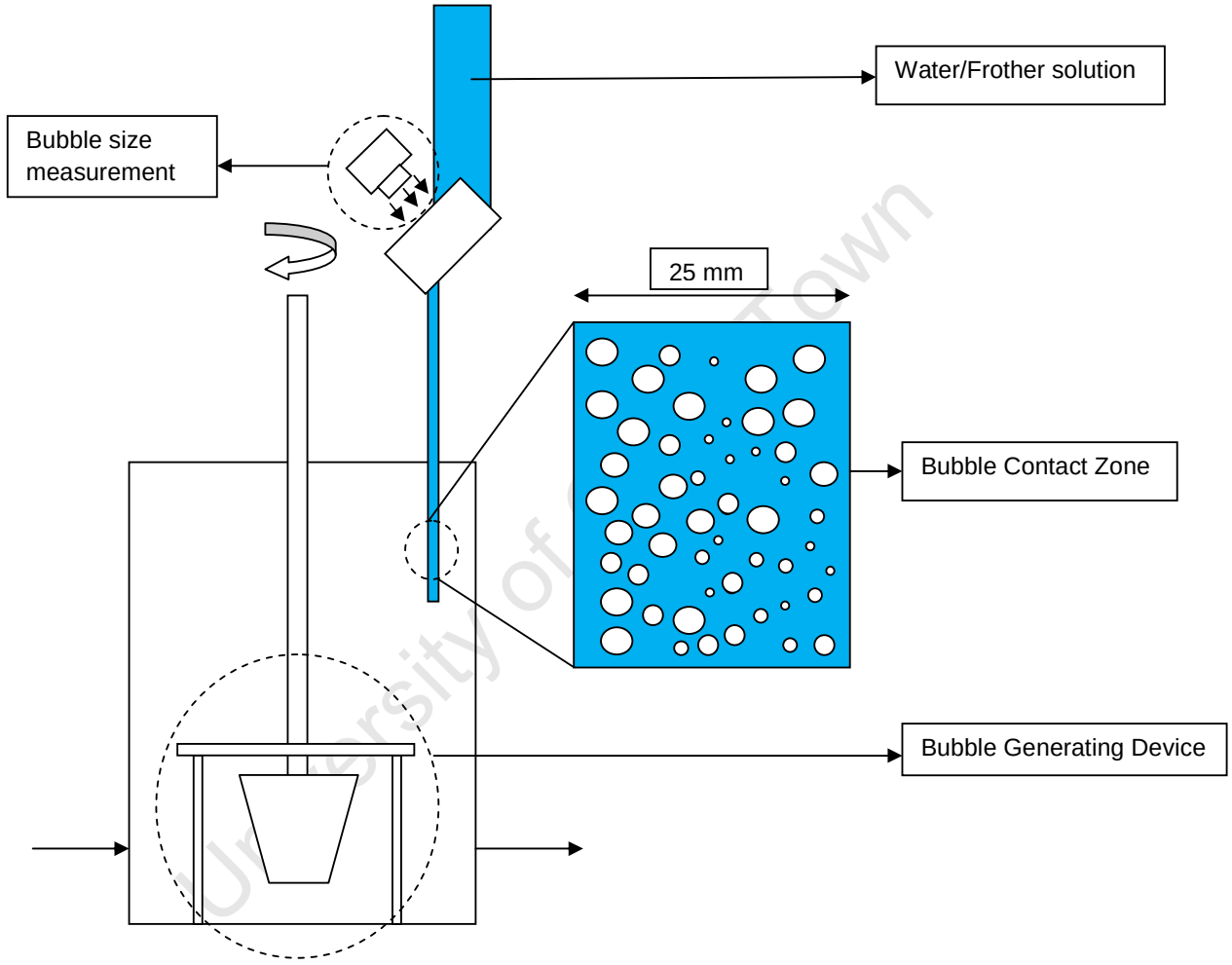

Figure 67: Experimental set up for technique 2

This technique was first applied at Plant A which was using Betafroth 206C as the plant frother. Rustenburg tap water was used to make up the frother concentrations. The results are shown in Table 5, Table 6, Figure 40 and Figure 41. For test 1 the bubble size was large at zero frother concentration and as the frother concentration increased the bubble size decreased until after a point there was no further reduction in bubble size with increasing frother concentration. This was similar to the relationship found in literature (Cho and Laskowski, 2002; Finch et al, 2008; Nesset et al, 2006; Nesset et al, 2007; Grau et al, 2005). However the experimental concentrations used did not clearly define the decay portion of the relationship, the CCC appeared to be close to 10 ppm. Hence the technique was repeated with more data points in the 0-10ppm range (test 2). Figure 40 showed that the experimental concentrations for test 2 clearly defined the decay portion of the relationship. Furthermore, the curves for test 1 and test 2 were clearly similar. Both test 1 and 2 were fitted with the

exponential decay relationship described by (Comley et al, 2002; Nesset et al, 2006). The fit of the model for both tests was excellent.

Grau et al (2005) showed that the CCC of a given frother is a material constant, hence for different bubble generation mechanisms the measurement of the CCC will be the same. Hence the CCC was compared to the CCC of a polyglycol frother similar molecular weight measured in literature. For both test 1 and test 2, the CCC was at approximately 7-8 ppm for Betafroth 206C which was in the typical range for polyglycol frothers of molecular weight 200 g/ mol (Nesset et al, 2006).

Figure 41 shows the bubble size frequency distributions obtained for test 2. The relationship shows that the bubble size distribution at zero frother concentration (tap water) was bimodal. There were predominantly coarse bubbles and fine bubbles of sizes 3.5 and 0.30 mm respectively. As the frother concentration increased bubble size distribution became narrower and approached a unimodal distribution. In other words, the amount of coarse and fine bubbles decreased and the bubble size distribution approached unimodal. This was in agreement with bubble size distributions obtained by Nesset et al (2006) which are shown in Figure 9. These bubble size distributions can be compared because Nesset et al (2006) used a similar bubble generating mechanism; a forced air mechanical cell. Finch et al (2008) showed that this bubble size distribution is a result of the bubble coalescence mechanism. Finch et al (2008) took high rate camera images to investigate the mechanism from bubble-bubble contact to coalescence. These images are shown in Figure 12. The images show for Montreal tap water that there is an elongation of the bubbles when bubble-bubble contact occurs, and after coalescence a larger bubble is formed and a much finer bubble is released. It is also shown that with the addition of frother, the bubbles contact each but do not elongate and coalescence but merely bounce off each other. Hence this explains why the bubble size distribution gets narrower with increase in frother concentration. As the frother concentration increases, the coalescence mechanism is reduced and the amount of fine and coarse bubbles generated as a result decreases. The above results were in excellent agreement with the results obtained in literature. This implied that technique 2 is able to determine the relationship between frother concentration and bubble size on a full scale plant. The robustness of this technique was then tested by applying it on a different plant, a different frother, different cells and different cell sizes.

Test 3 and Test 4 were applied to test the application of technique 2 to a different frother, Sasfroth 200 to test reproducibility of technique 2. The measurements were performed in a 70m^3 Outokumpu forced air mechanical cell, which is the same cell size used for test 1 and 2. However, this was done in a different plant, Plant B UG2 Concentrator. Rustenburg tap water used to make up the frother concentrations. Test 3 and 4 were applied to investigate the application of technique 2 in 2 different cells of the same size, type and impeller speed but can be expected to have slightly different cell characteristics and bubble size distributions. The results are shown in Table 7, Table 8, Figure 42, Figure 43 and Figure 44. Similarly to previous tests the exponential decay relationships between bubble size and frother concentration was observed. Both experimental data sets and fitted data sets are in excellent agreement with the exponential decay relationship described by (Comley et al, 2002; Nesset et al, 2006). Figure 42 shows the comparison between the graphs obtained for test 3 and test 4. It can be seen that the graphs are almost identical; the experimental data points for both tests appear to lie on the same common line. Furthermore, the CCC for both tests 3 and 4 were almost identical at 10 ppm. Although the cell size, type and impeller speed were identical for both cells, it can be expected that these cells will have different characteristics such as gas dispersion and bubble size distributions because of differences in wear of the cell internals. However, it can be seen that under these conditions, the results obtained were identical and it can be said that technique 2 is reproducible.

Figure 43 and Figure 44 show the bubble size frequency distributions for test 3 and test 4. It can be seen that both distributions were bimodal at zero frother concentration. In both tests, the change in the bubble size distributions was the same. As the frother concentration increased, the bubble size

distribution became narrower and the proportion of fine and coarse bubbles decreased until the distribution approached a unimodal distribution. However there was a difference in the actual bubble size distributions for each test. By comparing the bubble size distribution at zero frother concentration this difference can be explained. Test 3 had an almost equal proportion of fine and coarse bubbles in the bimodal distribution but test 4 had a larger proportion of coarse bubbles than fine bubbles. Furthermore, there was a significant difference in the coarse bubble size. Test 3 had coarse and fine bubble sizes of approximately 3 and 0.28 mm. Test 4 had coarse and fine bubble sizes of 2.2 and 0.28 mm respectively. This can be explained using the coalescence mechanism described by Finch et al (2008). The differences can be attributed to bubble coalescence. It is possible that the degree of coalescence at zero frother concentration for test 4 was less than test 3. This is indicated by the smaller coarse bubble size of 2.2mm compared to 3 mm in test 3. Furthermore, the proportion of fine bubbles which is a product of bubble coalescence was less, implying lesser coalescence. There is the possibility that test 4 may have been contaminated with frother. Care was taken to ensure there was no frother present in the tap water used and that the rougher cell was depleted of frother. Contamination of the tap water is unlikely but the presence of residual frother in the rougher cell could be possible. This could have been due to the pumping of spillage containing frother into the cell which is not an uncommon event in process plants. Another observation between test 3 and test 4 is the above mentioned fine bubble size is the same for both tests, which is 0.28 mm. This is common in both tests which imply that this bubble size could be the size of the fine bubbles released during the coalescence mechanism, and hence could be an indication of the degree of coalescence.

Test 2 and Test 3 were used for comparison between Betafroth 206C and Sasfroth 200 respectively. Both Betafroth 206C and Sasfroth 200 are polyglycol type frothers and are reported by their manufacturer to have a molecular weight of approximately 200 g/mol. Both of these frothers are mixtures of organic molecules, hence it can be expected that the mixture compositions for Betafroth 206C and Sasfroth 200 will be different. Figure 45 shows the graphs of the relationships between Sauter mean bubble diameter and frother concentration for Betafroth 206C and Sasfroth 200. It can be seen that both frothers have a similar exponential decay relationship between bubble size and frother concentration. However, the graph of Betafroth 206C is shifted down relative to the graph of Sasfroth 200 in the decay portion of the relationship. This could imply that Betafroth 206C has a slighlty stronger reduction in bubble size with frother concentration than Sasfroth 200. This is proved by the fact that the CCC of Betafroth 206C was 8 ppm, which is lower than the CCC for Sasfroth 200, which was 10 ppm. This is possible because the actual compositions of the mixture for each frother could be different. **Error! Reference source not found.** shows the typical composition of Sasfroth 200. It can be seen that there is a mixture of different organic molecules which are polyglycol ethers and alcohols. Cho and Laskowski (2002) and Nesset et al (2006) showed that different pure organic molecules will have different effects on bubble size. The general trend was that alcohols have lesser effect in reducing bubble size compared to polyglycol ethers. Hence depending on the compositions of alcohols and polyglycol ethers, the effect of the overall mixture could be different. In addition, it has been shown that certain frother mixtures result in a synergistic effect (Tan et al, 2005). Hence the difference in compositions between Betafroth 206C and Sasfroth 200 could have resulted in the different effect on bubble size. Frother manufacturers do not disclose the mixture compositions because of the protection of intellectual property. However, when manufacturers propose alternative frother mixtures that are cheaper or more effective, testing them in this way will provide an indication of the relative difference between the frothers. Cho and Laskowski (2002) showed that the strength of different frothers in a two phase air/water system could be characterised by CCC and the dynamic foamability index (DFI). It was shown that the frothers with lower CCC resulted in a higher DFI. There is difference in full scale plants because the froth phase is a three phase air/water/solid system. By inferring that the effect on froth stability (DFI) in two phase system will apply to a three phase system, the CCC can be used as an indication of the strength of the frother when comparing similar frother types.

Test 5 and 6 were done to investigate the application of technique 2 using the same frother in a rougher cell of different size. This was done at Plant C UG2 concentrator on the first rougher cell which was a 50m^3 Outokumpu forced air cell. Sasfroth 200 was the frother tested and also the frother used in the process plant. Potable water was used to make up frother concentrations. It will be useful to compare the results of applying this technique for the same frother but on different cell sizes. The difference in cell size will have a significant difference in the cell characteristics such as gas dispersion and bubble size generation compared to the 70m^3 rougher cell used in previous tests. This is important because it will provide an indication of the robustness of the application of technique 2 under completely different hydrodynamic conditions. The results for test 5 and 6 are shown in Table 10, Table 11, Figure 46, Figure 47, and Figure 48. Furthermore, test 5 and 6 were performed on the same rougher cell on different days; which provided an indication of the effect of different plant operating conditions. The results show that both test 5 and test 6 shows the exponential decay relationship seen in the previous tests. Hence the results are in agreement with the findings of (Cho and Laskowski, 2002; Nesset et al, 2006; Grau et al, 2005). The fitted model described by Comley et al (2002) and Nesset et al (2006) also fits the experimental data well. Figure 46 shows the graphs of the relationship between bubble size and frother concentration for test 5 and test 6. The graphs for test 5 and 6 overlap each other and are almost identical in the lower frother concentration region. However, there is a slight difference in the limiting bubble diameter at the higher frother concentrations which is approximately a 0.2 mm difference which is outside the experimental error of 2% for bubble size measurements. This could have been due to a difference in the air rates with possibly a slightly higher air rate for test 5 which elevated the limiting bubble size. Although the CCC95 is different between test 5 and test 6, the graphs obtained are very similar even under different plant operating conditions. However it should be considered that the CCC95 is close to the flat portion of the curve where the frother concentration is very sensitive to bubble size, Figure 47 and Figure 48 show the bubble size frequency distributions for test 5 and 6 respectively. The effect of frother concentration on the bubble size distribution is the same as those observed in test 3 and 4.

Figure 49 shows a comparison of the graphs of Sauter mean bubble diameter and frother concentration for Sasfroth 200 for tests 3,4,5 and 6 which were established on different cells, different cell sizes, different plants and at different times. It can be seen that all the graphs lie on the same common line which describes the relationship between frother concentration and bubble size for Sasfroth 200. The CCC95 for all the tests was an average of 10.6 ppm with a relative standard error of 4.4% which was within a 10% experimental error at an air rate of 0.7-0.9 cm/s in performed on a full scale plant which has much larger instability than a laboratory or pilot scale set up. Hence this implies that technique 2 can be considered to be robust, repeatable and reproducible on different plants, cell sizes and cell characteristics for mechanical forced air cells. Similarly this finding also agrees with the findings of Grau et al (2005) in which the CCC for a given frother could be treated as a material constant. Grau et al (2005) found that the measurement of the CCC for a given frother was the same by using different bubble generating devices.

For all the tests conducted on Sasfroth 200, the measurement of the CCC was approximately 10.6 ppm on average. From the bubble size distributions, it can be seen that the distributions approached unimodal at a concentration of 15ppm, which represents the distribution generated by the impeller (Cho and Laskowski, 2002). Hence on a plant, when setting frother dosages it is desired that this bubble size distribution at impeller is preserved in the cell and coalescence is minimised. The exact mathematical estimation of the CCC and CCC95 has been defined by Cho and Laskowski (2002) and Nesset et al (2006). However a practical consideration when dosing frother on a plant could be that: dose at the frother concentration that gives a unimodal bubble size distribution which would be minimum of approximately 15ppm in this case.

7.2 Technique for estimating frother concentration in process streams

There are a few techniques reported in literature for determining frother concentration in process streams (Gelinas and Finch, 2007; Tsatouhas et al, 2005; Hadler et al. 2005; Weber et al, 2003). These included calorimetry, gas chromatography, total organic carbon, and using gas hold up as a proxy for frother concentration.

The above techniques (Gelinas and Finch, 2007; Tsatouhas et al, 2005; Hadler et al. 2005) require special experimental equipment which includes gas chromatographs, UV spectrophotometers etc. which are expensive and are better suited to a laboratory type of environment. Furthermore, these will require chemists to operate and maintain. These items will cost capital to install as well as maintenance costs which will be difficult to motivate on a plant. The technique described by Weber et al (2003) is more suitable to a plant environment; however it does require capital investment and maintenance cost for the experimental apparatus. Furthermore the technique described by Weber et al (2003) uses the effect of frother on gas hold up as an indication of frother concentration. Gas hold up and bubble size are related, the smaller the bubbles, the smaller the bubble rise velocity and the higher the gas hold up. The available tools on a plant are limited to the AAPBS which measures bubble size. Hence the use of bubble size as a proxy for frother concentration was investigated.

In this technique the AAPBS was set up on the first rougher cell in the same method as described for technique 2. The relationship between frother concentration and bubble size was then determined for the frother using technique 2. Samples of the process streams were taken and filtered. The aqueous solution for each process stream was then added into the AAPBS, and the bubble size was measured. This measurement of the bubble size using the aqueous solution is a measure of the effect of the solution on preventing bubble coalescence. Hence the bubble size can be translated into an equivalent concentration using the equation described by (Comley et al, 2002; Nesset et al, 2006) shown in equation 19 or graphically as shown in Figure 68. The A, B and d_{lim} are determined by model fitting the experimental data. The equivalent frother concentration (EFC) can be defined as the concentration of frother that would have the same effect on bubble coalescence as the process stream aqueous solution.

$$C_{frother} = \frac{\ln\left(\frac{d_{32}-d_{lim}}{A}\right)}{-B} \quad (19)$$

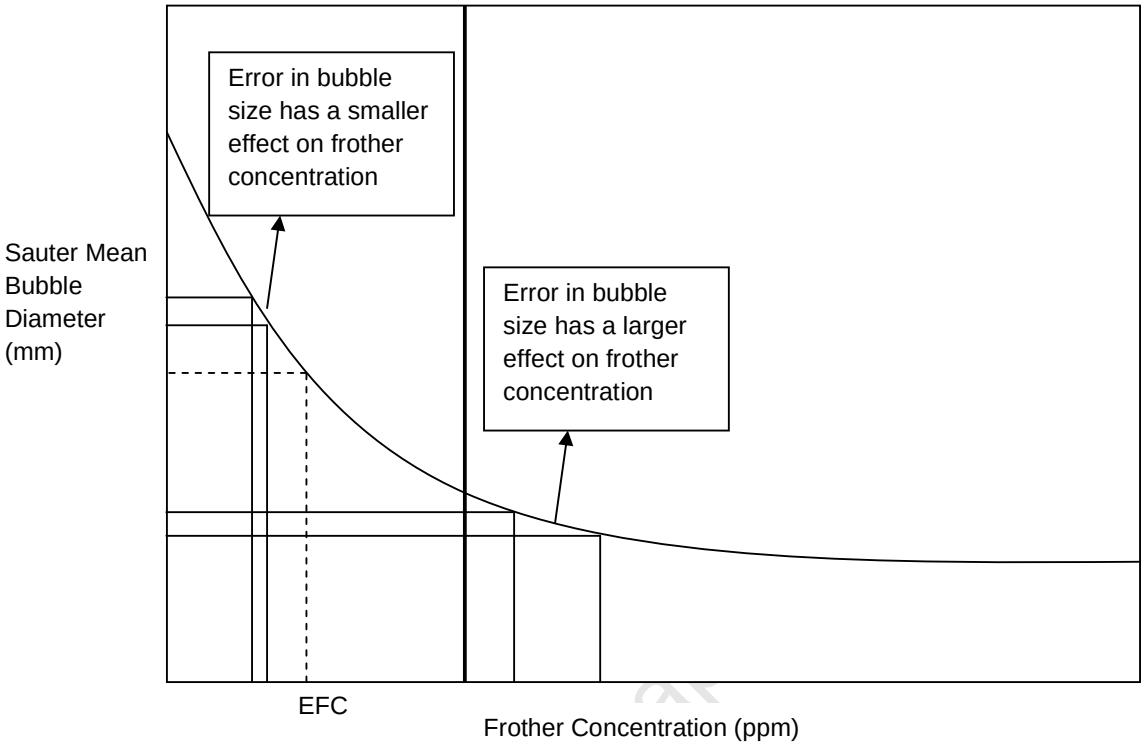

Figure 68: Measuring the equivalent frother concentration graphically

The above measurement of the EFC requires the bubble size measured to be in the decay portion of the relationship shown in Figure 68. The slope of the curve decreases as the frother concentration increases; this implies that, as the bubble size approaches d_{lim}, a small change in bubble size will result in a big change in the frother concentration which escalates the effect of experimental error in the bubble size measurement. In the case of the process stream aqueous solutions, the bubble size generated may be small due to already high concentration of frother present. This requires dilution of these solutions with potable water to ensure the bubble size measured is within the decay portion of the curve. This EFC is then multiplied by the dilution factor to determine the actual EFC in the aqueous solution of the process stream. The EFC measured in each process stream aqueous solution will include the effects of ions which are known to affect bubble size at high concentrations (Quinn et al, 2007).

7.2.1 Frother Balance at Plant C UG2 concentrator

This technique for measuring the EFC was applied to a rougher bank at Plant C UG2 concentrator as shown in Figure 50. The frother used on the plant was Sasfroth 200 which is a mixture of polyglycol ethers and alcohols. A survey of the rougher bank was performed where mass flow rates were taken of the rougher concentrates. Samples and mass percentage solids were taken of the rougher feed, concentrates and tail streams. These measurements were used to perform a water balance across the rougher bank. The samples of the process streams were filtered and the filtrate or aqueous solution was measured using the above technique. The EFC and water flows were used to perform a

frother balance for the rougher bank. The results are shown in Table 12, Table 13, Figure 52 and Figure 53.

The results shown in Table 12 showed that the aqueous solution from each of the process streams did affect bubble coalescence significantly implying the presence of frother. Furthermore these solutions had to be diluted with potable water in order for the bubble size measured to occur in the decay portion of the relationship. Potable water was used because it is known to contain zero frother concentration and it will be simpler to calculate the actual EFC for each stream using the dilution factors.

Table 13 showed that there was a small difference between the measured and balanced EFC implying the measured EFC data reconciled well. There was little difference between the rougher feed and rougher tail EFC and this implied that the most of the frother remained in the bulk water stream of the rougher bank which was also found by (Gelinas and Finch, 2007; Tsatouhas et al, 2005; Hadler et al. 2005). The rougher concentrates' EFC were generally higher than the EFC of the rougher feed and tails. It can be expected that frother will enter the froth phase either adsorbed onto bubbles or with entrained water entering the frother. The bulk of water recovered to the concentrate would be due to entrainment, with a small contribution from the films and from the Plateau borders of the froth structure. The frother concentration at these bubble interfaces would naturally be higher than the bulk water stream EFC accounting for the higher EFC found in the concentrates.

The differences between the rougher concentrates EFC could be due to the difference in cell operating conditions such as air rate and froth depth. Frother may enter the concentrate either by adsorption onto the bubbles or by entrained water. It can be expected that the adsorption of frother onto the bubble film will be at a higher concentration than in the entrained water stream. Hence air rates and froth depths may influence the amount of entrained water and number of bubbles reporting to the concentrates which could affect the overall frother concentration. This could also explain the difference in frother concentrations in the cells down the bank. Figure 69 shows the EFC for each of the rougher concentrates against the mass percentage solids of the concentrates. It can be seen that at a high percentage solids, the EFC was high and then decreased and remained relatively constant at a concentration similar to the bulk water concentration for any further decrease in mass percent solids. This is a complex mechanism but it appears there may be relationship with mass percent solids. At low percent solids, the mass is diluted with a lot of water and, therefore, one would expect the frother concentration to be similar to the bulk frother concentration. However, at high percent solids, the concentrate is relatively undiluted and much of the solids reporting to the concentrate did so by true flotation. Thus, the frother reporting to the concentrate is also relatively undiluted with water and gives a higher EFC.

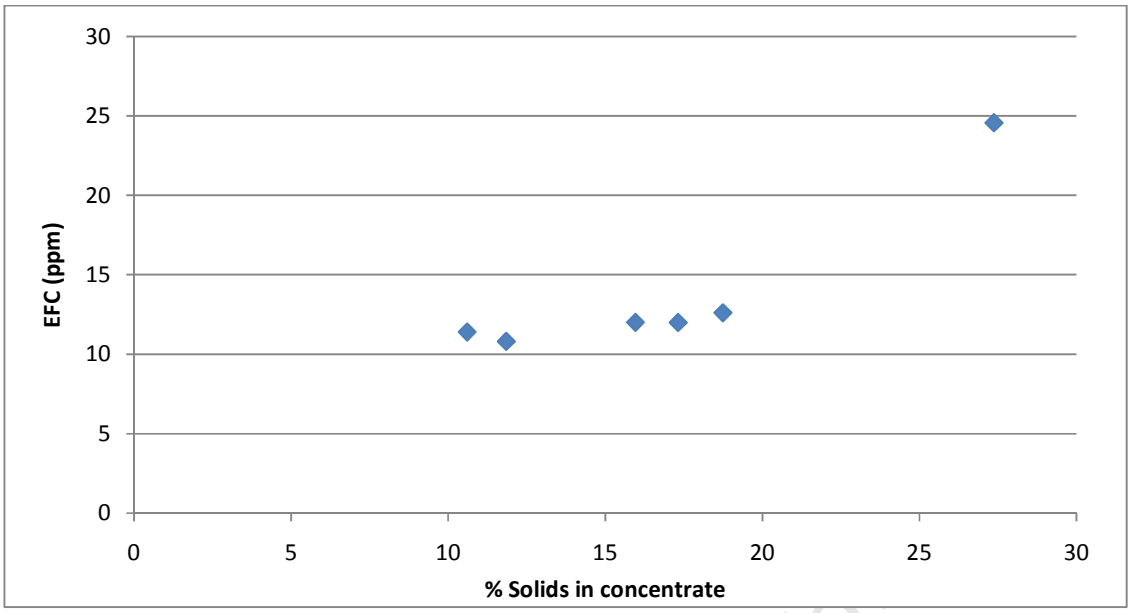

Figure 69: EFC vs. % solids of the concentrates in the rougher bank at Plant C UG2 concentrator

Figure 53 shows the cumulative frother recovery (based on EFC) and the cumulative water recovery for the rougher bank. It can be seen that the relationship is linear and can be fitted with a straight line passing through the origin. Hence this further illustrates that frother tends to follow the water stream.

7.2.2 Measurement of the concentration of dissolved ions in process stream aqueous solutions

Two sets of measurements were performed on the process stream aqueous solutions to measure the concentration of dissolved ions in solution which is shown in Table 14. The measurements indicate that the concentration of the ions in process streams are much lower than concentrations necessary to significantly affect bubble coalescence as shown by Quinn et al (2007). However, Manono et al (2013) showed that there was a small effect on bubble size with increasing ionic strength of process water. However, this was small (in the order of 0.2 mm) and probably lying within the range of experimental error. Hence it is unlikely that the dissolved ions would have significantly affected the EFC measurement. In any event, the concentration of ions in solution would have been more or less constant and would have exhibited a constant effect on the bubble size. From the above, it could be concluded that the effect on bubble coalescence of each of the solutions would have been predominantly due to frother.

7.2.3 Frother Balance at Plant B UG2 Concentrator

A frother balance was performed similarly at Plant B UG2 Concentrator on the rougher banks as shown in Figure 54. Sasfroth 200 was the frother used on the plant. The rougher at Plant B UG2 Concentrator consists of two parallel banks. The samples taken were of the feed, concentrates and tail. Mass flow rates were taken of the rougher concentrates. Mass percent solids were taken for all the sampled streams. A water balance was then performed for the rougher bank. The EFC were measured for the aqueous solutions of each of the process stream samples and the results are shown in Table 15, Table 16, Figure 56 and Figure 57. The EFC's of all streams was high (31 to 47 ppm). This was expected to be much lower, however there could have been spillage containing frother being pumped into the rougher feed which resulted in the elevated EFC. This highlights the importance of

making measurements of frother concentration on plant. There may be high residual frother concentrations on the plant that could lead to identification of problem areas or reduce the need for high frother dosages. The mass balance results are shown in Table 16 and were relatively good however; there were significant adjustments in the rougher tails streams which expected because these samples were poor.

Table 13 shows the measurement of the EFC for each of the aqueous solutions of the process streams. For this test, the EFC measurements for a few of the process streams were measured at different dilution ratios. It can be seen that when the bubble size measured is large enough to be in the decay portion of the frother vs. bubble size relationship, which is the case for rougher conc 3, 4, 7 and the rougher feed; there is good reproducibility of the measurements. However if the bubble size is small and occurs close to the flattened portion of the curve which is the case for rougher conc 2; the reproducibility of the measurement is poor. Hence the correct dilution factor is important when performing measurements to ensure the resulting bubble size is large enough to be in the decay portion of the curve.

Figure 56 shows the EFC of the process streams in the rougher banks. It can be seen that the concentrate EFC for rougher concentrates of cells 1-4 were generally higher than the other rougher concentrates. This could be a result of the differences in operating conditions of the cells such as air rate and froth depth. The EFC of the rougher feed after frother addition and the rougher tails showed little difference, which implied that the bulk of the frother remained in the bulk water stream which was also observed by (Gelinas and Finch, 2007; Tsatouhas et al, 2005; Hadler et al. 2005).

Figure 57 shows the cumulative equivalent frother recovery against cumulative water recovery for the individual rougher banks and the combined rougher bank. This relationship was fitted with a straight line passing through the origin and the fit was excellent with an R^2 greater than 0.98. This was a similar result to Amandelbult described above. Furthermore, the cumulative equivalent frother recoveries were similar to the cumulative water recoveries, and this was a similar result obtained by Tsatouhas et al (2005) using gas chromatography. In Figure 57, the slope of the line for rougher concentrates 1-5 was greater than the slope of the line for rougher concentrates 6-10. This could have been due to the different cell operating conditions which is reflected by the differences in cumulative water recoveries between the two banks.

Frother can enter the concentrate adsorbed onto bubbles or by entrained water which was discussed above. Similarly the relationship between EFC and mass percentage solids is shown in Figure 70 below. Similarly to Plant C UG2 concentrator results, the EFC appears to increase with increase in mass percent solids although the relationship is not as clear. The mass percent solids is an indication of the amount of solids recovered relative to the amount of water recovered. The higher mass percent solids would indicate more solids relative to water and less entrainment because of less water recovered. Hence, it could be possible that the increase in EFC with mass percent solids could be due to a lower proportion of entrained frother compared to adsorbed frother which resulted in an overall higher EFC. Hence there could be a relationship that describes the concentration of frother in process streams with the mass percent solids.

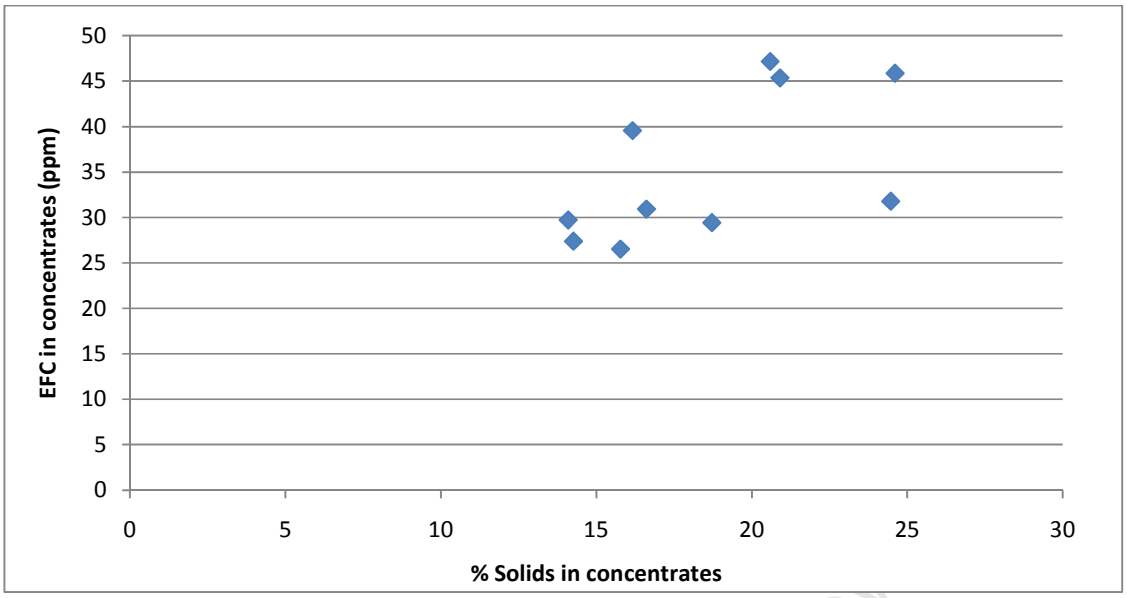

Figure 70: EFC vs. % solids in the concentrates of the rougher banks at Plant B UG2 Concentrator

7.3 Investigating the relationship between the Sauter mean bubble diameter and superficial gas velocity and its application in detecting frother depletion

Nesset et al. (2007) investigated the effects of hydrodynamic parameters on the d_{32} as well as the effects of frother in a mechanical forced air pilot cell. It was shown by Nesset et al (2007) that there exists an almost linear relationship between the Sauter mean bubble diameter and superficial gas velocity, and this relationship is different at different frother concentrations. As the frother concentration increases the straight line shift downwards because of the reduction in bubble coalescence. As the frother concentration exceeds the CCC, the relationship would not change because coalescence would be minimized, and the effects would be as a result of the impeller (Cho and Laskowski).

Gorain et al (1995) showed that increasing gas flow rate increased the mean bubble size for different impellers running at different speeds in a forced air mechanical cell. However, the effect of air rate for each impeller was different, implying the different impellers dispersed air differently. In addition, at a constant impeller speed, increasing air rate increased the spread of the bubble size distribution and the bubble size.

Hence for a bank of identical cells with identical impellers in series operating at the same speed, at a frother concentration exceeding the CCC, the relationship between the Sauter mean bubble diameter and superficial gas velocity should all lie on the same line. This was tested at Plant D concentrator on the secondary cleaners and cleaner scavengers. Frother was being dosed in the secondary cleaners in excess of the CCC, which was taken to be approximately 10 ppm as a reference for Betafroth 206 from the measurements done on Betafroth 206C. Furthermore, from a visual assessment, the bank appeared to have good froth stability. The relationship between Sauter mean bubble diameter and air flow rate was then established and is shown in Figure 58 for the first four cells in the secondary cleaner bank. Figure 58 showed that all the curves were on a common line, implying that the concentration of frother was above the CCC in each of the cells.

The cleaner scavenger bank receives the secondary cleaner tail as the feed to the bank. Frother is not dosed at this bank and a visual assessment indicated poor froth stability in the last three cells of the bank. Furthermore, these last three cells were struggling to recover concentrate and the bank was not able to achieve the targeted mass recovery even at high air rates and cell levels. The relationship between Sauter mean bubble diameter and superficial gas velocity was then established and shown for all the cells in the bank in Figure 59. Figure 59 shows the graphs for each of the cells down the bank. It can be seen that the first two cells, which are FT 59 and 60 are on the same common line. However from FT 61-64 the curves gradually shifted upwards which indicated that the bubble size was increasing which could be due to decreasing frother concentration below the CCC which resulted in bigger bubbles due to bubble coalescence. The impeller speed, type and size for all the cells were the same. Hence in conjunction with the visually poor froth on these cells and the above relationship, this effect was likely due to a decrease in the frother concentration to below the CCC from FT 61. Hence it was decided to dose frother on FT61 and the method for choosing the dosage rate was shown in Figure 60. The bubble size on the last cell FT64 was measured at a fixed air rate and the frother dosage was gradually increased until the bubble size decreased significantly to a minimum which was effectively dosing at a concentration close to the CCC. This resulted in a frother dosage rate that was equivalent to 15 ppm based on the bulk water flow in the cleaner scavenger bank, excluding any residual frother already in the bank.

The relationship between Sauter mean bubble diameter and superficial gas velocity was then established on the cells after frother addition on FT61 and is shown in Figure 61. The measurements of bubble size and superficial gas velocity were performed at the same position on the cell as previous measurements. The results showed that curves of bubble size versus superficial air velocity

for all the cells were now on a common line. This implied that frother depletion was in fact the problem. This also indicated that the frother concentration in each cell was now close to the CCC. Furthermore, the visual froth structure on the cells improved significantly and the bank was able to achieve the mass recovery at even lower air rates and cell levels than previously.

The cleaner scavenger bank was surveyed before and after frother addition to determine the effect on metallurgical performance of the bank. Figure 62 shows the process flow diagram of the bank and the sampling points in the bank. The bank operates with a recycle and the first two concentrates report to final concentrate on the plant. The tail stream is recycled back into the scavenger flotation circuit. A mass balance was performed to determine the overall bank performance. The surveys before and after frother addition are called S1 and S2, respectively. Figure 63 and showed the base metal and PGM grades for S1 and S2 for the final concentrate stream. The results showed a slight decrease in copper grade, but significant increases in the nickel and PGM grades. Figure 64 showed the solids flow rate of the final concentrate for S1 and S2. There was an increase in solids flow rate with the addition of frother and this was expected because the froth stability improved and concentrate pull rate improved on cells FT61-64. Figure 65 shows the bank recoveries of copper, nickel and PGMs. It can be seen that there was a significant increase in copper recovery and an almost two fold increase in nickel and PGM recovery. This was a result of improved grade and increased solids flow rate in the final concentrate. The improvement in both grade and recovery for nickel and PGM implies a significant shift upwards in the grade/recovery relationship of nickel and PGM for the bank. From a flotation kinetics perspective, these significant improvements in flotation performance can be attributed to improvement in the pulp phase and froth phase kinetics. The smaller bubble sizes would have increased the bubble surface area flux which resulted in an increase in the flotation rate constant as shown by Gorain et al (1998). Furthermore there was a significant visual improvement in the stability of the froth phase which would have improved the froth recovery (Tsatouhas et al, 2005).

8 Conclusions

A technique for determining the relationship between bubble size and frother concentration on a full scale plant has been established using the AAPBS on forced air industrial mechanical flotation cells. The results obtained are in agreement with literature and are reproducible and repeatable on different plants, cells and cell sizes. The relationship between bubble size and frother concentration has an excellent fit with the exponential decay relationship described by Comley et al (2002). Furthermore, this technique can be used as a comparison between different frothers on a full scale plant with the CCC as an indication of the relative strength of the frothers.

This technique has been extended to measure the equivalent frother concentrations in process streams by using effect of the process stream aqueous solution on bubble coalescence as a proxy for frother concentration. Bubble coalescence in these aqueous solutions will be affected by the ionic strength of the solution but this effect will be negligible. Hence the effect on bubble coalescence will therefore be predominantly due to frother which will allow the technique to be a good proxy for estimating frother concentration.

The relationship between bubble size and superficial gas velocity in a bank of identical flotation cells on a full scale plant operating at the same impeller speed and at a concentration of frother greater than or equal to the CCC is linear and the same for each cell. A shift in this relationship upwards at any point in the bank may indicate a decrease in frother concentration to below the CCC and will require additional dosage of frother. This technique was successfully applied to a cleaner scavenger bank on a full scale plant to detect depletion of frother. Additional frother was dosed on the cell that showed depletion of frother concentration midway through the bank and metallurgical performance of the cleaner scavenger improved significantly after the addition of frother. The recovery of copper increased by 27%; 4E PGM and nickel recovery increased by 100%. The 4E PGM grade and nickel grade increased by 30%.

9 References

1) Ata S., Ahmed N., Jameson G.J., 2004. The effect of hydrophobicity on the drainage of gangue minerals in flotation froths, Minerals Engineering, vol. 17, pp 897-901.

2) Barbian N., Hadler K., Ventura-Medina E., Cilliers J.J., 2005. The froth stability column: Linking froth stability to flotation performance, Minerals Engineering, vol. 18, pp 317-324

3) Becker M., Harris P.J., Wiese J.G., Bradshaw D.J., 2009. Mineralogical Classification of naturally floatable gangue in Merensky Reef ore flotation. International Journal of Mineral Processing, vol. 93, pp 246-255.

4) Cappuccitti F., Finch J.A., 2008. Development of new frothers through hydrodynamic characterisation, Minerals Engineering vol. 21, pp 944-948.

5) Cawthorn R.G., 1999. The Platinum and Palladium resources of the Bushveld Complex, South African Journal of Science, vol. 95, pp 481-489.

6) Cho Y.S., Laskowski J.S., 2002. Effect of flotation frothers on bubble size and foam stability, International Journal of Mineral Processing vol. 64, pp 69-80.

7) Comley B.A., Harris P.J., Bradshaw D.J., and Harris M.C. 2002. Frother characterisation using dynamic surface tension measurements. *International Journal of Mineral Processing,* Vol. 64. pp. 81-100.

8) Farohkpay S., 2011. The significance of froth stability in mineral flotation- A review, *Advances in Colloid and Interface Science*, vol. 166, pp 1-7.

9) Finch J.A., Nesset J.E., Acuna C., 2008. Role of frother on bubble production and behavior in flotation, Minerals Engineering, vol 21, pp 949-957.

10) Gorain B.K., Franzidis J.P., Manlapig E.V., 1998. Studies on Impeller type, impeller speed and air flow rate in an industrial scale flotation cell. Part 4: Effect of Bubble Surface Area flux on Flotation Performance, Minerals Engineering vol 10, pp 367-379.

11) Gorain B.K., Franzidis J.P., Manlapig E.V., 1995. Studies on Impeller type, impeller speed and air flow rate in an industrial scale flotation cell. Part 1: Effect on Bubble Size Distribution, Minerals Engineering vol 8, no. 6, pp 615-635.

12) Grau R. A., Laskowski J.S., Heiskanen K., 2005. Effects of frothers on bubble size, International Journal of Mineral Processing, vol. 76, pp 225-233.

13) Hadler, K., and Cilliers J.J. 2009. The relationship between the peak in air recovery and flotation bank performance. *Minerals Engineering*, vol. 22. pp. 451–455.

14) Hadler, K., Aktas, Z., and Cilliers, J.J. 2005. The effects of frother and collector distribution on flotation performance. *Minerals Engineering*, vol. 18 pp. 171-177.

15) Hadler K., Greyling M., Plint N., Cilliers J.J., 2012. The effect of froth depth and air recovery on flotation performance, Minerals Engineering, vol 36-38, pp 248-253

16) Hay M.P., Roy R., 2010. A case study of optimising UG2 flotation performance Part 1: Bench, pilot and plant scale factors which influence Cr_2O_3 entrainment in UG2 flotation, Minerals Engineeing, vol. 23, pp 855-867.

17) Malysa, K., Czubak-Pawlikowska, J., Pomianowski, A., 1978. Frothing properties of solutions and their influence on the floatability. Proc. 7th Int. Congress Surface Active SubstancesŽMoscow, 1976., vol. 3, Gordon and Breach, London, pp. 513–520

18) Malysa, K., Lunkenheimer, K., Miller, R., Hartenstein, C., 1981. Surface elasticity and frothability of *n*-octanol and *n*-octanoic acid solutions. Colloids Surf. 3, 329–338.

19) Manono M.S., Korin K.C., Wiese J.G., 2013. The effect of ionic strength of plant water on foam stability: A 2-phase flotation study, Minerals Engineering, vol. 40, pp. 42-47.

20) Morar S.H., Bradshaw D.J., Harris M.C., 2012. The use of froth surface lamellae burst rate as a measure as a froth stability measurement, Minerals Engineering, vol. 36-38, pp 152-159.

21) Mhlanga S.S., O'Connor C.T., Mcfadzean B., 2012. A study of the relative adsorption of guar onto pure minerals. Minerals Engineering, vol. 36-38, pp 172-178.

22) Nesset J.E., Finch J.A., Gomez C.O., 2007. Operating Variables affecting the bubble size in Forced Air Mechanical Flotation Machines, Ninth Mill Operators Conference, Fremantle, WA, pp 55-65.

23) Nesset, J.E., Hernandez-Aguilar, J.R., Acuña, C., Gomez, C.O., Finch, J.A., 2006. Some gas dispersion characteristics of mechanical flotation machines. Minerals Engineering 19, 807–815.

24) Quinn J.J., Kracht W., Gomez C.O., Gagnon C., Finch J.A., 2007. Comparing the effects of salt and frother (MIBC) on gas dispersion and froth properties. Minerals Engineering, vol. 20, pp 1296-1302.

25) Sweet, C., van Hoogstraten, J., Harris, M.C., Laskowski, J.S., 1997. The effect of frothers on bubble size and frothability of aqueous solutions. In: Finch, J.A., Holubec, I. (Eds.), Processing of Complex Ores—Proc.2nd UBC-McGill Symposium. Canadian Institute of Mining, Metallurgy and Petroleum, Montreal, pp.235–246.

26) Subrahmanyam T.V., Forssberg E., 1988. Froth Stability, Particle entrainment and drainage in Froth Flotation-A review, International Journal of Mineral Processing, vol.23, pp 33-53.

27) Tan S. N., Pugh R.J., Fornasiero D., Sedev R., Ralston J. 2005. Foaming of polypropylene glycols and glycol/MIBC mixtures, Minerals Engineering, vol. 18, pp. 179-188.

28) Tsatouhas G., Grano S.R., Vera M., 2006. Case studies of the performance and characterisation of the froth phase in industrial flotation circuits. Minerals Engineering, vol. 19, pp 774-783.

29) Valenta M., 2007. Balancing the reagent suite to optimise grade and recovery, Minerals Engineering, vol. 20, pp 979-985.

30) Vera, M.A., Franzidis, J.P., and Manlapig, E.V. 1999. Simultaneous determination of collection zone rate constant and froth zone recovery in a mechanical flotation environment. *Minerals Engineering*, vol. 12, no. 10. pp. 1163-1176.

31) Weber T., Gomez C.O., and Finch J.A. 2003. A frother concentration meter. *Proceedings of the 35th Annual Meeting of the Canadian Mineral Processors*, pp. 639-652.

32) Wiese J., Harris P., Bradshaw D., 2007. The response of sulphide and gangue minerals in selected Merensky ores to increased depressant dosages, Minerals Engineering, vol. 20, pp 986-995

33) Wiese, J., Harris, P., and Bradshaw, D. 2011. The effect of the reagent suite on froth stability in laboratory scale batch flotation tests. *Minerals Engineering*, vol. 24. pp. 995–1003.

34) Wiese, J. and Harris, P. 2012. The effect of frother type and dosage on flotation performance in the presence of high depressant concentrations. *Minerals Engineering,* vol 36-38, pp 204-210